

FINAL PROGRAM

**25th Annual Meeting
of the
Council on Ionizing Radiation Measurements and Standards**



“PAST, PRESENT AND FUTURE”

March 27 – 29, 2017

**National Institute of Standards and Technology
Gaithersburg, Maryland**

TABLE OF CONTENTS

Sponsors	3
CIRMS Officers and Subcommittee Chairs	5
Meeting Focus and Needs Report	6
Full Meeting Agenda at a Glance	7
- Agenda for the Afternoon Industrial Applications and Material Effects (IAME) Breakout Sessions	10
- Agenda for the Afternoon Medical Applications Breakout Sessions	11
- Agenda for the Afternoon Radiation Protection Breakout Sessions	13
Abstracts of Morning Plenary Sessions	15
Abstracts of Afternoon Medical Applications Breakout Sessions	18
Abstracts of Afternoon Radiation Protection Breakout Sessions	22
Abstracts of Afternoon Industrial Applications and Material Effects (IAME)	26
Breakout Sessions	
Abstracts of Student Presentations and Posters	28
Past CIRMS Presidents	74
Caswell Award Winners	74
Student Grant Recipients	75
Next Year's CIRMS Meeting Announcement (Save The Date!)	81
Information on Becoming a CIRMS Sponsor	82



25TH ANNUAL MEETING



**MARCH 27-29, 2017
AT NIST
GAITHERSBURG, MD**

CIRMS SPONSORS

American Association of Physicists
in Medicine (AAPM)

American College of Radiology (ACR)

ASTM International

Bruker BioSpin Corporation

Ecker & Ziegler Isotope Products

Hopewell Designs, Inc.

IBA Industrial, Inc.

Kent State University

Landauer, Inc.

National Institute of Standards and
Technology (NIST)

ScanTech Sciences

Steris Corporation

SUNY – ESF

The University of Texas at Dallas

University of Wisconsin -
Madison ADCL

UT MD Anderson Cancer Center ADCL

NIST
NATIONAL INSTITUTE OF
STANDARDS AND TECHNOLOGY
U. S. Department of Commerce

www.cirms.org

**THE COUNCIL ON IONIZING RADIATION MEASUREMENTS AND
STANDARDS GRATEFULLY THANKS ITS DISTINGUISHED SPONSORS**

CORPORATE

Bruker BioSpin Corporation

Ecker & Ziegler Isotope Products

Hopewell Designs, Inc.*

IBA Industrial, Inc. *

Landauer *

ScanTech

Steris Corporation

Sterigenics

Theragenics Corporation

ORGANIZATIONAL

American Association of Physicists in
Medicine

American College of Radiology

ASTM International *

Kent State University

National Institute of Standards and
Technology

RadTech

SUNY - ESF

University of Texas at Dallas

University of Wisconsin Madison ADCL

UT MD Anderson Cancer Center ADCL

* Sponsors of the Students Travel Awards

CIRMS 2017 OFFICERS AND SUBCOMMITTEE CHAIRS

President: Mark S. Driscoll, State University of New York at
Syracuse - ESF

1st Vice-President: Zhichao Lin, U.S. Federal Drug Administration

2nd Vice-President: To be determined

Secretary: Ryan Howell, Hopewell Design Inc.

Treasurer: Regina Fulkerson, Standard Imaging

Administrative Assistant: Renata Freindorf, University of Texas - Dallas

Immediate Past President: Walter E. Voit, University of Texas - Dallas

Science & Technology: Walter E. Voit, University of Texas - Dallas

Radiation Protection: Michael P. Unterweger, NIST

Industrial Applications and Materials Effects: Kim M. Morehouse, U.S. FDA Division of Analytical
Chemistry
Roberto Uribe-Rendon, Kent State University

Medical Applications: Ronaldo (Ronnie) Minniti, NIST
Regina Fulkerson, Standard Imaging
Wesley Culberson, University of Wisconsin - Madison

MEETING FOCUS

The 25th Annual Meeting of the Council on Ionizing Radiation Measurements and Standards will focus on the “Past, Present and Future” of CIRMS. For twenty-five years, CIRMS has played an important role in serving as a public forum for discussion of radiation measurements and standards issues for industry, academia and government. The technical program this year will consist of oral and poster presentations and three parallel working group sessions that address measurement and standards needs in the following topics:

- Medical Applications [proton therapy, dosimetry for radiation biology applications, nuclear medicine and diagnostic 3D real-time imaging for orthopedic applications]
- Radiation Protection [personnel dosimetry, electronic dosimeters, radiation protection instrumentation, document standards, food safety and consequence management]
- Industrial Applications and Materials Effects [dosimetry for radiation processing, radiobiology, safety at radiation facilities, food irradiation, medical device sterilization and nanomaterials]

The CIRMS Executive Committee has developed a program and agenda to celebrate our past, focus us on the present and help us influence the future. We have a diverse group of topics that will be covered this year including: radiation effects in space, 3D real time x-ray imaging for orthopedic applications, quantitative imaging, proton therapy, radiation biology irradiators, radiation protection instrumentation, document standards, food safety, nanomaterials, food irradiation, sterilization and much more.

NEEDS REPORT EXECUTIVE SUMMARY

The Council on Ionizing Radiation Measurements and Standards (CIRMS) is an independent, non-profit council that draws together experts involved in all aspects of ionizing radiation to discuss, review and assess developments and needs in this field. Drawing upon expertise from government and national laboratories, agencies and departments, from the academic community and from industry, CIRMS has issued four triennial reports on “Needs in Ionizing Radiation Measurements and Standards.” Such needs are delineated in Measurement Program Descriptions (MPDs) that indicate the objective, state background information, define needed action items and resource requirements in terms of personnel and facilities.

Each of the subcommittees of the CIRMS Science and Technology Committee has prepared a series of MPDs pertinent to their area of expertise. These emerge through data sharing and focused discussion at CIRMS meetings and workshops. These three subcommittees are:

- The Medical Applications Subcommittee
- The radiation Protection Subcommittee
- The Industrial Applications and Materials Effects Subcommittee

The most recent Needs Report published in 2016 is available on the CIRMS website at http://www.cirms.org/w/index.php?title=Executive_Summary

FULL MEETING AGENDA AT A GLANCE

Monday, March 27, 2017

Morning Plenary sessions: Green Auditorium

Afternoon Breakout Sessions: Lecture Rooms A, B and D

- 8:30 am Continental Breakfast/Registration
- 9:15 am **President's Welcome**
Dr. Mark S. Driscoll, President, CIRMS
- Welcome to NIST**
Dr. Lisa R. Karam,
Chief, Radiation Physics Division, Physical Measurement Laboratory
National Institute of Standards and Technology, MD
- 9:30 am **Intro to NEEDS REPORT and Student Award Introduction**
Dr. Walter E. Voit
University of Texas at Dallas
- 9:45 am **Keynote Address**
Dr. Bert M. Coursey, NIST
CIRMS: A Retrospective and Look Forward
- 10:15 am **Randall S. Caswell Award for Distinguished Achievement in the Field of Ionizing Radiation Measurements and Standards presented to:**
Dr. Peter R. Almond, UT MD Anderson Cancer Center (retired)
- 10:30 am Coffee Break
- 10:45 am **Plenary Session I**
Dr. Larry DeWerd, University of Wisconsin - Madison
Caswell Fellows and Calibration Standards from NIST using Secondary Laboratories as an Example
- 11:15 am **CIRMS Student Travel Grant Awards Presentations:**
- CIRMS Student Travel Grant – sponsored by ASTM International
Alexandra Bourgouin – Carleton University, Canada
Vacuum Current: A Possible Systematic Error in Absolute Dose/Kerma Measurements with Ion Chambers
- CIRMS Student Travel Grant – sponsored by Hopewell Designs, Inc.
James Renaud – McGill University, Canada
Aerrow: A Probe-Format Graphite Calorimeter for Use as a Local Absorbed Dose Standard for High-Energy Photon Beams in the Clinical Environment
- CIRMS Student Travel Grant – sponsored by Bruker IBA Industrial, Inc.
Susannah Hickling – McGill University, Canada
Measuring Radiation Dose through the Detection of Radiation-Induced Acoustic Waves
- CIRMS Student Travel Grant – sponsored by Landauer
Manik Aima – University of Wisconsin – Madison

Dose Distribution Measurements of a New Directional Pd-103 Low-dose Rate Brachytherapy Source

- 11:55 am **Poster Summaries**
- 12:05 pm **Poster Viewing**
- 12:45 pm Lunch
- 1:45 pm **Concurrent Working Group Sessions** (see separate agenda for afternoon sessions)
speakers below)
 Medical Applications – Lecture Room A
 Radiation Protection – Lecture Room B
 Industrial Applications – Lecture Room D
- 1:45 pm **Working Group Session I** (see separate agenda for afternoon sessions)
- 3:30 pm Coffee Break
- 3:45 pm **Working Group Session II** (see separate agenda for afternoon sessions)
- 5:30 pm Adjourn

Tuesday, March 28, 2017

Morning Plenary sessions: Green Auditorium

Afternoon Breakout Sessions: Lecture Rooms A, B and D

- 8:30 am Continental Breakfast
- 9:15 am **President's Welcome**
 Dr. Mark S. Driscoll, President, CIRMS
- 9:30 am **Plenary Session II**
 Dr. Edward F. Jackson, University of Wisconsin - Madison
 Quantitative Imaging
- 10:00 am **Plenary Session III**
 Kevin O'Hara, Sterigenics
 Sterilization Standards
- 10:30 am Coffee Break
- 10:45 am **Plenary Session IV**
 Dr. Ruthan Lewis, National Aeronautics and Space Administration (NASA)
 Radiation -- A Cosmic Hazard to Human Habitation in Space
- 11:15 am **Poster Summaries**
- 11:30 am **Poster Viewing**
- 12:45 pm Lunch
- 1:45 pm **Concurrent Working Group Sessions (continued):**
 Medical Applications – Lecture Room A
 Radiation Protection – Lecture Room B
 Industrial Applications – Lecture Room D

- 1:45 pm **Working Group Session III** (see separate agenda for afternoon sessions)
- 3:30 pm Coffee Break
- 3:45 pm **Working Group Sessions IV** (see separate agenda for afternoon sessions)
- 5:30 pm Adjourn Day 2
- 6:15 pm Bus from the hotel to the restaurant
- 6:45 pm **Gala Dinner @ Smokey Glen Farm BBQ**
16407 Riffle Ford Rd, Gaithersburg, MD 20878

Wednesday, March 29, 2017

Morning Plenary sessions: Green Auditorium

- 8:30 am Continental Breakfast
- 9:15 am **Welcome Back**
Dr. Mark S. Driscoll, President, CIRMS
- 9:30 am **Plenary Panel**
Dr. Jonathan W. Engle, LANL/University of Wisconsin - Madison
Alpha Therapy
- 9:45 am **Plenary Panel**
Dr. Ileana Pazos, NIST
Chip-scale Calorimetry for Industrial Dosimetry
- 10:00 am **Plenary Panel**
Dr. Stephanie Healey, Food and Drug Administration
Food Defense during a Radiological Emergency
- 10:15 am **Plenary Panel**
Panel Discussion with three panelists
- 10:30 am Coffee Break
- 10:45 am **Capstone Speaker**
Dr. Vasilis Ntziachristos, Technical University of Munich, Germany
Biological and Medical Imaging
- 11:15 am **Report on Needs in Ionizing Radiation**
Dr. Anthony Berejka, Ionicorp
Past MPD Recap
Group leaders

Dr. Walter E. Voit, University of Texas at Dallas
Current/Future Work
- 12:30 pm **Closing Address/ New Officers**
Dr. Mark S. Driscoll, President, CIRMS
- 12:45 pm Lunch
- 1:45 pm **ExComm Meeting**

Agenda for the Afternoon **Industrial Applications and Material Effects (IAME) Breakout Sessions**

Monday March 27, 2017 (afternoon)

Chairs: Roberto Uribe (Kent State University) and Kim M. Morehouse (FDA)

Breakout Session I: Food Irradiation

- 1:45-2:05 Anuradha Prakash, Chapman University
Shedding Light on Food Irradiation: A Comparison with Alternative Food Technologies
- 2:05-2:25 Vanee Komolprasert, Food and Drug Administration/ CFSAN
Packaging for Irradiated Fresh Produce
- 2:25-2:45 Laura Jeffers, U.S. Department of Agriculture/APHIS
Phytopathological Irradiation Treatments: An Important Mitigation Tool in the Agriculture Quarantine Inspection (AQI) Toolbox
- 2:45-3:05 Chip Starns, ScanTech Sciences Inc.
Cross-border Produce Irradiation using E-beam; an Emerging Market with Great Potential
- 3:05-3:30 Questions for speakers and discussion on "current needs"
- 3:30-3:45 Break

Breakout Session II: Nanomaterials

- 3:45-4:30 Mohamad Al-Sheikhly, University of Maryland
Electron Beam Synthesis of Magnetic Nanomaterials and Nanocomposites
- 4:30-4:50 Dianne Poster, NIST
Production of Nanomaterials in Water using Ionizing Radiation
- 4:50-5:10 Michael Postek, NIST
Nanomaterials Analysis and Standards
- 5:10-5:30 Questions for speakers and discussion on "current needs"
- 5:30 Adjourn

Tuesday March 28, 2017 (afternoon)

Breakout Session III: Dosimetry for High Dose Applications

- 1:45-2:15 Lonnie Cumberland and Ileana Pazos, NIST
High Dose Calibration at NIST (Gamma)
- 2:15-2:45 Fred Bateman and Ronald Tosh, NIST
Accelerator-Based Standards for Industrial Dosimetry
- 2:45-3:15 Spencer Mickum, Hopewell Designs Inc.
New Design Basis Analysis for Self-Contained, Dry-Storage Irradiators
- 3:15-3:30 Questions for speakers and discussion on "current needs"
- 3:30-3:45 Break

Breakout Session IV: Sterilization of Medical Devices

- 3:45-4:15 Sherry Formica, Johnson & Johnson
Process Verification – How to Ensure Process Effectiveness
- 4:15-4:45 Kevin O'Hara, Sterigenics
Sterilization of Medical Devices
- 4:45-5:15 Deepak Patil, Steris Corporation
Establishing Process Parameters and Process Acceptance
- 5:15-5:45 Questions for speakers and discussion on "current needs"
- 5:30 Adjourn

Agenda for the Afternoon **Medical Applications** Breakout Sessions

Monday March 27, 2017 (afternoon)

Chairs: Regina Fulkerson (Standard Imaging), Wesley Culberson (University of Wisconsin), and Ronaldo (Ronnie) Minniti (NIST)

Breakout Session I: Radionuclides for nuclear medicine

- 1:45-2:15 Reid Townson, Ph.D., National Research Council of Canada
Realistic Simulation of Radionuclide Sources in Egsnrc: A Predictive Model of the Vinten Ionization Chamber
- 2:15-2:45 Brian Zimmermann, Ph.D., NIST
From Level Scheme to Diagnosis: Nuclear Data and The Development of Standards for Quantitative Medical Imaging.
- 2:45-3:15 John Keightley, Ph.D., National Physical Laboratory, UK
Development of Standards for Alpha Emitting Radionuclides for Nuclear Medicine
- 3:15-3:30 Questions for speakers and discussion on "current needs"
- 3:30-3:45 Break

Breakout Session II: Radiation Biology and Dosimetry

- 3:45-4:15 Wesley Culberson, Ph.D., University of Wisconsin - Madison
Current Status of Radiobiology Dosimetry
- 4:15-4:45 Paul DeJean and Bill McLaughlin, Precision X-Ray
Advances in Pre-Clinical Image Guided X-Ray Irradiation
- 4:45-5:15 Adrian Treverton, Ph.D., Xstrahl Inc.
Towards Better Repeatability and Accurate Dosimetry in Image-Guided Small-Animal Irradiators
- 5:15-5:30 Questions for speakers and discussion on "current needs"
- 5:30 Adjourn

Agenda for the Afternoon **Medical Applications Breakout Sessions**

Tuesday March 28, 2017 (afternoon)

Working Group Chairs: Regina Fulkerson (RKF Consultants), Wesley Culberson (Univ. of Wisconsin) and Ronaldo (Ronnie) Minniti (NIST)

Breakout Session III: Real Time Imaging for Orthopedic Applications

- 1:45-1:55 Introduction to the session by the chairs: *The need for developing 3D imaging tools for evaluating orthotics. How can we improve the current practice?*
- 2:00-2:30 Kevin Wilson, Ph.D., Hologic
Low dose, mini C-arm fluoroscopy for hand and foot applications
- 2:30-3:00 Stuti Singh, Ph.D., Curvebeam
Why Cone Beam CT can make 3D the Standard of Care in Extremity Imaging
- 3:00-3:15 Regina Fulkerson, Ph. D., RKF Consultants
A quick overview of a weight bearing 3D imaging system for horses
- 3:15-3:30 Questions for speakers and discussion on needs in this area
- 3:30-3:45 Break

Breakout Session IV: Proton Relative Biological Effectiveness (RBE)

- 3:45-4:10 Ramin Abolfath, Ph.D., MD Anderson & University of Pennsylvania
Biological Responses of Therapeutic Ionizing Radiation and Charged Particles
- 4:10-4:35 Paige Taylor, M.Sc., MD ANDERSON (IROC)
Proton Therapy National Ion Chamber Intercomparison
- 4:35-5:00 Darshana Patel, Ph.D., MD Anderson
Experimental Investigation of RBE as a Function of Dose and LET
- 5:00-5:25 Michael Butkus, M.S., Yale
Multi-Ion Analysis of RBE using the Microdosimetric Kinetic Model
- 5:30 Adjourn

Agenda for the Afternoon Radiation Protection Breakout Sessions

Monday March 27, 2017 (afternoon)

Chairs: Stanley Mavrogianis (NSWC) and Michael Unterweger (NIST)

Breakout Sessions I: Instrumentation

- 1:45-2:15 Dr. Luis Benevides, Naval Surface Warfare Center, Carderock Division
Aligning US Navy Dosimetry with NIST
- 2:15-2:45 Jeancarlo Torres, CHP Naval Surface Warfare Center, Carderock Division
IM-276/PD Next Generation Navy Battlefield Dosimeter – System Overview and Test Summary
- 2:45-3:15 Joe Rotunda, Rotunda Scientific Technologies LLC
The Future Direction of Passive Dosimetry
- 3:15-3:30 Questions for speakers and discussion on "current needs"
- 3:30-3:45 Break

Breakout Sessions II: Document Standards

- 3:45-4:15 Dr. Chad McKee, JPL – Radiological and Nuclear Defense
Conformal Testing for Dosimeters against Prompt Neutron and Gamma Exposures
- 4:15-4:45 Keith D. Turner, PE, US Navy RADIAC Standards Program
An Overview of Current US NAVY Alpha, Beta, Gamma, and Neutron Radiation Calibration Standards and the Processes Used to Ensure NIST Traceability
- 4:45-5:15 Meredith Wood, Naval Surface Warfare Center, Carderock Division
Pitfalls of Revising National Standards – A Portable Survey Instrument Standard (ANSI 42.17AC)
- 5:15-5:30 Questions for speakers and discussion on "current needs"
- 5:30 Adjourn

Agenda for the Afternoon Radiation Protection Breakout Sessions

Tuesday March 28, 2017 (afternoon)

Chairs: Jacqueline Mann (NIST) & Stephanie Healey (FDA)

Breakout Sessions III: Consequence Management

- 1:45-2:05 Robert L. Jones, CDC, NCEH, Division of Laboratory Sciences
CDC's Need for Reference Materials to Validate Analytical Methods for Public Health Exposure Assessments after a Radiological or Nuclear Incident
- 2:05-2:25 John Griggs (EPA)
EPA's Needs for Radiological Reference Materials to Support Response and Recovery Activities Following a Radiological or Nuclear Incident
- 2:25-2:45 Stephanie Healy (FDA-WEAC)
An Intercomparison Study on Radiological Methods Used by FDA Food Emergency Response Radiological Laboratory Network
- 2:45-3:30 Questions for speakers and discussion on "current needs"
- 3:30-3:45 Break

Breakout Sessions IV: Consequence Management (continued)

- 3:45-4:05 Zhichao Lin (FDA-WEAC)
Development of Rapid Liquid Scintillation Counting Method for determination of Tritium in Foods
- 4:05-4:25 Zhichao Lin (FDA-WEAC)
Rapid Detection of Americium-241 in Food by Inductively-Coupled Plasma Mass Spectrometry
- 4:25-4:45 Clarence Rolle (FDA-WEAC)
A Comparison of Computational Approaches for the Detection of Gamma-Emitting Radionuclides in Foods
- 4:45-5:30 Questions for speakers and discussion on "current needs"
- 5:30 Adjourn

Conference Abstracts

Monday March 27, 2017 - Morning Plenary Sessions

CIRMS – A Retrospective and Look Forward

Dr. Bert Coursey, National Institute of Standards and Technology (NIST)

A quarter century ago the Council on Ionizing Radiation Measurements and Standards (CIRMS) was founded to give voice to the community of users of ionizing radiation and radioactivity who span different scientific and technological endeavors but share a common interest in development of measurements and standards. The decision was made by the founders that CIRMS would actively engage users from the industrial, governmental and academic fields and provide them a common forum for discussion of measurements and standards. The Scientific Committee of CIRMS through its subcommittees has produced since 1995 six reports on “Needs for Ionizing Radiation Measurements and Standards”. This account will look at the evolving roles of ionizing radiation and applications of radionuclides, how CIRMS has attempted to steer the development of measurements and standards for these evolving applications, and a brief look forward at the challenges and opportunities for the CIRMS communities.

The Caswell Fellows

Dr. Larry DeWerd, FAAPM

CIRMS instituted the honorary award called the Caswell fellowship, based on Randy Caswell. Randy was the first fellow. The fellowship is to recognize distinguished achievements in the field of Ionizing Radiation Measurements and Standards. A history of the awards will be presented. Peter Almond will be recognized for our 25th year.

Calibration Standards from NIST using Secondary Laboratories as an Example

Dr. Larry DeWerd, FAAPM

The radiation output of linear accelerators used for medical radiation therapy need precise calibrations. The accepted procedure is to calibrate ionization chambers on a two-year period. NIST used to calibrate all chambers but soon found that this was not feasible because of the volume. Robert Loevinger proposed to the AAPM that secondary laboratories be set up which would be directly traceable to NIST. The procedure and operation of such secondary labs will be reviewed and the methodology of maintaining traceability. A review of all the traceable quantities will be given.

Tuesday March 28, 2017 - Morning Plenary Sessions

Quantitative Imaging

Dr. Edward F. Jackson, University of Wisconsin - Madison

Over the past decade, increasing attention has been directed toward quantitative imaging biomarkers (QIBs), which are defined as “objectively measured characteristics derived from *in vivo* images as indicators of normal biological processes, pathogenic processes, or response to a therapeutic intervention”¹, and the applications of such QIBs. To translate current qualitative imaging assessments to the use of QIBs requires the development and standardization of data acquisition, data analysis, and data display techniques, as well as appropriate reporting structures. As such, successful implementation of QIB applications relies heavily on expertise from the fields of image science, radiology, statistics, metrology, and informatics as well as collaboration from vendors of imaging acquisition, analysis, and reporting systems. When successfully implemented, QIBs will provide image-derived metrics with known bias and variance that can be validated with relevant measures, including treatment response (and the heterogeneity of that response) and outcome. Such non-invasive quantitative measures can then be used effectively in clinical and translational research and will contribute significantly to the goals of precision medicine. This presentation will focus on 1) outlining the opportunities for QIB applications, with examples to demonstrate applications in both research and patient care, 2) discussing key challenges in the implementation of QIB applications, and 3) providing

overviews of efforts to address such challenges from federal, scientific, and professional organizations, including, but not limited to, the RSNA, NCI, FDA, and NIST. ¹Sullivan, Obuchowski, Kessler, *et al.* *Radiology* 277(3):813-825, 2015.

Medical Product Sterilization: Past, Present and Future

Kevin O'Hara, Director of Radiation Physics, Sterigenics

The medical product sterilization landscape has changed dramatically of the last sixty years. New materials make it very important to understand the effects of sterilization on end use of the device. Materials such as biodegradables, orthopedic implants, nanotechnology applications or surface modifications are all part of the orthopedic landscape. Mitigating sterilization risks by utilizing the knowledge of radiation chemistry and mechanical properties of both the packaging and device materials is a key to successful sterilization.

Many current medical devices are profoundly different with respect to materials of construction and complexity of design. In addition to metals such as titanium alloys, orthopedic implants now contain different types of polymers and engineering plastics, composites, absorbable polymers, biological materials, and embedded electronics. Most device manufacturers outsource the sterilization process to contract service providers who annually process millions of cubic feet of medical products. The sterilization of large volumes of commodity medical product may not be operationally compatible with the sterilization of lower volumes of specialized devices, but on-going collaboration between the device manufacturer and the sterilization-service provider will lead to innovative technology breakthroughs. A number of precision dose irradiators are now available for small- to medium-volume complex medical product, but a high-volume precise dose irradiator will yield the best of both worlds: reduction in sterilization costs associated with high-volume irradiation of medical product. Other processes are available for sterilization of medical devices that are based on hydrogen peroxide, peracetic acid, nitrogen dioxide, chlorine dioxide, and seeded gas plasma. Sterilization processes have evolved and new ones have been developed to meet the challenges posed by many new medical devices. For ionizing radiation, several strategies will be discussed, including: utilizing precision gamma irradiators to narrow the range of dose that products receive; optimal presentation of the device to the radiation field, and processing product at low temperature and/or under nitrogen to preserve drug/biologic attributes. Medical devices have become more sophisticated. In some cases, optimal sterilization methods have to be evaluated on a case-by-case basis, but finding the right sterilization solution takes in-depth knowledge of the product, potential constraints on the sterilization process, and collaboration between the manufacturer and sterilization service provider.

Radiation -- A Cosmic Hazard to Human Habitation in Space

Dr. Ruthan Lewis, National Aeronautics and Space Administration (NASA)

Radiation exposure is one of the greatest environmental threats to the performance and success of human and robotic space missions. Radiation "permeates" all space and aeronautical systems, challenges optimal and reliable performance, and tests survival and survivability. We will discuss the broad scope of research, technological, and operational considerations to forecast and mitigate the effects of the radiation environment for deep space and planetary exploration.

Wednesday March 29, 2017 - Morning Plenary Sessions

Alpha Therapy

Dr. Jonathan W. Engle, LANL/University of Wisconsin - Madison

In the last decade, clinical trials of late-stage cancer patients have established that targeted radiotherapy offers immense, untapped treatment potential. Challenges in the large-scale production of alpha- and electron-emitting radionuclides are being addressed by dedicated research efforts and federal investment. I will describe work conducted to expand the availability of these radionuclides at Los Alamos National Laboratory and the University of Wisconsin, emphasizing unanswered questions in their formation by high intensity charged particle irradiations, isolation from radiochemical impurities, and application in the treatment of human disease.

Chip-scale Calorimetry for Industrial Dosimetry

Dr. Ileana Pazos, National Institute of Standards and Technology (NIST)

The high-dose dosimetry program supports radiation-processing applications by assuring NIST traceability of absorbed dose to a product which is often closely regulated. The firmly established alanine-based dosimetry system is an integral part of the NIST transfer service and internal calibrations based on Co-60 radioactive sources. However, many industrial and medical applications utilize accelerator-based radiation sources for which only secondary standards are available. The development of high-precision chip-scale nano-photonic calorimeters that improve spatial resolution will transform clinical and material applications where characterization of non-uniform radiation fields is critical.

Food Defense during a Radiological Emergency

Stephanie Healey, Zhichao Lin, and Patrick Regan, Food and Drug Administration

Proven analytical methods and a competent laboratory network are essential for the Food and Drug Administration (FDA) to implement food defense and safety measures under the Food Safety Modernization Act (FSMA). With growing risks imposed by global aging nuclear facilities and proliferation of radioactive materials, FDA faces increasing challenges in safeguarding the nation's food supply from radioactive contamination. In order to mitigate the imposing threats to food safety and public health, a radiological Food Emergency Response Network (FERN) consisting of federal and state laboratories was established. This network serves to strengthen the FDA's ability to respond to a nuclear/radiological incident. FDA's decision-making during an incident will be based on large pools of data from diversified analytical methods. Ambiguous findings will inhibit FDA's ability to take prompt action on protecting public health. Measurement capability, data comparability, and an efficient data reporting mechanism are essential for emergency response when analytical data from FERN laboratories are used for post-incident risk assessment and management.

The FDA's Winchester Engineering and Analytical Center (WEAC) has engaged the FERN network radio analytical labs in a number of activities in recent years to assess and improve their capability and capacity. This presentation will summarize method development, proficiency testing, training, and emergency response exercises performed by the FERN radiological laboratories. Lessons learned, future activities, and the FERN's readiness for emergency response will also be discussed.

Optoacoustics Meets Ionoacoustics: 3D imaging of the Bragg Peak

Dr. Vasilis Ntziachristos, Technical University of Munich, Germany

For the past 10 years, we have developed optoacoustic (photoacoustic) tomography for biomedical applications. The technology illuminates tissue at multiple wavelengths, typically utilizing pulsed lasers, and records ultrasonic waves generated within tissue. By unmixing images obtained at different wavelengths, multispectral optoacoustic tomography (MSOT) can then resolve tissue physiological and molecular parameters, including angiogenesis, hypoxia, inflammation or metabolism. Recently, we adapted this technology to measuring ion beams and introduce ionoacoustic tomography based on detection of ion induced ultrasound waves. The detected ultrasonic data are treated through mathematical reconstruction to deliver 3D images of the Bragg peak inside phantoms and tissues. Ionoacoustic tomography can be therefore employed as a technique to provide measurements and real-time feedback on the ion beam profile. We show imaging in the case of 20 MeV with submillimeter accuracy and combinations with ultrasound and optoacoustic imaging.

Monday March 27, 2017: Afternoon Medical Applications Breakout Sessions

Medical Applications Breakout Session I: Radionuclides for Nuclear Medicine

Realistic Simulation of Radionuclide Sources in EGSnrc: A Predictive Model of the Vinten Ion Chamber

Dr. Reid Townson, National Research Council of Canada

Monte Carlo simulations are widely used to evaluate experimental conditions involving radionuclides. Recently, the ability to simulate radionuclide decays based directly off the ENSDF (Evaluated Nuclear Structure Data File) format has been integrated into the EGSnrc Monte Carlo code. The new radionuclide source model includes simulation of decay chains and correlated internal transitions, allowing for detailed event-by-event analysis. This can be a powerful predictive tool of experimental conditions. In particular, a Vinten ionization chamber has been investigated.

From Level Scheme to Diagnosis: Nuclear Data and the Development of Standards for Quantitative Medical Imaging.

Brian Zimmermann, Ph.D., NIST

Development of Standards for Alpha Emitting Radionuclides for Nuclear Medicine (^{223}Ra & ^{227}Th)

Dr. John Keightley, National Physical Laboratory, Teddington, UK

Alpha-particle emitting radiopharmaceuticals are becoming increasingly important as cancer therapeutic agents, and dosimetry associated with their use requires accurate activity standards coupled with improvements to existing nuclear data. An Ac-227 generator (half-life 21.8 years) may be used to produce the two radionuclides Th-227 and Ra-223 (half-lives 18.7 days and 11.4 days respectively). These are ideal for transport from production facilities to clinical sites, and both radionuclides are of great recent interest in the field of Targeted Alpha Therapy. Radium-223, used as radium chloride, targets bone growth in metastases of various cancers (since radium and calcium exhibit similar chemical properties), whereas Th-227 has broader applications (as targeted thorium conjugates) due to the availability of chelates which can be attached to targeting proteins such as antibodies for delivery to tumour cells. The standardisation of these two isotopes has been the subject of considerable recent effort at National Metrology Institutes worldwide, and this is the main focus of the presentation, coupled with the determination of improved nuclear data, and the determination of appropriate dose calibrator dial factors. This important work ultimately enables the administration of accurate (and traceable) patient doses.

Medical Applications Breakout Session II: Radiation Biology and Dosimetry

Current Status of Radiobiology Dosimetry

Dr. Wesley Culbertson, University of Wisconsin - Madison

In the past decade, there has been an increased interest in the standardization of dosimetry in radiobiological experiments. For radiobiology researchers to accurately compare and reproduce studies, both accurate reporting and dosimetry calculations are imperative. The proceedings from a recent symposium on dosimetry in radiobiology research titled, "The importance of standardization of dosimetry in radiobiology" outlined the methods required for accurate radiobiology dosimetry standardization. A literature reviews by our group following this symposium showed that very few of the suggested reporting criteria are actually being reported. Radionuclide-based irradiators are slowly being phased out in favor of x-ray cabinet irradiators due to licensing requirements and expensive resourcing. Radionuclide-based irradiator dosimetry tends to be straightforward due to the predictable nature of the sources and available radionuclide-based calibrations for dosimeters. Advances in small-animal conformal irradiator technology means more complicated dosimetry. Treatment planning systems have been developed to assist in these high-tech delivery machines, but the basic measurements of output with NIST-traceability are still difficult to perform. A review of the NIST-traceable radiobiology dosimetry techniques available today will be presented as well as the challenges moving forward.

Advances in Pre-Clinical Image Guided X-Ray Irradiation

Paul DeJean and Bill McLaughlin, Precision X-Ray

Towards Better Repeatability and Accurate Dosimetry in Image-Guided Small-Animal Irradiators

Dr. Adrian Treverton, Xstrahl Inc

Tuesday March 28, 2017: Afternoon Medical Applications Breakout Sessions

Medical Applications Breakout Session III: Real Time Imaging for Orthopedic Applications

The need for developing 3D imaging tools for evaluating orthotics.

How can we improve the current practice?

Introduction to the session by the working group chairs: R. Minniti, R. Fulkerson & W. Culberson

Low Dose, Mini C-Arm Fluoroscopy for Hand and Foot Applications

Dr. Kevin Wilson, Hologic

Mini C-arms typically have low scatter radiation and are used primarily by extremity orthopedic surgeons, and to a lesser extent, by podiatric surgeons and emergency physicians. The mini C-arm is especially popular with hand and foot surgeons due to its small size and ease of use. Surgeons find that these devices help reduce procedure time, tourniquet time and time spent in the operating room compared with full size C-arms. This is due in large part to their ability to operate the system themselves versus having to utilize radiology staff. Outside of the operating room mini C-arms can be used to provide immediate imaging capabilities to help diagnose and reduce fractures of the extremities, remove foreign bodies, assist in castings or intra-articular injections. While mini C-arms can record fluoroscopic images, they are primarily utilized for still radiographic images. Most modern mini C-arms are based on digital plate technology and have an image receptor area of approximately 200 cm² and run at 30 frames per second. The FDA has special guidelines for mini C-arm x-ray fluoroscopic devices. By regulation, mini C-arms are limited to extremity imaging and must have a source to detector distance less than 45 cm and a source to skin distance of 10 cm or greater. Mini C-arm capabilities and examples of their uses will be presented with an emphasis on their applications for foot and ankle imaging.

Why Cone Beam CT Can Make 3D the Standard of Care in Extremity Imaging

Dr. Stuti Singh, Curvebeam

Cone Beam CT technology gives doctors access to 3D, dimensionally accurate images of osseous structures at the point of care at a relatively low radiation dose, where previous modalities would have been impractical primarily due to access and cost issues. The technology revolutionized the dental and maxillofacial industry, allowing for accurate assessment of conditions and planning of procedures in the specialty including orthodontic bite correction and dental implants. Presently, the recent advent of Cone Beam CT devices for upper and lower extremities has started a transformation in diagnosis, surgical planning, and post-operative analysis techniques for orthopedic doctors and podiatrists. These devices make it possible to perform 3D weight bearing imaging of the feet and knees, allowing for visualization of the biomechanics of lower extremities under load as never before. 3D weight-bearing images offer undistorted views to measure bone distances and angles as well as joint spaces. This new data is enabling specialists to challenge the conventional methods for classifying pathologies and develop new paradigms. The new Torque Ankle Lever Arm System (TALAS) analyzes the foot as a 3D tri-pod and calculates the forces that may throw this tripod out of alignment. A study of the joint spaces in the knees has helped advance the early detection of osteoarthritis. Assessment of post-operative scans allows a doctor to verify if bones have successfully fused and determine if a patient can safely bear weight on the foot. In addition, advances in the technology are providing cleaner images and new algorithms can correct for patient motion and metal artifact. Such advances will allow these devices to be viable tools for a wider pool of patients. Future advancements may even allow for bone density measurements and soft tissue visualization.

A quick overview of a weight bearing 3D imaging system for horses

Regina Fulkerson, Ph. D., RKF Consultants

Medical Applications Breakout Session IV: Proton Relative Biological Effectiveness (RBE)

Biological Responses of Therapeutic Ionizing Radiation and Charged Particles

Ramin Abolfath, Dept. Radiation Physics – MD Anderson Cancer Center

Biological systems are exceptionally complex. In particular, cancer progression and treatment present several challenges that require multi-scale modeling. In this talk, I briefly review practical and computational approaches in modeling the interaction of ionizing radiation with biological systems. Based on recent experimental data analysis, I will discuss that extensions to conventional mechanistic approaches are necessary to interpret and fit the observed RBE's as a function of dose and linear energy transfer (LET). I will discuss the possibilities in improving the current models and introduce a novel approach to enable studies the real-time DNA damage-repair pathway in the cell-survival biological endpoint *in-silico* to quantify the radiobiological effectiveness of proton and heavy ion beams. Specific goals for potential enhancements in therapeutic applications and treatment planning will be sketched. For illustration of the methodology, the predicted population of DSBs along the proton track with the highest occurrence frequency in the Bragg peak and a quantitative comparison demonstrating the agreement between theoretical predictions and more recently reported experimental data based on γ H2AX counting will be presented.

Proton Therapy National Ion Chamber Intercomparison

Paige Taylor, IROC Houston QA Center

With its Bragg peak dose deposition and potential for normal tissue sparing, proton therapy is rapidly increasing as a radiotherapy treatment modality. Several new proton centers open in the USA each year. The ICRU 59 report developed a calibration procedure for therapeutic proton beams, which was shortly followed by the IAEA TRS 398 calibration protocol. The ionization chamber intercomparison was an experiment with 11 proton therapy institutions. The goal was to compare various calibration protocols (ICRU 59, TRS 398, and any institution's customized calibration procedure) as well as the various ion chambers used by participating institutions. The dose per monitor unit (MU) was measured and calculated for simulated brain and prostate proton treatment fields. 11 thimble and 12 parallel plate ion chambers were used. For the ICRU 59 protocol, both the N_x and $N_{D,w}$ methods were used and dose per MU was calculated by the experiment organizers. The N_x method gave a smaller spread than the $N_{D,w}$ method (e.g. 1.0% 2σ versus 3.8% 2σ for the brain field). When institutions calculated their own dose per MU using the TRS 398 protocol, the spread of results for the same field was within 3.0%. When the organizers performed the TRS 398 calculation using the same raw data, the spread was within 2.3%. The TRS 398 protocol provides acceptable consistency for use with multi-institutional clinical trials. Several of the chambers did not have k_Q values defined by the protocols, so institutions had determined their own value or used one from a similar chamber. The spread of the dose per MU values could be reduced by using k_Q values of 1.014 for the Standard Imaging Exradin T1v2 and T1v3 thimble chambers, 1.010 for the PTW Markus TN23343 chamber, 0.997 for the PTW Advanced Markus TN34045 chamber, and 1.007 for the IBA PPC05 chamber.

Experimental Investigation of RBE as a Function of Dose and LET

Darshana Patel¹, Lawrence Bronk¹, Fada Guan¹, Christopher Peeler¹, Dragan Mirkovic¹, David Grosshans¹, Oliver Jäkel², Amir Abdollahi^{2,3}, Radhe Mohan¹ and Uwe Titt¹

¹The University of Texas MD Anderson Cancer Center, Houston, TX, ² Deutsches Krebsforschungszentrum (DKFZ), Heidelberger Ionentherapiezentrum (HIT), Heidelberg / Germany, ³ National Center for Tumor diseases (NCT), Heidelberg / Germany

Purpose: Investigate and quantify the effect of dose and LET on the RBE of Protons, Helium and Carbon ions.

Methods: A custom designed, high-throughput and high accuracy experimental design was employed to investigate the Relative Biological Effectiveness (RBE) dependence on dose and Linear Energy Transfer (LET) values for proton, helium and carbon ion beams. The experiment was conducted at the HIT facility in collaboration with the DKFZ in Heidelberg/Germany. Clonogenic assay of human lung cancer cell line, H460, was investigated in this study. The experimental setup was designed and optimized using the Geant4 Monte

Carlo toolkit incorporating the horizontal beam line design available at the HIT facility. Specific points along the Bragg curve corresponding to well-defined doses and LET values were chosen by appropriate selection of the pre-absorber thicknesses.

Results: Approximately 16,000 samples of cancer cells were irradiated during 23 hours of beam time. The preliminary results of the survival curves for both cell lines show a distinct dependence on LET for a given dose with decreased survival fractions at increasing LET values, encountered at the Bragg peak and in the distal falloff.

Conclusion: Our preliminary findings are indicative of the ability of this experimental setup in providing massive amount of data using our high-throughput experimental setup. This will be leading to deeper insights into the RBE of heavy ions for possible future heavy ion therapy facilities in the US.

Multi-Ion Analysis of RBE using the Microdosimetric Kinetic Model

Michael P. Butkus^{1,2} and Todd Palmer²

¹Yale School of Medicine, ²Oregon State University: Department of Nuclear Engineering

To better quantify the relative biological effectiveness (RBE) of potential ions to be used in hadron therapy, the PHITS Monte Carlo code paired with a microscopic analytical function was used to determine probability distribution functions of lineal energy in 0.3 μ m diameter spheres throughout a water phantom. Pencil beams of 0.6cm diameter for ⁴He, ⁷Li, ¹⁰B, ¹²C, ¹⁴N, ¹⁶O, and ²⁰Ne were simulated at energies that corresponded to physical Bragg peak depths of 50, 100, 150, 200, 250, and 300mm. The acquired probability distribution functions were scored every millimeter transversely, and in annuli with outer radius of 1.0, 2.0, 3.0, 3.2, 3.4, 3.6, 4.0, 5.0, 10.0, 15.0, 20.0, and 25.0mm and then reduced to dose-mean lineal energies and applied to a modified microdosimetric kinetic model for five different cell types to calculate RBE at the 10% survival threshold. The product of the calculated RBEs and the simulated physical dose was taken to create biological dose and comparisons were then made between the various ions. For all beams the radial fluctuations in RBE were less than 4.2% while physical dose was greater than 1% of the maximum dose. Transversely, for the 50mm depth beams ⁷Li was seen to provide the most optimal biological dose profile. However, at higher initial energies, fragmentation reduced the biological advantages of ⁷Li and ¹⁰B was seen to provide the most optimal biological dose profile, followed by ¹²C. The differences in these two beams reduced as initial energy was increased. Greater variance in cell-specific biological dose were seen for the more massive ions.

Monday March 27, 2017: Afternoon Radiation Protection Breakout Sessions

Radiation Protection Breakout Session I: Instrumentation

Aligning US Navy Dosimetry with NIST

Dr. Luis Benevides, Naval Surface Warfare Center, Carderock Division

The US Navy has 17 National Voluntary Laboratory Accredited Program accreditations in ionizing radiation passive Dosimetry. The US Navy utilizes a passive Thermoluminescent (TLD) dosimetry (LiF:Mg, Cu, P) manufactured by Thermo-Fisher Scientific consisting of a Harshaw 8840/8841 card and holder assembly. The NVLAP accreditation scope includes ANSI Standard 13.11-2008 category IA, IIA, IIIA, and IVAB and VCB for the whole body dosimeter. The challenge is to maintain this diverse distributed system aligned with our nation's standards. The US Navy achieves this by a rigorous program of calibration protocols, intercomparison and routine program reviews, the US Navy maintains secondary and tertiary calibrations throughout its network ensuring compliance with all applicable national standards.

IM-276/PD Next Generation Navy Battlefield Dosimeter – System Overview and Test Summary

Jeancarlo Torres, CHP, NSWCCD, West Bethesda, Md, Radiation Technology Group (RTG)

The Navy's current Battlefield Dosimeter is the IM-270/PD. As stated on the Navy's Radiation Health Protection Manual (NAVMED P-5055), the IM-270/PD dosimeter is a personnel accident dosimeter that uses metal oxide semiconductor field effect transistor (MOSFET) technology. This legacy Battlefield Dosimeter has limited capabilities such as; battery life, gamma only sensitive device, and a dynamic range that starts from 0.1 Gy (10 rads) to 10 Gy (1,000 rads). Due to ongoing battery failures and the limited radiological detection capabilities of the IM-270/PD, the Navy has recently acquired the IM-276/PD as a replacement and Next Generation Battlefield Dosimeter. An overview of the new dosimeter will be provided along with test results obtained from the ongoing acceptance testing.

The Future Direction of Passive Dosimetry

Joe Rotunda, Rotunda Scientific Technologies LLC

The concept of passive dosimetry was first discovered in 1663 and it took until the 1920s for it to be used in radiation measurements by Marie Curie during her research, just under 300 years later. Since that time many forms of passive dosimetry have been developed and commercialized. With the advent of miniature electronics, active personal dosimeters came on the scene and while the expectation that they would replace passive dosimetry they have not yet fulfilled that goal. Now the line between passive and active dosimetry is blurred with the introduction of the Direct Ion Storage devices. Other systems have now been developed that work in both passive and active mode. In this talk we will review the history and more importantly provide a vision of what the technologies and future might hold for passive dosimetry. This will include potential new requirements for Standards and calibration.

Radiation Protection Breakout Session II: Document Standards

Conformal Testing for Dosimeters against Prompt Neutron and Gamma Exposures

Dr. Chad McKee, Joint Project Leader for Radiological and Nuclear Defense; Dr. Chad Weaver, Joint Project Leader for Radiological and Nuclear Defense; Frank Andrews, SVAD, White Sands Missile Range; Dr. T.

Mike Flanders, SVAD, White Sands Missile Range

The Department of Defense has the mission not only to survive, but to operate and to win on a nuclear battlefield. For small tactical nuclear weapons (under 50 kT), the prompt radiation is one the most predominate causes of casualties, more than the blast wave and thermal (Ref. 1). Prompt neutrons result almost exclusively from the energy producing fission and fusion reactions, while prompt gamma radiation includes that arising from these reactions as well as that resulting from the decay of short-lived fission products (Ref. 1). Therefore, tactical dosimetry must accurately measure the dose from prompt events. Ensuring the dosimetry meets the accuracy requirements is challenging because of the significant ranges of

dose and spectrum, the limited number of test facilities capable of doing the tests, and the lack of rigorous traceability back to a national standard. The talk will focus on the challenges faced by the military in ensuring the accuracy of its dosimeters for such a unique radiation hazard. Reference 1. FM 8-9, NATO Handbook on the Medical Aspects of NBC Defensive Operations, 1996.

An Overview of Current US NAVY Alpha, Beta, Gamma, and Neutron Radiation Calibration Standards and the Processes Used to Ensure NIST Traceability

Keith D. Turner, P. E., NMCLANT Yorktown, VA., RADIAC Calibration Standards Program (RCSP)

U. S. NAVY Alpha, Beta, Gamma, and Neutron Radiation Detection, Indication and Computation (RADIAC) instruments and dosimetry devices require periodic calibration. The goal is to ensure both reliability and NIST traceable accuracy are evident in each calibrated RADIAC and ultimately provide end users with confidence in the device. Seven RADIAC Calibration Laboratories (RCLs) throughout the United States accomplish NIST traceable calibrations on the entire inventory of U. S. Navy RADIAC instruments. Calibrators located at each RCL are maintained and verified by the RADIAC Calibration Standards Program (RCSP) in Yorktown, VA. These alpha, beta, gamma, and neutron radiation calibrators provide data that is directly traceable to NIST. An overview of these calibrators and the processes used by the RCSP team to accomplish this goal is provided.

Pitfalls of Revising National Standards – A Portable Survey Instrument Standard (ANSI 42.17AC)

Meredith Wood, Naval Surface Warfare Center, Carderock Division

National Standards require periodic revision in order to reflect modern instrumentation characteristics and test methodologies. The revision process requires a critical eye—in addition to a thorough understanding of the original document—so that the standard can be updated to match the best practices available. Several members of the Radiation Technology Group at Naval Surface Warfare Center, Carderock Division (NSWCCD) along with representatives from commercial industry and other Government entities are developing a revised American National Standards Institute (ANSI) performance standard for radiation detection instrumentation (ANSI 42.17 AC). A discussion on the problems associated with updating a National Standard and advice for overcoming these issues will be provided within the context of the ANSI 42.17AC revision.

Tuesday March 28, 2017: Afternoon Radiation Protection Breakout Sessions

Radiation Protection Breakout Session III: Consequence Management

CDC's Need for Reference Materials to Validate Analytical Methods for Public Health Exposure Assessments after a Radiological or Nuclear Incident

Robert Jones, Center for Disease Control

One of the key tasks of responding to a radiological or nuclear incident is the capability and capacity of rapid screening and quantitative analysis of human clinical samples in order to direct short and long-term medical care. Without these rapid laboratory analytical results, exposures of health significance will likely be missed, medical treatment will be misguided and ineffective, and prevention of additional exposures will be impaired. It has been estimated from past radiological and chemical incidents, of national significance, that tens to hundreds of thousands of people may need to be screened and tested to determine their contamination/exposure to radiological materials to guide medical management. This has brought on the need to develop rapid analytical methods using a minimum amount of urine for the analytical tests due to the fact that only spot urine samples can be logistically collected in a public health emergency. This will enable the decision makers to have high quality data to make sound consequence management decisions and provide for the efficient and effective use of limited medical countermeasures. To ensure that these new rapid analytical methods are properly validated for both the identification and quantification of the radionuclides of interest, there is a critical need for both aqueous and clinical (urine) Certified and Standard Reference Materials (SRM and CRM) for both the validation and ongoing performance testing (PT) of these newly developed rapid analytical methods (radio-bioassays) to ensure the proper estimation of radiological contamination/exposure so that the correct medical management can be applied, if needed. These clinical

tests are regulated under the Clinical Laboratory Improvement Amendments of 1988, and that regulation requires an ongoing performance or proficiency testing (PT) process twice a year along with a required calibration verification twice a year. The validation, PT and calibration verification require materials of the highest quality to ensure that the bioassay testing results are of the highest quality for critical medical decisions. Therefore, both aqueous and clinical CRMs and SRMs containing the priority radionuclides (as determined by the federal interagency workgroups) are needed to ensure that this process has the materials needed to ensure the medical community receives the highest quality data, so that the limited medical countermeasures in the Strategic National Stockpile (SNS) are effectively used on the population that will need them the most. These CRMs and SRMs will be used by laboratories that will be analyzing clinical samples from hundreds to thousands of people suspected to be exposed to radiological materials. The specific needs of the Centers for Disease Control and Prevention (CDC) for CRMs and SRMs will be discussed.

**EPA's Needs for Radiological Reference Materials to Support Response and Recovery Activities
Following a Radiological or Nuclear Incident**
John Griggs, Environmental Protection Agency

In the event of a major radiological or nuclear incident such as multiple RDDs or an IND there will be hundreds of thousands of samples that will require laboratory analyses to protect human health and in general to support response, cleanup and monitoring activities. The samples will include typical environmental matrices such as air particulates, drinking water, waste water, soil and vegetation as well as urban matrices such as cement, brick, asphalt, etc. The demand for laboratory data to support decision making in a timely manner will be intense. Given the large number of samples involved a large number of laboratories will be called upon to analyze the samples and to provide data. It is critical that the laboratory data be both accurate, comparable, timely and defensible to support a range of response, cleanup and monitoring activities. Critical to the generation of accurate, comparable and defensible data is the availability of radiological reference materials to support method validation efforts, proficiency testing and quality control measures. It is essential that the radiological reference materials closely match the radionuclide/matrix combinations analyzed by the laboratories. In the absence of needed radiological reference materials there will be significant delays in laboratory data generation resulting in delays in decision making which could potentially negatively impact public health and result in even greater negative economic impacts due to delays in cleanup and restoration of normal operations in major cities.

**An Intercomparison Study on Radiological Methods Used by FDA Food Emergency Response
Radiological Laboratory Network**
Stephanie Healey, Food and Drug Administration-WEAC

Proven analytical methods and a competent laboratory network are essential for the Food and Drug Administration (FDA) to implement food defense and safety measures under the Food Safety Modernization Act (FSMA). With growing risks imposed by global aging nuclear facilities and proliferation of radioactive materials, FDA faces increasing challenges in safeguarding the nation's food supply from radioactive contamination. In order to mitigate the imposing threats to food safety and public health, a radiological food emergency response network (FERN) consisting of federal and state laboratories was established. This network serves to strengthen the FDA's ability to respond to a radiological emergency. FDA's decision-making during a nuclear emergency will be based on large pools of data from diversified analytical methods. Ambiguous findings will inhibit FDA's ability to take prompt action on protecting food safety and public health. Measurement capability, data comparability, and an efficient data reporting mechanism are essential for emergency response when analytical data from cooperative laboratories are used for post-incident risk assessment and management. To evaluate different radiological methods currently used by member laboratories for food analysis, intercomparison studies were conducted using water and various food samples containing mixed several radionuclides at different radioactivity levels. This presentation details the sample preparation and verification, insightful data analysis on evaluating method performance characteristics, recommendations for developing harmonized methods for food analysis, and future needs for radiological food reference materials and standards.

Radiation Protection Breakout Session IV: Consequence Management (continued)

Development of Rapid Liquid Scintillation Counting Method for determination of Tritium in Foods

Zhichao Lin, Food and Drug Administration-WEAC

Distillation technique was widely used as the simplest method for extraction of tritium (^3H) as a form of free water from various environmental, bioassay, and food samples. However, vacuum distillation of ^3H from foods is very time consuming and unsuitable for high throughput emergency response. This study investigated two different approaches for rapid determination of free-water ^3H , i.e., heating mantle distillation of food and purification of food extract by Eichrom's tritium column, followed by liquid distillation (LS) counting. A variety of fresh produce samples was spiked with ^3H and analyzed using the proposed procedures. For heating mantle distillation method, a total of 10 samples in each batch were distilled for approximately an hour and a half inside a radiological fume hood to further prevent the analyst from any untoward exposure to ^3H . Sample preparation and subsequent batch distillation process took approximately two hours for a total of 10 samples. Hence 40 samples could be prepared each day for counting. Each 8 mL sample mixed with 12 mL LS cocktail was counted for 100 minutes, well over the time required to reach the data quality objective of detection limit for ^3H in drinking water and food. However, for emergency response scenarios, a lower counting time would be deemed acceptable depending on the counting efficiency and background radiation level. For Eichrom's tritium column method, various food extracts were directly loaded on to the tritium column for obtaining ^3H counting samples. ^3H extracted from different food samples was determined using three different liquid scintillation spectrometers i.e., Quantulus 1220, TriCarb 3170 TR/SL, and Hidex 300 SL. Instrument settings, cocktail types, and sample parameters were studied and compared for enhancing ^3H analysis. Both internal and external laboratory control samples containing normal background and variable amounts of ^3H were analyzed to evaluate method performance characteristics. The developed method would provide an alternative approach to devise a more effective and efficient method for routine analysis and emergency response efforts.

Rapid Detection of Americium-241 in Food by Inductively-Coupled Plasma Mass Spectrometry

Zhichao Lin, Food and Drug Administration-WEAC

The recommended intervention level for ^{241}Am in food is 2 Bq/kg (16 pg/kg) as per FDA regulatory guideline. Detection of ^{241}Am in food based on its 59 keV photon emission by gamma ray spectrometry is impractical due to high photon mass attenuation and low maximum permissible concentration. A sensitive and rapid radioanalytical method is essential for ensuring and improving food safety compliance and emergency response. A quadrupole ICPMS coupled with an Aridus II desolvation nebulizer system was applied for analyzing ^{241}Am in a wide variety of foods following a simple radiochemical separation. Quantification of ^{241}Am in food was achieved by isotope dilution technique using ^{243}Am tracer. Eichrom's DGA resin was used for separation of ^{241}Am from sample matrices and isobaric interferences after sample mineralization. A 5-fold enhanced sensitivity for ^{241}Am was achieved by using a desolvation nebulizer and optimizing ion optics for achieving maximum ion transmission. The study results showed that the method has the ability to positively detect ^{241}Am in various foods at concentration of ~ 1 pg/kg (0.13 Bq/kg) and to quantify ^{241}Am at 1/3 of the recommended intervention level with accuracy better than $\pm 20\%$.

A Comparison of Computational Approaches for the Detection of Gamma-Emitting Radionuclides in Foods

Clarence Rolle, Food and Drug Administration-WEAC

Monday March 27, 2017: Afternoon Industrial Applications and Materials Effects Sessions

IAME Breakout Session I: Food Irradiation

Shedding light on food irradiation: A comparison with alternative food technologies

Anuradha Prakash, Chapman University

Globally, food irradiation is used primarily to eliminate disease causing microorganisms and extend shelf-life, and to a lesser extent to sterilize insect pests on fresh fruit and inhibit sprouting of root vegetables. A recent estimate suggests that 500,000 metric of food is currently irradiated worldwide, with China processing nearly 40% of that volume. In terms of growth areas, irradiation use for phytosanitary treatment of fruit has increased at a faster rate than any other use of food irradiation. In the last decade, volumes of fruit treated have increased year to year with exports directed primarily to the US. And even more recently, trade between trans-Pacific countries is picking up driven in large part by the phasing out of chemical fumigants. In this talk, I will discuss the various drivers for growth of phytosanitary irradiation. I will also offer a comparison of irradiation with other food technologies to highlight the benefits and challenges, as well as to identify the barriers that seem to preclude the growth of this technology for food safety in most markets.

Packaging for Irradiated Fresh Produce

Vanee Komolprasert, Food and Drug Administration

Ionizing radiation is an effective means for controlling foodborne pathogens and is applicable to fresh produce. The U.S. Food and Drug Administration permits the safe use of ionizing radiation for control of food-borne pathogens and extension of shelf-life in fresh iceberg lettuce and fresh spinach using energies not to exceed 4.0 kGy. However, the lack of suitable packaging materials is likely a factor that delays the commercialization of irradiated prepackaged fresh produce. Additionally, the irradiated foods are ready for shipping to the market immediately after irradiation. However, ionizing radiation can induce chemical changes to the packaging materials, which may result in the formation of breakdown products that may readily migrate into foods. Therefore, the packaging materials holding food being irradiated are required to undergo premarket authorization prior to use. This presentation discusses the Agency's current thinking in evaluating the suitability of packaging materials for use during ionizing radiation of prepackaged fresh produce.

IAME Breakout Session II: Nanomaterials

Nanomaterials Analysis and Standards

Michael T. Postek¹, Dianne L. Poster¹, Mark Driscoll², Jay LaVerne³, Mohammed Al-Sheikhly⁴

¹National Institute of Standards and Technology, Gaithersburg, MD, United States

²Chemistry, State University of New York College of Environmental Science and Forestry, Syracuse, NY, United States

³Department of Physics, University of Notre Dame, Notre Dame, IN, United States

⁴Department of Materials Science and Engineering, University of Maryland, College Park, MD, United States

Metrology and standards are critical to advanced manufacturing. This presentation will focus on the strong joint collaboration between NIST and its academic partners in pursuit of the demonstration of applied ionizing radiation to the manufacturing and characterization of novel nanomaterials. Included is the development of the necessary measurements and standards which are a key component to this success. Only through detailed dimensional metrology studies can the level of detail be obtained to further the growth of large scale radiation processing for plant materials. One of the major components of this research is nanocellulose. Nanocellulose is a high value material that has gained increasing attention because of its high strength, stiffness, unique photonic and piezoelectric properties, high stability and uniform structure. Nanocellulose can be produced in large volumes from wood at relatively low cost via radiation processing. Ionizing radiation

causes significant break down of the polysaccharide and leads to the production of potentially useful gaseous products such as H₂ and CO. Interestingly, the application of radiation processing to the production of nanocellulose from non-wood sources, such as field grasses, bio-refining by-products, industrial pulp waste, and agricultural surplus materials remains an open field, ripe for innovation and application. Elucidating the mechanisms of the radiolytic decomposition of cellulose and the mass generation of nanocellulose by radiation processing is key to tapping into this source array of nanocellulose for the growth of nanocellulostic-product development. More importantly, understanding the structural break up of the cell walls as a function of radiation exposure is key and only through the development of the necessary metrology and standards.

Tuesday March 28, 2017: Afternoon Industrial Applications and Materials Effects Sessions

IAME Breakout Session III: Dosimetry for High Dose Applications

New Design Basis Analysis for Self-Contained, Dry-Storage Irradiators

Spencer Mickum, Robert Rushton, Zachary Hope
Hopewell Designs Inc.

The present work explores the irradiation field parameters of a high dose rate research irradiator concept in comparison to the performance of a legacy irradiation system. A mainstay legacy irradiation system used internationally is the Gammacell 220 which is a self-contained, dry storage research irradiator developed in the late 1950s by Atomic Energy of Canada Limited and later Nordion. This system is capable of irradiating samples within a 20.47 cm tall by 15.49 cm diameter cylindrical chamber at Co-60 activities approaching 24kCi (nominally, 1.75 Mrad/hr). This talk includes an overview of the overall modeling effort, Gammacell 220 irradiation field performance, estimates of an improved irradiation design baseline and expected irradiation chamber dose uniformity ratio and absolute exposure rates for the new concept irradiator. Several high-fidelity monte-carlo models utilizing the Los Alamos National Laboratory MCNP N-particle transport code (MCNP6) were developed for this investigation. As a technical starting point, estimates of the Gammacell 220 irradiation field parameters were modeled to determine dose uniformity ratios and absolute exposure rates achieved by the system. The dose uniformity figure of merit was revisited as an applicable metric to determine if it provides sufficient details for categorizing irradiation chamber performance. Furthermore, a new design basis analysis for self-contained, dry-storage irradiators was examined. The new approach provides insight to the field uniformity of the irradiation chamber as a function of the symmetric field lines.

Students' Abstracts

CIRMS Student Travel Grant – sponsored by ASTM International

Vacuum Current: A Possible Systematic Error in Absolute Dose/Kerma Measurements with Ion Chambers (Poster 1)

Alexandra Bourgouin¹, Malcolm McEwen²

¹Carleton University, Ottawa, Ontario, K1S 5B6, Canada

²Ionizing Radiation Standards, National Research Council of Canada, Ottawa, Ontario, K1A 0R6, Canada

Purpose: The output of an ionization chamber is assumed to be uniquely due to ionization from the air within the cavity. However, in the 1950s and '60s, a 'vacuum' current' (V_c) consisting of slow electrons emitted from the electrodes, was observed and investigated. The effect was ignored for several decades, considered to be not significant or cancelling between chamber calibration and use. In the mid-2000s it was investigated again by LaRussa *et al*, using for kV x-ray beams, and McEwen *et al* (2010) carried out preliminary research in high-energy electron beams. This work expands on that previous investigation with the aim of obtaining high-quality and high-resolution data.

Methods: Five different ionization chambers (ICs) were used: 3 Farmer-type and 2 parallel-plates. Each ion chamber was positioned in a vacuum vessel where the ambient air pressure was varied from 0.1 to 1.0 atmosphere. Three different radiation fields were used (^{90}Sr , ^{60}Co and high energy electron beams from an Elekta Precise linac). A protocol was developed to ensure that the air pressure and temperature within the chamber cavity was at equilibrium with the measured vessel pressure and temperature, and measurements were repeated to verify consistency. The measurement set-up was then reproduced using the EGSnrc Monte Carlo system for comparison.

Results: Analysis of the data obtained indicated that at least three effects were contributing to the ion chamber response:

- i) A change in the energy deposition due to the variation in air density (ideal gas law, P_{TP}).
- ii) A variation in the dose deposition dependent with air pressure due to IC design characteristics (P_{MC} , determined from Monte Carlo calculation).
- iii) A pressure-independent effect, interpreted to be the 'vacuum' current (V_c) proposed by Greening *et al* (BJR, 1954).

The 'vacuum' current is extracted from measurement data and is shown in Table 1.

Table 1: Vacuum current for all IC, beams and polarities.

Type Ion Chamber	Model	Sensitive volume cm^3	Vacuum ion current (%)				
			^{90}Sr	^{60}Co	4 MeV	18 MeV	22 MeV
Parallel-Plane	PTW - Markus	0.055	0.17	0.26			
	PTW - Roos	0.35	0.06	0.14			
Cylindrical	PTW - 30013	0.60	0.16	0.05			
	IBA - FC65G	0.65	0.19	0.40			
	Exradin - A19	0.62	0.46	0.12	0.74	1.02	0.98

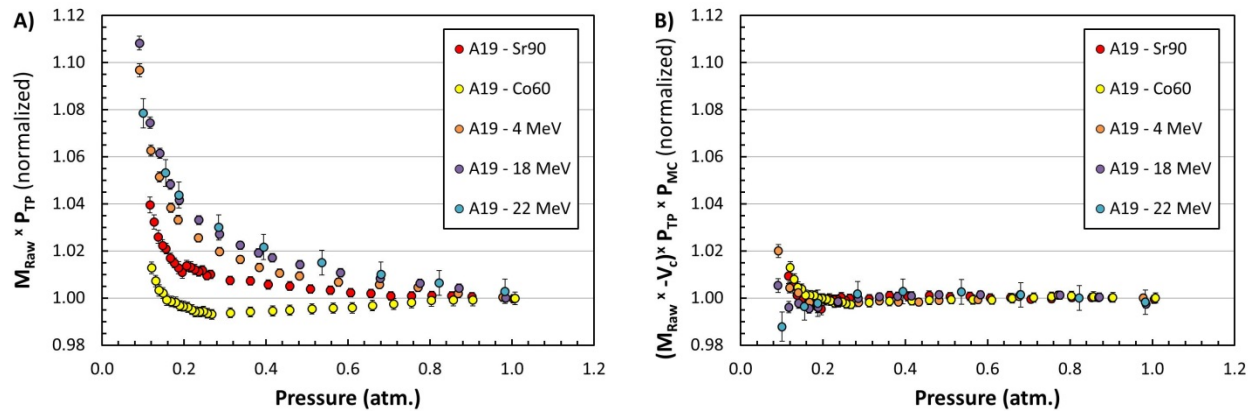


Figure 1: Farmer chamber results (M_{Raw}) corrected for pressure using A) temperature-pressure correction factor, P_{TP} ; and B) P_{TP} together P_{MC} and the vacuum current, V_C .

Conclusion: A signal that is consistent with the 50-year-old concept of a vacuum current has been measured and found to be significant when considering the stated uncertainties in primary air kerma determinations in photon beams. However, secondary instruments that are calibrated against a primary standard will only show a differential effect, e.g. due to small pressure (altitude) differences, which, for the chamber types investigated here, should be less than 1%. It is often assumed that ionization chambers are old technology and therefore well understood, but there is clearly still much in their functioning that is not fully explained.

CIRMS Student Travel Grant – sponsored by Hopewell Designs, Inc.

Aerrow: A Probe-Format Graphite Calorimeter for Use as a Local Absorbed Dose Standard for High-Energy Photon Beams in the Clinical Environment (Poster 2)

James Renaud – McGill University, Canada

The Past: For more than sixty years, calorimeters of various designs have been applied to radiation dosimetry. Owing to a myriad of technical refinements achieved over this time, calorimeters now form the basis of primary absorbed dose standards in many countries around the world. To date, calorimeter designs have primarily been driven by national metrology institutes, whose principle motivation is to achieve the lowest possible measurement uncertainty. Utility and usability of the devices are secondary considerations, and as a result, most calorimeters today are generally both bulky and fragile, and are operated by only handful of individuals possessing the required specialized equipment and tacit knowledge.

The Present: Clinical reference dosimetry of high-energy photon beams is generally based on calibrating ionization chambers in a standard ^{60}Co field. The emergence of specialized and non-conformal radiation delivery modalities incapable of producing a standard reference field has prompted the development of methodologies to adapt reference dosimetry traceability to smaller clinical fields. As a more direct alternative method to realize absorbed dose in non-standard fields, new transportable graphite and water calorimeters are being developed to permit operation at the user's facility. Despite their aforementioned advantages over other dosimetry systems, calorimeters have yet to be incorporated into regular clinical use.

The Future: Mainstream calorimetry for the radiotherapy clinic is no longer a matter of 'if', but 'when'. It is unrealistic to expect a dose standards laboratory to possess (or even have access to) every specialized and non-conventional radiotherapy modality that is brought to market. In the long run, it will be more practical for standards laboratories to perform some dose calibrations directly in the user's beam with a calorimeter transfer standard, such as the one presented in this work.

Purpose: The aim of this project is to design, develop, and fabricate a practical, mass-producible calorimeter system for the absolute determination of the delivered dose in the radiation therapy clinic. To this end, an

ionization chamber-sized calorimeter prototype (Aerrow; patent filing no. PCT/CA2013/000523; Figure 1) has been built, characterized, and successfully benchmarked against current clinical absorbed dose standards. My short-term career goal is to champion the first successful commercial translation of absorbed dose calorimetry from the standards laboratory to the clinical environment.



FIG. 1. The comparable size of the Aerrow to that of a Farmer-type ionization chamber is illustrated by the Exradin A12 positioned alongside the probe calorimeter (internal Aerrow structure is shown as a blended rendering) and a 5-cent coin (21 mm wide) for scale.

Methods: In contrast to nearly all other graphite calorimeters, the Aerrow design (Figure 2) incorporates aerogel-based material as opposed to a vacuum to achieve thermal isolation from the surrounding environment. This design choice was made to simplify the assembly process, to maximize the compactness, and to improve the structural robustness of the device.

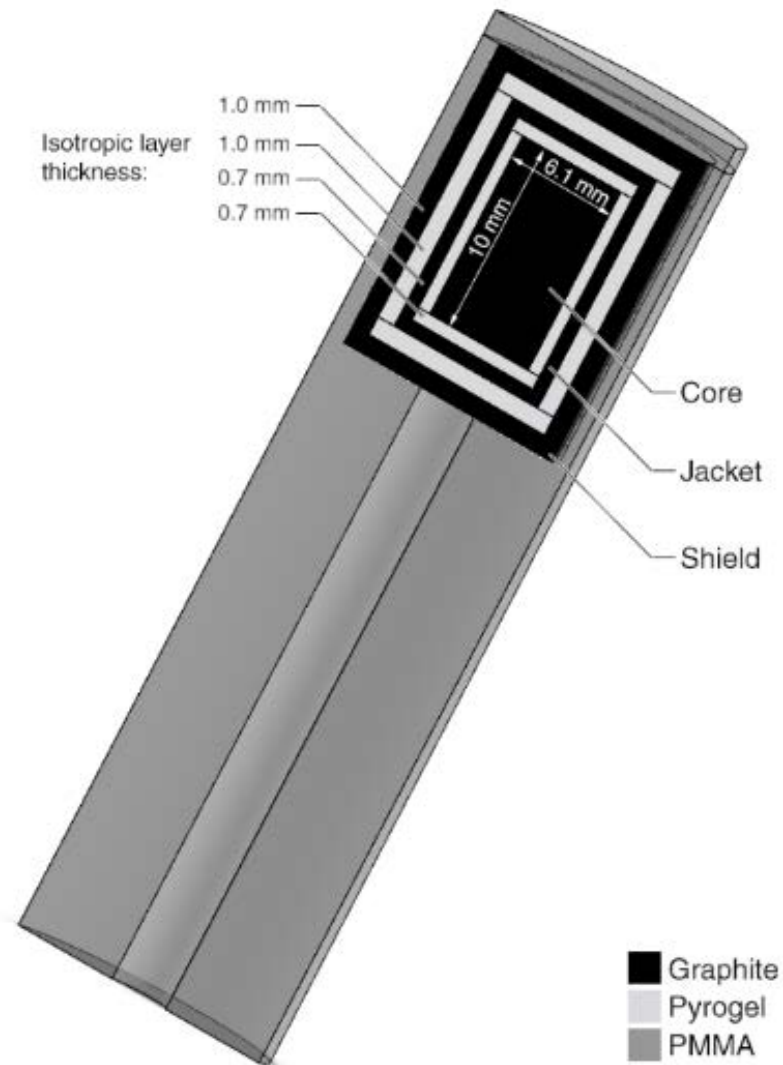


FIG. 2. A cross-sectional schematic diagram of the Aerrow design. The graphite components of the calorimeter are arranged in a nested cylindrical geometry and are separated by a 0.7 mm and 1.0 mm isotropic layer of aerogel-based thermal insulation (Pyrogel).

The Aerrow operates isothermally, meaning that each graphite component is maintained at a constant set point temperature throughout operation, and absorbed dose determination is based on an electrical substitution method. Under irradiation, a constant temperature is maintained by reducing the rate of electrical energy dissipated in the detector by an amount equal to the rate of energy deposited by the radiation (Figure 3). By integrating the electrical power deficit over the timespan of irradiation, the total deposited radiation energy, and hence the dose, can be derived.

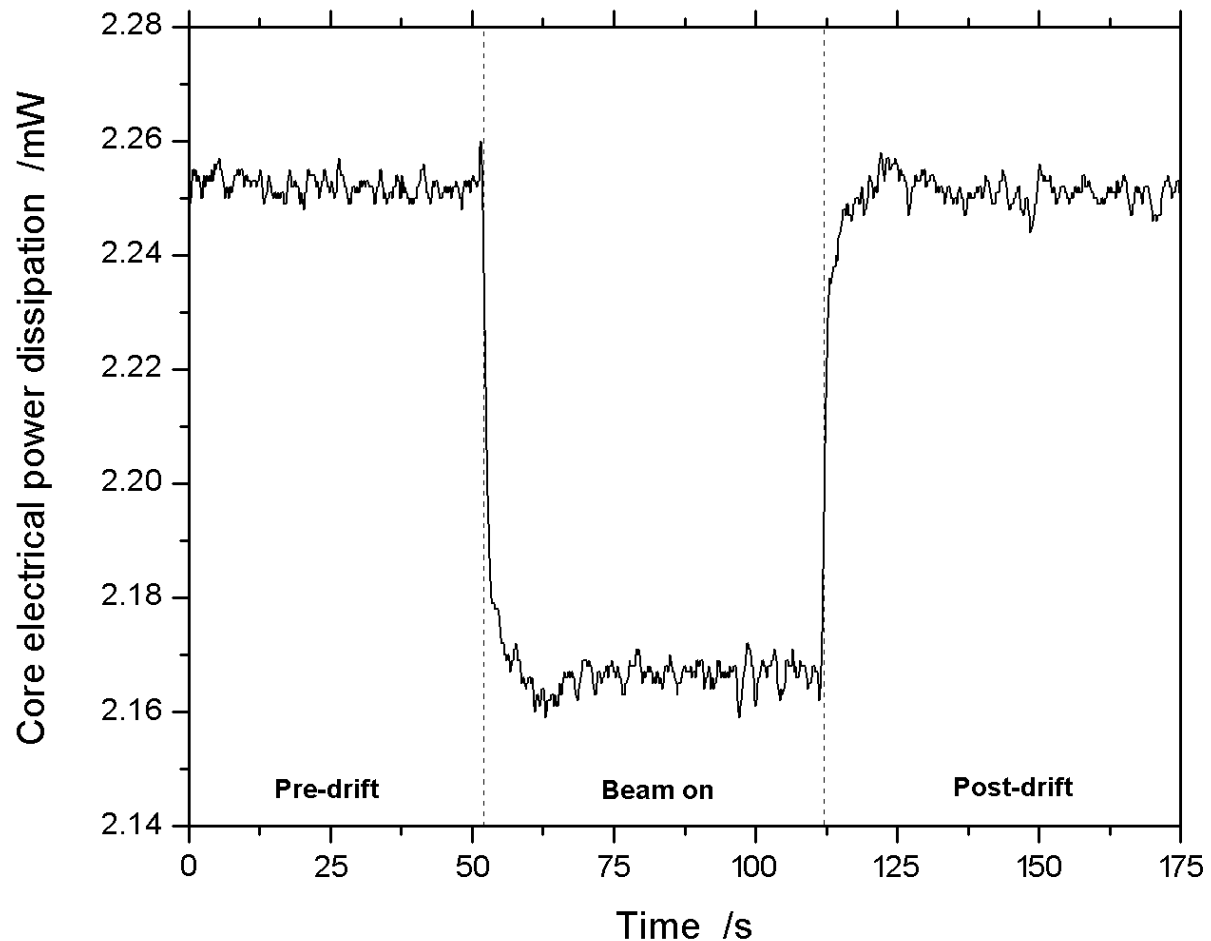


FIG. 3. Example of a 60 s isothermal mode measurement acquired using the Aarrow in a 6 MV photon beam at a dose rate of approximately 7.5 Gy/min. During the beam on period, a decrease in the electrical power dissipated in the sensitive volume resulting from the addition of a radiation-induced energy contribution is recorded. This power deficit is directly proportional to the absorbed dose rate.

Results: In one experiment, the Aarrow was used to measure the absolute output of five high-energy photon beams, under reference conditions, in a water equivalent phantom. These results were directly compared to the output measured using a calibrated reference class ion chamber (Figure 4). Overall, statistically significant agreement was observed for all output measurements. The error bars in Figure 4 reflect the combined standard uncertainty (0.9 %; $k = 1$) for both measurement techniques.

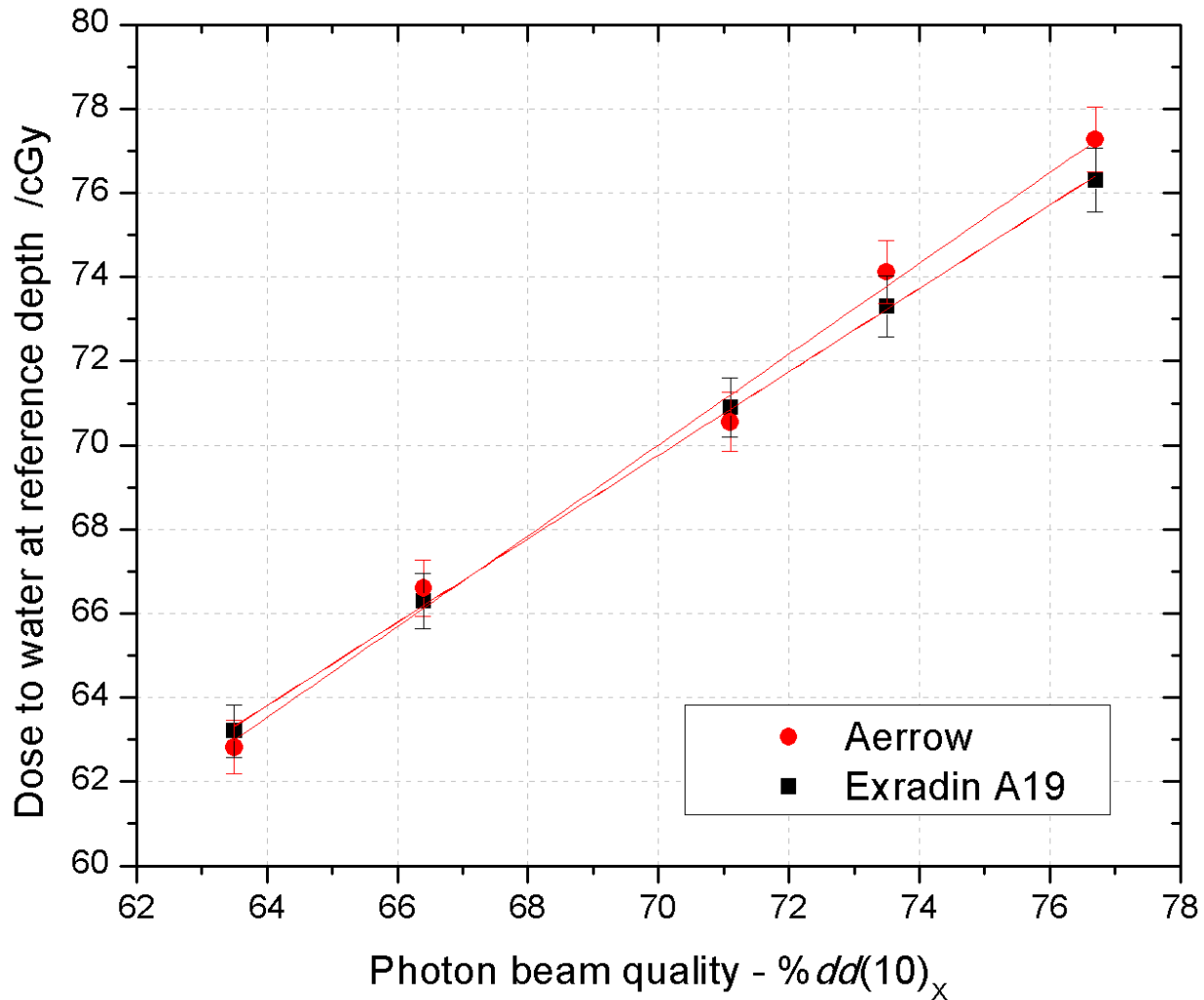


FIG. 4. A comparison of output measurements for five high-energy photon beam qualities at a depth of 10 cm, as determined with the Aerrow operating in isothermal mode and a reference class ionization chamber (Exradin A19). Statistically significant agreement is seen for all included beams. On average, the Aerrow measured an output 0.3 % greater (range: -0.6 % to 1.3 %) than that derived from the chamber.

Conclusion: Within combined uncertainties, the doses to water measured with the Aerrow in the clinical photon beams are in good agreement with those derived from TG-51 using a calibrated reference class ionization chamber. Collectively, these results demonstrate the feasibility of measuring absolute clinical photon doses to within a 2 % accuracy using this type of probe-format calorimeter. This is an important finding, as currently, there is no other means of realizing absolute dose to water outside of the established primary dose standard calibration chain. Furthermore, no other calorimetry-based technology suitable for mainstream use has ever been shown to be a potential independent alternative to ionization chambers for clinical reference dosimetry. Keeping that in mind, any mainstream adoption of calorimetry by physicists in the radiotherapy clinic will necessitate a high degree of dependability, robustness, and a relative ease of use (*i.e.*, practicality) on the part of the detector.

Collaborators: Dr. Jan Seuntjens, McGill University
 Dr. Arman Sarfehnia, University of Toronto
 Julien Bancheri, McGill University

**Measuring Radiation Dose through the Detection of Radiation-Induced Acoustic Waves
(Poster 3)**

Susannah Hickling^a, Hao Lei^b, Maritza Hobson^a, Issam El Naqa^{a,c}

^a Medical Physics Unit, McGill University, Montreal, Canada

^b Department of Mechanical Engineering, University of Michigan, Ann Arbor, USA

^c Department of Radiation Oncology, University of Michigan, Ann Arbor, USA

Purpose: It has been proposed that detecting the acoustic waves induced following irradiation by a clinical linear accelerator (linac) can be used as a radiotherapy dosimetry technique. The rapid deposition of heat energy following a pulse of linac irradiation causes a temperature increase and thermoelastic expansion, resulting in the induction of a differential pressure distribution and the propagation of acoustic pressure waves via the thermoacoustic effect. By detecting these acoustic waves at various angles surrounding the irradiated region, an image of the induced pressure distribution can be reconstructed. This imaging modality is called x-ray acoustic computed tomography (XACT)¹. Since the induced pressure distribution can be related to radiation dose using thermoacoustic principles, it has been proposed that XACT could be a useful dosimetry technique. While the feasibility of XACT as a dosimetry technique has previously been demonstrated through simulations², experimental work has been limited to detecting the acoustic waves induced following irradiation of metal blocks³. This work aims to experimentally investigate XACT as a tool for relative water tank dosimetry.

Methods: Acoustic waves induced in a water tank irradiated with a clinical linac were detected using an immersion ultrasound transducer. Signals were acquired every 6° surrounding the radiation field and an XACT image was reconstructed using a back projection algorithm. XACT images were formed for a variety of radiation field sizes and shapes. Based on the thermoacoustic wave equation, these XACT images are relative dose images. Therefore, relative dose information was extracted directly from XACT images and compared to established radiotherapy dosimetry techniques, such as ion chamber (IC) and film measurements. A previously developed simulation workflow² to model XACT was used to help interpret experimental results and identify factors affecting XACT image accuracy.

Results: XACT images were found to closely reproduce the shape of a variety of radiation fields. For a 4 cm x 4 cm radiation field, the normalized root mean square error when comparing 2D XACT and film dose distributions inside the field region was 12.2%. Fig. 1 demonstrates the ability of XACT to image a puzzle piece shaped radiation field. Fig. 1a displays the field shape as defined by the linac multi-leaf collimators. Fig. 1b and Fig. 1c show the experimental and simulated XACT images, respectively. Profiles were extracted from the XACT images along the x-axis at Y=-15 mm and compared to ion chamber (IC) measurements in Fig. 1d. When comparing the experimental XACT profile to the simulated XACT and IC profiles in the collimator defined field size region from -35 mm to +35 mm, the normalized root mean square errors were 17.2% and 10.9%, respectively. Through simulations, it was found that transducer central frequency and bandwidth, linac radiation pulse length and reconstruction algorithm can affect the accuracy of dose information extracted from XACT images. The accuracy of the experimental XACT images obtained in this work could likely be improved using a focused transducer with a larger bandwidth, as well as decreasing the length of the linac radiation pulse.

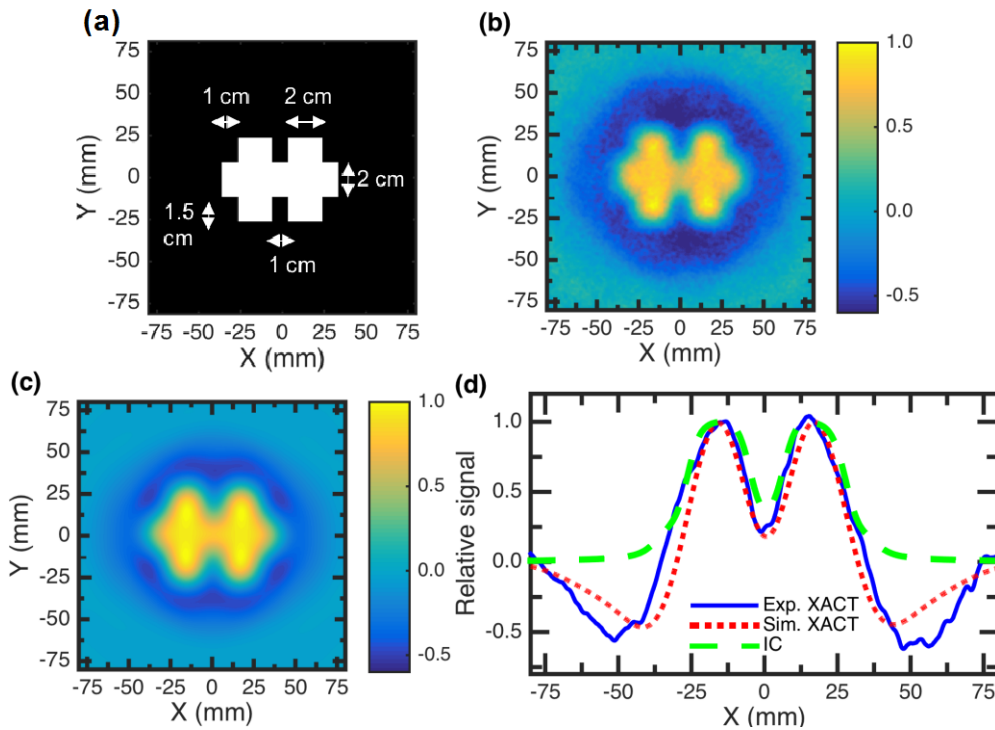


Fig. 1. (a) Block diagram showing the radiation field, where the white region represents the primary beam. (b) Experimental and (c) simulated XACT images of the field at 10 cm depth. (d) Comparison of profiles extracted from experimental and simulated XACT images to IC measurements along the x-axis at $Y=-15$ mm.

Conclusion: While further work is required to improve the accuracy of XACT prior to clinical implementation, this work has provided the first experimental demonstration of the feasibility of using XACT for relative water tank dosimetry. Some of the advantageous characteristics of XACT for dosimetry applications include the fact that it is inherently a 3D technique, has the potential to be real time, does not perturb the radiation beam, and could be combined with diagnostic ultrasound imaging to overlay dosimetric information on an anatomical image. XACT has the potential to be a useful dosimetry tool that could fill various existing clinical needs, such as 3D dose mapping, small field dosimetry, and *in vivo* dosimetry.

This project is of interest to the CIRMS community since it deals with applying a fundamental physical phenomenon, namely the thermoacoustic effect, to measuring ionizing radiation for radiation dosimetry applications. The 2016 CIRMS Needs Report indicated the need for “Standards for Small Fields in External Beam Therapy” and “3D Dosimeters for Non-Standard External Beam Therapy Dosimetry”. While further developments are required, XACT-based methods have the potential to fill such roles. In theory, the amplitude of detected pressure waves can be quantitatively related to dose in absolute terms using the thermoacoustic wave equation. Therefore, XACT could be used for absolute dosimetry purposes and be a stand-alone standard measurement technique, although this has not yet been investigated. This research fits in with the conference theme of “Past, Present & Future of Ionizing Radiation Measurements and Standards” since discussion with other conference attendees on how current methods of measuring ionizing radiation were developed in the past will help guide the evolution of XACT into a viable technique that can be used clinically and in standards labs in the future.

Following the completion of my PhD, I intend to pursue a career combining both research and clinical medical physics. In particular, I am interested in the experimental development of new techniques based on fundamental physics principles. This PhD project has been an excellent opportunity for me to undergo that process, namely using thermoacoustic principles and applying them to radiation dosimetry.

References

- [1] L. Xiang, B. Han, C. Carpenter, G. Pratz, Y. Kuang and L. Xing, *Med. Phys.* **40**, 010701 (2013).
[2] S. Hickling, M. Hobson and I. El Naqa, *Int. J. Rad. Biol. Phys.* **90**, S843 (2014).
[3] S. Hickling, P. Leger and I. El Naqa, *IEEE Trans. Ultrason. Ferroelectr. Freq. Control.* **63**, 683 (2016).

CIRMS Student Travel Grant – sponsored by Landauer Inc.

Dose Distribution Measurements of a New Directional Pd-103 Low-Dose Rate Brachytherapy Source (Poster 4)

Manik Aima¹, Larry A. DeWerd¹, Wesley S. Culbertson¹

¹University of Wisconsin Medical Radiation Research Center, Madison, WI

Purpose: A new directional low-dose rate (LDR) brachytherapy source called the CivaSheet™ has been developed by CivaTech Oncology, Inc. (Durham, NC). The CivaSheet is a planar source comprised of an array of discrete directional elements called “CivaDots.” Each CivaDot contains radioactive Pd-103 isotope held within a polymer capsule. The capsule also consists of a gold shield that attenuates radiation on one side of the device, and thus helps in defining the hot and the cold sides of the device. The source geometry and design for the CivaSheet vary significantly from conventional LDR brachytherapy sources. Guidelines and dosimetric formalisms have been recommended by the American Association of Physicists in Medicine (AAPM) for conventional LDR sources.¹⁻⁴ Currently, there is no standard protocol for planar or directional LDR sources. The use of AAPM Task Group No. 43 update (TG-43 U1) proposed formalism¹ is precluded due to the directional as well as planar nature of the CivaSheet array. Additionally, gold shield x-ray fluorescence is observed in the CivaDot energy spectrum. Thus, a thorough investigation needs to be conducted to ascertain the source strength and the dosimetric characteristics of the source prior to its clinical use. Previous work by the authors addressed the source strength determination for a CivaDot.⁵ This work aims to help in the dosimetric characterization of the CivaDot by performing in-phantom dose distribution measurements, and using Monte Carlo simulations.

Materials and Methods: Figure 1 is an illustration of the CivaDot, consisting of a polymer capsule with epoxy sealing containing Pd-103 and a gold shield, encased within a bioabsorbable membrane.

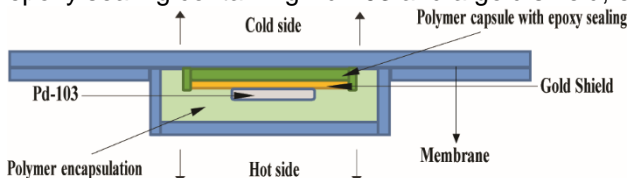
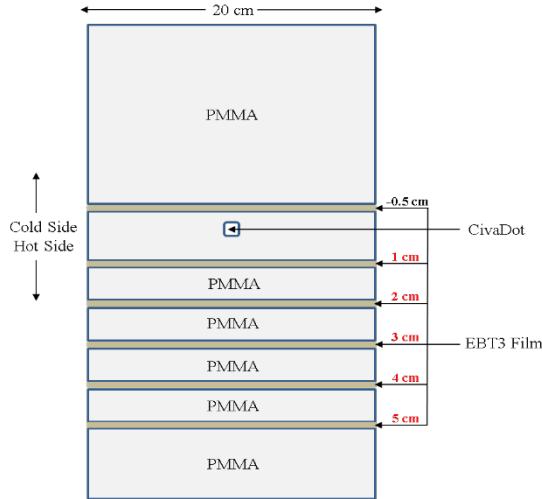


Figure 1: An illustration of the CivaDot with its components in a cross-sectional view.⁵

A Polymethylmethacrylate (PMMA) phantom was designed to perform dose-to-water measurements of the CivaDot using Gafchromic™ EBT3 film manufactured by Ashland, Inc. (Convington, KY). Figure 2 is an illustration of the PMMA phantom (20×20×12 cm³) setup used for these measurements. The CivaDot source was placed in the center of the phantom, and six EBT3 films (12×12 cm²) were irradiated simultaneously along its central axis at various depths. Five EBT3 films were placed on the hot side of the source (1, 2, 3, 4, 5 cm) and one on the cold side of the source (0.5 cm). For conventional brachytherapy sources, this measurement is usually performed on the source transverse axis. The orientation was adapted to an on-axis measurement considering the directional as well as planar nature of the CivaDot. Air-kerma strength was determined for these sources using the University of Wisconsin Variable-Aperture Free-Air Chamber (UW VAFAC)⁶ and methods outlined by Aima *et al.*⁵



(1)

Figure 2: A cross-sectional illustration of the PMMA film stack phantom setup for the CivaDot dose distribution measurements, using six Gafchromic EBT3 films placed at different depths on the source cylindrical axis. The illustration is not to scale.

The dose-to-water rate for the CivaDot for a given region of interest using the EBT3 film measurements can be determined with the implementation of Equation 1. The EBT3 films were read out using an EPSON 10000XL flatbed scanner. A calibration curve was determined for these measurements by irradiating additional films using the University of Wisconsin NIST-matched M40 x-ray beam (effective energy: 19.2 keV, 40 kV_p). A total of sixty-two dose-to-water values were used for the calibration curve, with four films irradiated for each dose. The CivaDot source and the phantom setup were modeled using the Monte Carlo N-Particle Transport Code 6 (MCNP6) version 1.0. The phantom/detector corrections were calculated using MCNP6. The intrinsic-energy correction value for this measurement was assumed to be unity based on the findings of Morrison *et al.*⁷ and Chiu-Tsao *et al.*⁸

$$\begin{aligned}
 (\dot{D}_{\text{water}})_{\text{water}}^{\text{CivaDot}} &= \frac{\lambda}{(e^{-\lambda t_1} - e^{-\lambda t_2})} \\
 \frac{(\text{netOD}_{\text{EBT3}})_{\text{phantom}}^{\text{CivaDot}} \cdot f((D_{\text{water}})_{\text{Cal}}^{\text{M40}}, (\text{netOD}_{\text{EBT3}})_{\text{Cal}}^{\text{M40}})}{\downarrow \text{Measurement}} & \cdot \frac{(\frac{(D_{\text{EBT3}})_{\text{phantom}}^{\text{CivaDot}}}{(M_{\text{EBT3}})_{\text{phantom}}^{\text{CivaDot}}}) \cdot (\frac{(M_{\text{EBT3}})_{\text{Cal}}^{\text{M40}}}{(D_{\text{EBT3}})_{\text{Cal}}^{\text{M40}}})}{\downarrow \text{Intrinsic-energy correction}} \cdot \frac{(\frac{(D_{\text{water}})_{\text{water}}^{\text{CivaDot}}}{(D_{\text{EBT3}})_{\text{phantom}}^{\text{CivaDot}}}) \cdot (\frac{(D_{\text{EBT3}})_{\text{Cal}}^{\text{M40}}}{(D_{\text{water}})_{\text{Cal}}^{\text{M40}}})}{\downarrow \text{Phantom/Detector correction}}
 \end{aligned}$$

where the notation is $(X_{\text{material}})_{\text{Geometry}}^{\text{Source}}$, D is dose, netOD is the net optical density, f is the calibration curve fit converting netOD to dose, λ is the Pd-103 decay constant and t_1 , t_2 are start and stop irradiation times, respectively.

Results: The measured dose-to-water distribution results of a CivaDot source (normalized to maximum dose value) at distance of 1 cm away from the source (hot side) are shown in Figure 3a. The measured dose-to-water distribution of the CivaDot was compared to the corresponding Monte Carlo predictions at the six depths measured in phantom. Figure 3b shows the results of the pixel-by-pixel difference map of the measured and the predicted dose-to-water distribution of the source at 1 cm depth. As observed in the figure, most differences were within 2–3%, with maximum differences up to 5%. Thus, good agreement was observed between measured and Monte Carlo predicted dose distributions given the overall uncertainty. Preliminary determination of the CivaDot dose-rate constant (DRC) analog was also performed. The difference observed between average measured DRC analog using EBT3 film from the MCNP6 predicted value was about 0.6% with a standard deviation of 2.3% for eight different CivaDot sources. Future work will involve the determination of other TG-43 analog dosimetric parameters such as analog radial dose function and source anisotropy functions. The parameters will be compared to Monte Carlo calculations and the feasibility of an adapted TG-43 dosimetric formalism will be tested.

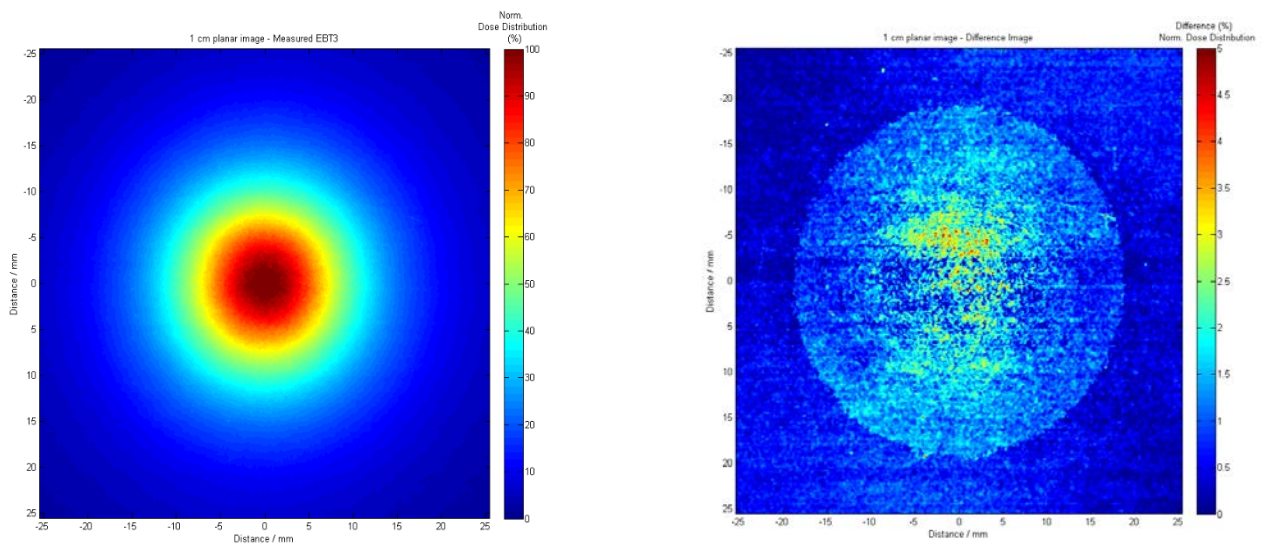


Figure 3: (a) The results of the CivaDot planar dose distribution measurement using EBT3 film at 1 cm away from the source along its cylindrical axis on the hot side of the device. (b) Difference in the measured dose distribution and the predicted dose distribution (MCNP6) at 1 cm. Please note that both the figures have been normalized to the maximum dose value.

Conclusions: Preliminary dose distribution measurements of the CivaDot using the EBT3 film stack PMMA phantom, and its subsequent comparison to Monte Carlo predicted dose distributions were encouraging. This work will aid in the eventual realization of a clinically viable dosimetric framework for the CivaSheet.

Relevance to CIRMS mission and first author’s goals:

This work is a subset of the doctoral work pursued by the first author based on the dosimetry of planar and directional brachytherapy sources. The first author currently works in a laboratory focused on the science of measurement and aims to become an academic/clinical medical physicist in the future. This work helps to better educate the author about the role of NIST in maintenance of primary ionizing radiation standards and the procedure of calibration as well as dosimetric characterization of a new brachytherapy source for clinical use.

References:

1. M. J. Rivard *et al.*, “Update of AAPM Task Group No. 43 Report: A revised AAPM protocol for brachytherapy dose calculations,” *Med. Phys.* 31 (3), 633–674, 2004.
2. R. Nath *et al.*, “Code of practice for brachytherapy physics: Report of the AAPM Radiation Therapy Committee Task Group No. 56,” *Med. Phys.*, 24 (10), 1557–1598, 1997.
3. W. M. Butler *et al.*, “Third-party brachytherapy source calibrations and physicist responsibilities: Report of the AAPM Low Energy Brachytherapy Source Calibration Working Group,” *Med. Phys.*, 35 (9), 3860–3865, 2008.
4. L.A. DeWerd *et al.*, “Calibration of multiple LDR brachytherapy sources,” *Med. Phys.*, 33 (10), 3804–3813, 2006.
5. M. Aima *et al.*, “Air-kerma strength determination of a new directional ¹⁰³Pd source”, *Med. Phys.* 42 (12), 7144-7152, 2015.
6. W.S. Culberson *et al.*, “Large-volume ionization chamber with variable apertures for air-kerma measurements of low-energy radiation sources,” *Rev. Sci. Instrum.*, 77 (1), 015105, 2006.
7. H. Morrison *et al.*, “Radiochromic film calibration for low-energy seed brachytherapy dose measurement,” *Med. Phys.*, 41 (7), 072101–1–11, 2014.
8. S.T. Chiu-Tsao *et al.*, “Dosimetry for ¹³¹Cs and ¹²⁵I seeds in solid water phantom using radiochromic EBT film,” *Appl Rad Isot*, 92, 102 – 114, 2014.

Reduction of Graphene Oxide via Electron Beam Irradiation Characterized by Structural and Resistivity Changes (Poster 5)

Jonathan Boyd, Roberto Uribe-Rendon
Kent State University

Purpose: Graphene is a fascinating material with exceptional properties and promises much technologic advancement, from more efficient solar cells to higher capacity batteries. Currently the use of graphene in commercial products is limited due to the difficulty of obtaining large pure sheets. Another material, graphene oxide, is similar to graphene except oxygen-containing functional groups are attached to the carbon lattice. The structural differences are shown in figure 1 below.

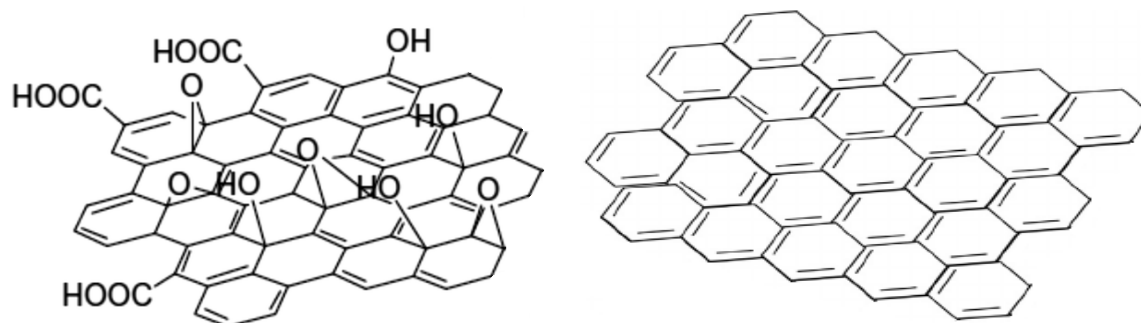


Figure 1: Graphene Oxide (left) and pure graphene (right)

Graphene oxide can be created in a lab by using a mix of acids to dissolve pieces of graphite. The functional groups attached to the Carbon lattice of graphene oxide reduce the electrical conductivity, one of the most desired properties of graphene. If these groups could be partially or fully removed from the material would possess properties closer to those of pure graphene. This process of removing oxygen groups is known as reduction and the final product is aptly called reduced graphene oxide. Other methods have successfully created reduced graphene oxide, the most notable being reduction with hydrazine vapors. Although successful, it takes up to 60 hours for maximum effectiveness, can let behind nitrogen impurities, and the byproducts from such a reduction are harmful. Other methods currently possess their own drawbacks, leaving many to look for better alternatives. We aim at investigating if radiation from an electron beam accelerator could reduce graphene oxide in a fast, safe, and controlled manner. This is a tried and tested technology that has been around for many years and already has industrial applications from crosslinking plastics to food sterilization. We hope that the technology can find a new use in creating materials for a new generation of products.

Methods: Samples of pre-prepared graphene oxide solution (from Graphene Supermarket Inc. USA) were deposited on glass slides, some of which were partially coated in Indium tin oxide. The slides were then put in an oven to bake at 65°C for around an hour to drive off the water from the solution. This temperature was well below the temperature range of possible thermal reduction (Seung Hun Huh) and was only intended to leave a thin coating of graphene oxide on the slides to prepare them for irradiation. After being dried, the samples were irradiated in the dose interval from 100 kGy to 1.6 MGy, using an electron beam accelerator at energies 80 keV and 120 keV. These energies were chosen to sample both above and below the calculated 86keV threshold for planar sp^2 hybridized Carbon-Carbon bond breaking by electron scattering (B. Smith & D. Luzzi). The samples were tested using Fourier transform infrared spectroscopy to determine any structural changes induced by the radiation, paying special attention to the absorbance peaks corresponding to carboxyl (-COOH) and alcohol (-OH) functional groups as well as the sp^2 hybridized Carbon-Carbon bond. The samples were etched off of the glass slides and then placed into the spectroscope. This removed any interference caused by the glass, which is active in absorbing portions of the IR spectrum. Four-probe resistivity measurements were later performed to determine the sheet resistance of the samples and characterize the conductivity changes caused by the radiation. The probes were connected to the Indium tin oxide coating of the glass. This coating acted as an electrode to allow for good electrical contact while preserving the graphene oxide layer from damage that the probes could cause.

Results: Samples that had been irradiated began to show a new peak in the infrared spectroscopy graphs. This peak is very similar to a peak formed in graphs of reduced graphene oxide that had been reduced with hydrazine vapors. This is a promising step in showing that some reduction was achieved through irradiation. A graph of the irradiated sample and the sample with the lowest dose is shown on the next page. Resistivity measurements are planned and will be reported at the conference.

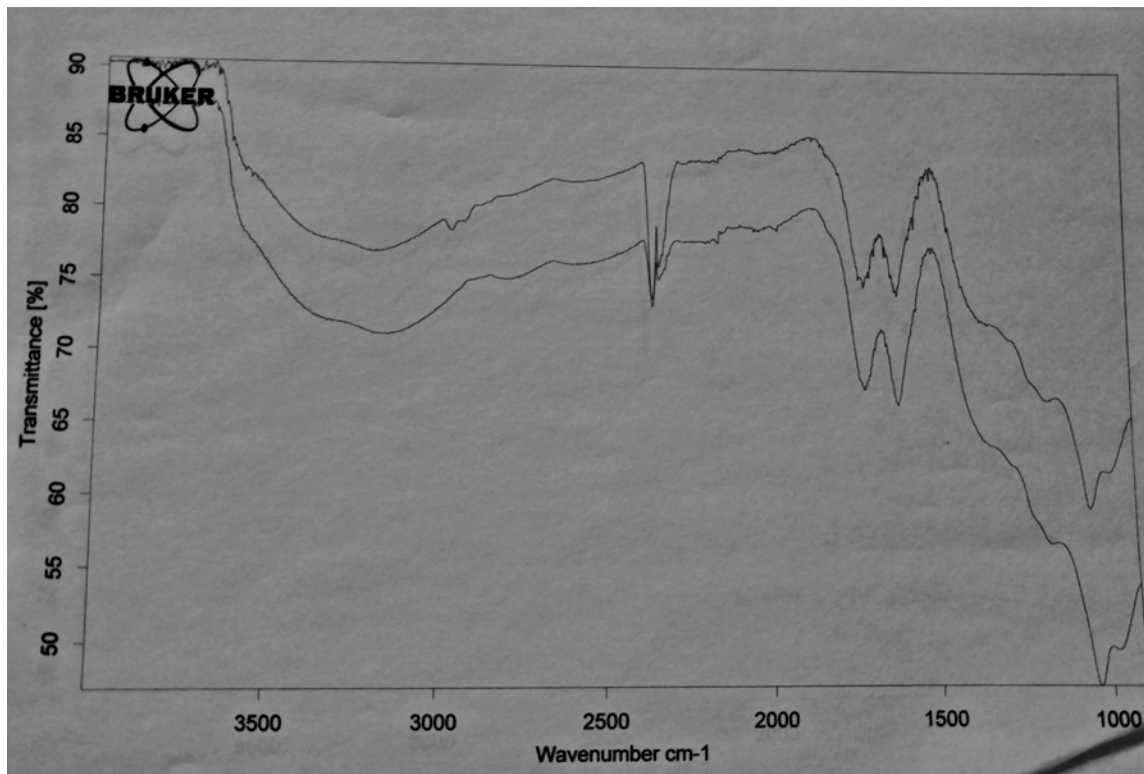


Figure 2: FTIR Spectrum of irradiated graphene oxide at 80keV and 100kGy (top line) and the control graphene oxide (bottom line). New peak emerged in the 2800-2900 wavenumber range.

Conclusion: Graphene and graphene-like materials are going to shape the future of technology. Small quantities are already being used in high performance racecars, cell phones, and professional sporting equipment. Once the method of production becomes reliable and inexpensive the products of these materials could become available for consumers. Currently we are working to get cleaner results for the infrared spectroscopy, focusing on better cleaning methods and longer scan times, as well as obtaining consistent results for the resistivity of the sheets that leave the samples intact. Ultimately, we want to use the technology developed in the past and combine it with research in the present to make the material of the future.

Computation of Transverse, Radial, and Cell-Specific RBE of Therapeutic Proton Beams Using the Microdosimetric Kinetic Model (Poster 6)

Michael P. Butkus^{1,2}, Todd Palmer²

¹Yale School of Medicine

²Oregon State University: Department of Nuclear Engineering

Purpose: The physical advantages of proton therapy are well understood and its clinical implementation has increased in recent years. Qualitatively, it is accepted that protons induce increased cell killing compared to equivalent photon doses. However, quantitative assessment and agreement on the magnitude of this

enhancement has proven difficult. Clinically, the standard is to assume that protons have a relative biological effectiveness (RBE) of 1.1. That is, they exhibit 10% cell killing enhancement over therapeutic photons. This 1.1 assumption is unvarying in all respects, including the differential lineal energy spectrums exhibited as protons become less energetic (see Fig. 1), radially away from the central ionizing axis (CAX), and for different cell lines. The aim of this work is to use the microdosimetric kinetic model (MKM) to computationally predict the RBE of protons transversely as they become less energetic, radially away from the CAX, and for differing cell types.

Characterization of the full spectrum of RBE values of protons is of principle concern to an organization such as CIRMS that wishes to further standardize and reduce the uncertainties in current and future treatments with protons.

Methods: The PHITS Monte Carlo code paired with a microscopic analytical function was used to determine probability distribution functions of the lineal energy in 0.3 μ m diameter spheres throughout a water phantom. Forty million protons were simulated as 0.6cm diameter pencil beams. Beam energies corresponding to physical Bragg peak depths of 50, 100, 150, 200, 250, and 300mm were used and evaluated transversely every millimeter and radially in annuli of 1.0, 2.0, 3.0, 3.2, 3.4, 3.6, 4.0, 5.0, 10.0, 15.0, 20.0 and 35.0mm outer radius. The acquired probability distribution functions were reduced to dose-mean lineal energies and applied to a modified MKM for five different cell types (V79, T1, nb1rgb, two HSG cell lines). The RBE compared to ^{60}Co beams at the 10% survival threshold (RBE_{10}) were then calculated and analyses made. The physical dose to each voxel was also scored to help in analyses.

Results: Transverse RBE_{10} : Figure 2 shows the radially-dose weighed RBE_{10} as a function of penetration depth for different energy beams. For all beams the RBE_{10} did not exceed 1.1 until 14-15mm proximal of the Bragg peak. Over this region, use of the 1.1 assumption would overestimate biological dose by an average of 1.90% for the least energetic beam and $2.32\pm 0.06\%$ for the other beams. From the point where RBE_{10} surpasses 1.1 up until the Bragg peak, the 1.1 assumption would underestimate biological dose by 5.85% for the least energetic beam and $8.46\pm 0.65\%$ for the other beams.

Radial RBE_{10} : Shown in Table 1 is the transverse-averaged RBE_{10} at different radius annuli from the CAX of the beam. RBE_{10} was seen to increase as distance from the CAX increased. However, large increases were only seen in low dose regions and their overall effects on the transverse biological dose remains low. In the entrance region of the phantom (first 10mm), the range of annulus specific RBE_{10} was 15.22 to 18.88% for different initial energies. At the Bragg peak, this difference ranged from 3.15 to 26.77%. Despite these rather large variations, the dose-weighted RBE_{10} and the CAX RBE_{10} varied by less than 0.14% at 10mm depth and less than 0.16% at the Bragg peak for all beams. Similarly, small variations were found at all depths proximal of the Bragg peak.

Cell Specific RBE_{10} : Minimal variations between cell-specific RBE_{10} were seen for all cell types except the HSG-2 cell. If the useful region of a beam is classified as the region in which biological dose is greater than 50% of the maximum dose, then the therapeutic RBE_{10} would be ratio of average RBE_{10} in the useful region to the average RBE_{10} proximal of the useful region. When normalized and compared to the therapeutic ratio of V79 cells difference of -0.43 ± 0.15 , 0.07 ± 0.07 , 0.38 ± 0.04 , and $2.57\pm 0.30\%$ were seen for T1, HSG-1, nb1RGB, and HSG-2 cells, respectively.

Conclusions: According to the MKM, application of the 1.1 assumption would underestimate biological dose to a treatment volume, while overestimating dose to normal tissues away from the Bragg region. Radial fluctuations in RBE_{10} , although seen, occur in low-dose regions and their presence only impacts the dose-weighted RBE_{10} on the order of 0.1-0.2%. Of the cell types examined, four of the cells exhibited therapeutic RBE_{10} ratios within $\pm 1\%$ of one another. However, HSG-2 cells, with a lowest saturation lineal energy, exhibited therapeutic RBE_{10} ratios 2-3.5% higher than the other cell types.

Investigation of the Formulation Dependence on Quenching In PRESAGE® By a Proton Beam (Poster 7)

Mitchell Carroll^{1,2} and Geoffrey Ibbott¹

¹Department of Radiation Physics, University of Texas MD Anderson Cancer Center, 1515 Holcombe Blvd., Houston, TX 77030 USA

²University of Texas at Houston Graduate School of Biomedical Sciences, Houston, TX 77030 USA

Abstract: The radiochromic dosimeter PRESAGE® has shown potential in conventional radiotherapies, but it suffers from dose under-responding, or signal quenching, in proton therapy as a result of dependence on variations in the linear energy transfer (LET). Early investigations have shown the under-response is affected by the chemical concentration of the active components, but as yet this relationship has not been comprehensively measured. This study investigated the impact of PRESAGE® formulation changes on signal quenching to determine the magnitude by which the quenching can be minimized.

1. **Purpose:** Radiotherapy techniques have advanced significantly over the last two decades and dose planning has also become significantly more complex [1]. This is explicitly seen in proton therapy, which includes extremely steep dose gradients as a result of the Bragg peak. Using conventional dosimetry systems to fully characterize complex dose distributions can be labor intensive and susceptible to volume interpolation errors [2]. A 3D dosimetry system could provide comprehensive volume measurements that are captured in a single irradiation and can potentially catch planning and delivery errors missed by conventional dosimetry systems.

PRESAGE® (Heuris Pharma, LLC, Skillman, NJ) is a radiochromic polyurethane three-dimensional (3D) dosimeter that has distinct advantages over many other 3D alternatives such as improved thermal and temporal stability, environmental robustness, and improved measurement accuracy through optical-CT imaging. Previous studies have demonstrated PRESAGE® can be successfully used to measure complex photon dose distributions [3-5].

Unfortunately, PRESAGE® suffers from a dose under-response, or signal quenching, in the Bragg peak region, making accurate proton dosimetry so far impossible [6-8]. This signal quenching has also been observed in polymer gels as well as most other 3D dosimetry alternatives and the source has been primarily attributed to LET-dependence [9]. The mechanisms of this quenching are believed to be recombination of the radical initiators rather than signal activation [10], local depletion of the signaling components [11], or some combination of the two. In our previous studies using commercially available PRESAGE®, we measured an under-response as high as 20% [12].

No known studies have comprehensively investigated relative concentrations of the radical initiator and leuco dye responder to chemically correct for PRESAGE® signal quenching in a proton beam. In this study, we investigated the relationship of these components on LET-dependence to assess the potential of a formulaic correction of this quenching effect.

2. **Methods:** 2.1 *PRESAGE® Manufacturing*

The PRESAGE® dosimeters used in this study were manufactured in-house using Leuco Malachite Green (LMG) dye, chloroform (CHCl₃) radical initiator, dibutyltin dilaurate as a catalyst, and polyurethane resin (Parts A and B, Crystal Clear 204, Smooth-On). Using a method described by Alqathami et al [13], 30 formulation batches were made with radical initiator concentrations varying between 3.0-30.0% (w/w) and LMG concentrations between 1.0-4.0% (w/w). After combining all ingredients, the formulations were poured into spectrophotometer cuvettes (1x1x4.5-cm³).

2.2 *Irradiation*

The cuvettes were irradiated using a 225-MeV (26.9-cm range) passively scattered proton beam modulated to deliver a 10-cm SOBP. A solid water phantom was used and cuvettes were positioned at four depths along the beam profile. The first depth was 10-cm and situated in the low LET dose plateau allowing dose normalization. Cuvettes were next irradiated at three points along the SOBP at the following depths to measure a uniform dose at varying LETs: 19-cm (the most proximal SOBP region), 22-cm (SOBP center), and 25-cm (the distal most SOBP region). Three cuvettes were independently irradiated at each position for each formulation. The cuvettes were irradiated to 387-MU (approximately 400 cGy to the SOBP). The beam profile was separately measured using a Zebra multilayer ion chamber (MLIC).

2.3 *Readout*

The dose signal was measured by the change in optical density (ΔOD) of the cuvettes using a Thermo Scientific GENESYS™ 10S UV-VIS spectrophotometer. Optical measurements were made at the absorption peak wavelength of 632-nm approximately 24 hours after irradiation. The ΔOD was determined by subtracting the pre-irradiation measured OD from the post-irradiation measured OD.

The ΔOD for each formulation was normalized to dose using the average of the measurements from cuvettes in the dose plateau region to the dose measured by the MLIC. The quenching magnitude for the measurements along the SOBP region was calculated as the difference of the normalized PRESAGE® signal to the ion chamber measurements made at each depth.

3. **Results:** Figure 1a illustrates quenching along the SOBPs while Figure 1b shows the magnitude of the quenching for better illustration. The relationship between quenching and radical initiator concentration was observed to be nonlinear. The maximum quenching magnitudes for all PRESAGE® formulations is shown in Figure 2. As LMG increased, a greater concentration of radical initiator was necessary before minimal dose quenching was minimized. As the concentration of radical initiator increased beyond this point, the quenching magnitudes sharply increased again. Minimal quenching was observed as the ratio of LMG-to-CHCl₃ approached 1:2-3. The 4% LMG, 9% CHCl₃ formulation showed the lowest quenching across the whole dose profile with a maximum under-response of 5.8%.

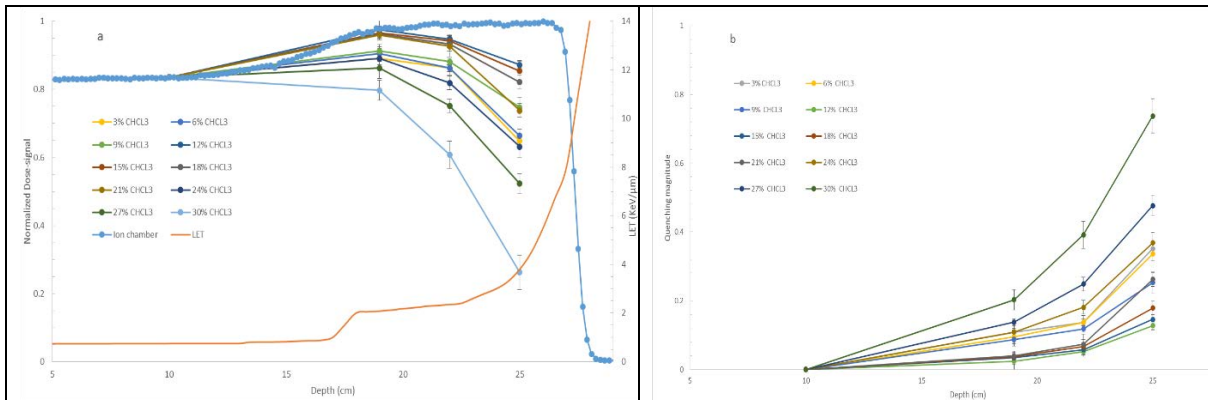


Figure 1: (a) The normalized dose-response curves for each PRESAGE® formulation irradiated by a proton beam compared with ion chamber measurements. The points are connected by straight lines to aid the eye. Additionally, the calculated LET_d is illustrated. (b) Only the magnitude of the quenching is shown as a function of depth.

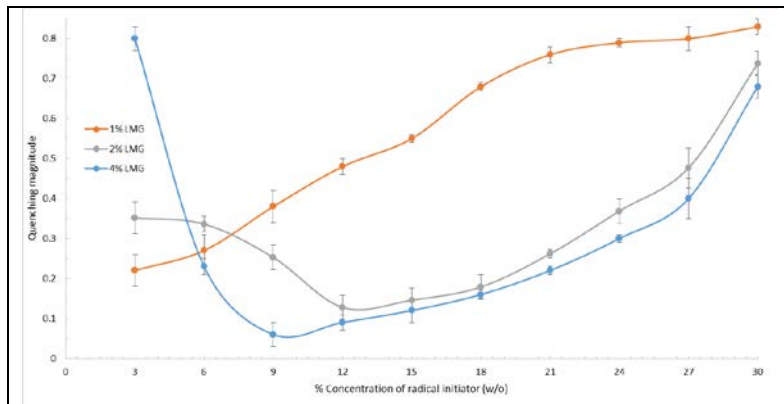


Figure 2: The quenching magnitudes at the high-LET measurement points for each PRESAGE® formulation as a function of radical initiator concentrations.

4. **Conclusions:** The concentration of the radical initiator in PRESAGE® dosimeters is shown to affect the magnitude of the dose quenching in a proton beam. We were able to decrease quenching from 20% down to 5.8%. Unfortunately, a limit to this quenching reduction was reached before it could be fully eliminated, but this is sufficient to demonstrate that further formulation optimization can improve the standard proton formulation available today.

This study also offers some insight into the physical processes resulting in quenching. As radical initiator concentrations increase beyond a point, the quenching magnitude begins to sharply increase which demonstrates that radical recombination likely plays a role in the quenching effect. Saturation of the leuco dye was also observed at low concentrations. Further studies are needed to determine the impact on quenching from leuco dye saturation as well as to determine if the quenching can be further reduced with chemical substitutions.

5. Relation to CIRMS: The focus of CIRMS has been, in large part, the measurement of radiation in its application to medical therapies. CIRMS is still setting the fundamentals that will be used in proton clinics. One of the objectives of their Measurement Program Descriptions A.9.0 is selecting appropriate dosimeters that can “harmonize protocols” amongst proton centers. My graduate research has been adapting PRESAGE® to be fully compatible to proton therapy and developing it as a tool for remote and in-house dose verification. As proton therapy is still a relatively new tool in the clinical setting, conventional radiation detectors of the past and present are still not fully suited to provide accurate verification of treatment plan delivery. I believe that 3D dosimetry will become a standard for all clinical-based ionizing radiation measurements in the near future, but first understanding and reducing quenching in PRESAGE® (and other chemical dosimeters) is vital for its implementation in proton therapy quality assurance.

5. References:

1. Klein, E.E., et al., *Task Group 142 report: quality assurance of medical accelerators*. Med Phys, 2009. 36(9): p. 4197-212.
2. Summers, P., et al., *Radiological Physics Center (RPC) Approval of Proton Centers for NCI-Sponsored Clinical Trials*. Medical Physics, 2013. 40(6).
3. Klawikowski, S.J., et al., *PRESAGE 3D dosimetry accurately measures Gamma Knife output factors*. Phys Med Biol, 2014. 59(23): p. N211-20.
4. Juang, T., et al., *On the feasibility of comprehensive high-resolution 3D remote dosimetry*. Med Phys, 2014. 41(7): p. 071706.
5. Grant, R., et al., *Investigation of 3D dosimetry for an anthropomorphic spine phantom*. Journal of Physics: Conference Series, 2013. 444(1): p. 012020.
6. Wu, C.-S., et al., *Dosimetric assessment of the PRESAGE dosimeter for a proton pencil beam*. Journal of Physics: Conference Series, 2013. 444(1): p. 012055.
7. Zhao, L., et al., *Determination of the depth dose distribution of proton beam using PRESAGE dosimeter*. J Phys Conf Ser, 2010. 250(1): p. 12035.
8. Zhao, L., et al., *Feasibility of using PRESAGE(R) for relative 3D dosimetry of small proton fields*. Phys Med Biol, 2012. 57(22): p. N431-43.
9. Karger, C.P., et al., *Dosimetry for ion beam radiotherapy*. Phys Med Biol, 2010. 55(21): p. R193-234.
10. Gustavsson, H., et al., *Linear energy transfer dependence of a normoxic polymer gel dosimeter investigated using proton beam absorbed dose measurements*. Phys Med Biol, 2004. 49(17): p. 3847-55.
11. Schmid, A.I., et al., *Monomer consumption in MAGIC-type polymer gels in the Bragg-peak of proton beams observed by volume selective 1 H MR-spectroscopy (MRS): proof of principle for high resolution MRS-methodology with a sensitive rf-detector*. Journal of Physics: Conference Series, 2013. 444(1): p. 012096.
12. Carroll, M., et al., *Investigation of photon and proton overlapping fields in PRESAGE® dosimeters*. Journal of Physics: Conference Series, 2013. 444(1): p. 012059.
13. Alqathami, M., A. Blencowe, and G. Ibbott, *Experimental determination of the influence of oxygen on the PRESAGE(R) dosimeter*. Phys Med Biol, 2016. 61(2): p. 813-24.

Analysis of Strontium-90 in Samples of Soil Contaminated with Post-Detonation Debris to Characterize Environmental Transport over Time as a Basis for Evaluating Contaminated Urban Debris (Poster 8)

Staci Herman, University of Cincinnati

Purpose:

Cesium-137 (¹³⁷Cs) and strontium-90 (⁹⁰Sr) are the predominant, long-lived fission product contaminants that persist in the environment after detonation of a nuclear device. These isotopes present a risk to human health since they become incorporated into the food chain and eventually deposit in soft tissue and bone, respectively.¹ Scientists at Lawrence Livermore National Laboratory (LLNL) have studied cycling of ¹³⁷Cs in coral atoll ecosystems and proposed several practical remedial measures to aid in reducing risk from consumption of food products.^{2,3} However, much less is known about the long-term cycling of ⁹⁰Sr. This research project analyzes existing archive of samples collected by LLNL during field studies at coral atoll ecosystems to evaluate the long-term fate and transport of ⁹⁰Sr in coralline soils. Results of these analyses will benefit radionuclide remediation, horticultural practices, and consequence management following radionuclide contamination events.

Unlike continental soil that is high in silica, Table 1 shows that soil from a coral atoll ecosystems has a preponderance of calcium derived from coral and is somewhat analogous to urban rubble that would exist after a radiological incident. Availability of a robust, reliable method for separation of ⁹⁰Sr from a high calcium-content sample would also be an asset in conducting forensic investigations after detonation of an improvised nuclear device in an urban environment.

Methods:

Samples of soil were limited to 1-g aliquots and dissolved in concentrated nitric acid to a final volume of 8 mL.⁷ Multiple aliquots of soil were analyzed to characterize sample inhomogeneity. The dissolved samples are traced with ⁸⁵Sr. Some samples were wet ashed with nitric acid and addition of hydrogen peroxide every 30 minutes for up to 4 hours. Ion exchange chromatography with Eichrom Sr spec resin is used to separate strontium from the dissolved sample.^{8,9} The ⁸⁵Sr tracer was measured in each of the eluted samples using a gamma spectrometer to determine the strontium recovery. The activity of ⁹⁰Sr in each sample was determined using a liquid scintillator counter to measure the activity of its decay product, ⁹⁰Y, approximately 2 weeks after separation to insure activity equilibrium between parent and decay product.

Results

Initial research has been focused on developing a reliable radioanalytical method for measuring strontium in samples of commercial grade coral and reagent grade CaCO₃ as analogs for a calcium rich sample. The selected method exhibits a yield greater than 90 percent for samples in which precisely known quantities of ⁸⁵Sr has been added. This method has been used to analyze three archival soil samples collected in 1964 from different locations on Bikini Atoll, a coral sample from Bahama, and a sample of reagent grade calcium carbonate. Table 2 lists results of ⁹⁰Sr for these samples and demonstrates that the method yields recoveries greater than 90%. Of the archived samples, Bikini Atoll Soil 1 has the highest concentration of ⁹⁰Sr. Analyses on additional soil and vegetation samples are needed to evaluate the long-term fate and cycling of the ⁹⁰Sr present in this unique coralline environment.

Conclusion:

A reliable method has been developed to analyze strontium in samples of coralline soil. Initial results demonstrate that samples of soil collected from the Bikini Atoll are quite variable ranging from 27.6 Bq/ g to 0.37 Bq/g, with tracer recoveries above 90 percent.

My dissertation project is aligned with the CIRMS Public Radiation and Protection Subcommittee, more

Table 1: The percent calcium and silicon in Marshall Islands soil, continental soil, and concrete.

Location/ Sample	% Ca	% Si
Marshall Islands Soil ⁴	45	<.2
New York City Soil ⁵	6	61
Concrete ⁶	49	10

Table 2: Percent recovery of Sr-85 tracer from samples, and average Sr-90. Bahama coral and calcium carbonate had no added Sr-90.

Sample Identity	Sr-85 Recovery (%)	Sr-90 (Bq/g)
Bikini Atoll Soil 1	92.94 ± 3.90	27.6 ± 0.2
Bikini Atoll Soil 2	90.73 ± 3.91	1.78 ± 0.02
Bikini Atoll Soil 3	91.91 ± 3.78	0.37 ± 0.01
Bahama Coral	92.19 ± 2.82	0
Calcium Carbonate	91.57 ± 2.82	0

specifically, their interest in sorption of radioactive elements in contaminated soils, sediments, urban structural, and other materials, since my research is examining the cycling of ⁹⁰Sr in the environment. Furthermore, with Marshall Islands soil being similar in calcium content to that of soil, my improved method of isolating ⁹⁰Sr in this matrix aligns with one of the subcommittees main goals. We are currently working with a collaboration with Dr. Terry Hamilton at LLNL.

References:

1. UNSCEAR (2008) *Sources and Effects of Ionizing Radiation* UNSCEAR: New York, 2008; p254
2. Robinson, W.L.; Hamilton T.F.; Radiation doses for Marshall Islands Atolls affected by U.S. nuclear testing: all exposure pathways, remedial measures, and environmental loss of ¹³⁷Cs. *Health Physics* 2010, 98 (1), 1-11.
3. Hamilton, T. F.; Robison, W. L., The effective and environmental half-life of the ¹³⁷Cs at former U.S. nuclear testing site at the Marshall Islands. Lawrence Livermore National Laboratory Lawrence Livermore National Laboratory, 2004.
4. Emery, K. O.; Jr., J. I. T.; Ladd, H. S., *Geology of Bikini and Nearby Atolls*. Interior, D. o. t., Ed. United States Government Printing Office: Washington D.C., 1954.
5. Giminaro, A.; Stratz, S. A.; Gill, J.; Auxier, J.; Oldham, C. J.; Cook, M.; Auxier, J., II; Molgaard, J.; Hall, H., Compositional planning for development of synthetic urban nuclear melt glass. *Journal of Radioanalytical and Nuclear Chemistry* 2015, 306 (1), 175-181.
6. Sidney Mindess and J. Francis Young Prentice-Hall, Inc., 1981, pp. 671.
7. Muramatsu, Y.; Hamilton, T.; Uchida, S.; Tagami, K.; Yoshida, S.; Robison, W., Measurement of ²⁴⁰Pu/²³⁹Pu isotopic ratios in soils from the Marshall Islands using ICP-MS. *Sci Total Environ* 2001, 278 (1-3), 151-9.
8. Horwitz, P. E.; Renato, C.; Dietz, M. L., Novel Strontium-Selective Excretion Chromatographic Resin. *Solvent Extraction and Ion Exchange* 1992, 10 (2), 313-336.
9. Clark, S. B., Separation and determination of radiostrontium in calcium carbonate matrixes of biological origin. *J. Radioanal. Nucl. Chem.* 1995, 194 (2), 297-302.

Characterization of Cesium-Bearing Soil from the Marshall Islands Using Micro-Analytical Techniques (Poster 9)

Katie Hoffman¹, Chad Durrant², Ruth Kips², James Begg², Mavrik Zavarin², Annie Kersting², Roger Martinelli³, Terry Hamilton³

¹Department of Chemistry, University of Cincinnati

²Nuclear and Chemical Sciences Division, Lawrence Livermore National Laboratory

³Atmospheric, Earth, and Energy Division, Lawrence Livermore National Laboratory

Methods for detecting and measuring the radionuclides in soil and sediment have been well established, but reliable methods for evaluating the mechanisms behind the soil-radionuclides interaction are still being evaluated. This work examined the potential correlation between radioactive cesium (Cs) and other elements in the soil from the Marshall Islands. Samples previously collected from various locations around the Marshall Islands were characterized using micro-analytical techniques such as nano-scale secondary ion mass spectrometry (NanoSIMS) and scanning electron microscopy (SEM). NanoSIMS is a powerful tool for these analyses because it provides means to detect and map the spatial distribution of isotopes of interest on the nanometer scale. The sample preparation and NanoSIMS methods addressed the unique spectroscopic and geochemical challenges associated with Cs. First, samples were morphologically characterized using SEM to obtain a general sense of the soil's physical features. After the SEM analysis, the soil samples were mounted for NanoSIMS analysis in epoxy or deposited directly on glassy carbon planchets. To more reliably assess the amount of Cs in the soil matrix, it was also necessary to mount "standards" with known quantities of cesium alongside the actual soil samples for comparison during the analysis. Bulk soil sorption experiments were used to determine the best method for preparing the "standards". These preliminary NanoSIMS experiments were able to distinguish the different samples based on the Cs secondary ion intensity detected in the samples. Future NanoSIMS experiments will most likely include a revised sample preparation protocol that involves physical size fraction of soil particles before they are mounted for analysis.

This work performed under the auspices of the U.S. Department of Energy by Lawrence Livermore National Laboratory under Contract DE-AC52-07NA27344. We thank the U.S. Department of Energy's National Nuclear Security Administration, Office of Defense Nuclear Nonproliferation Research and Development, for financial support. LLNL-ABS-719873

In Vivo Evaluation of Genotoxic Potential of 2-Acb's in Liver Cells from Rats Fed With Irradiated Diet Using Flow Cytometry (Poster 10)

R. Martins^a, L.R. de Carvalho^a, D.P. Vieira^a, A.B. Barbezan^a, A.L.C.H. Villavicêncio^a

^a Instituto de Pesquisas Energéticas e Nucleares (IPEN) na Universidade de São Paulo (USP) Av. Prof. Lineu Prestes, 2242, Cidade Universitária, São Paulo/ SP CEP: 05508-000 – Brasil

*regianemartins@usp.br

1. Purpose:

Radiation sources became widely available since 1960's, and between its main uses are the applications in food irradiation and research of effects of ionizing radiation on food products. Despite some public concern, the process is safe, free from chemical residues and presents advantages for preservation and storage. Nevertheless, safety dose parameters must be adopted in irradiation procedures to inhibit formation of undesirable and/or toxic products, for example, 2-ACB's (2-alkylcyclobutanones) that are cyclic compounds containing four carbon rings that can be formed in food when its fat content is irradiated through breakdown of fatty acids. 2-ACBs are considered a unique class of compounds, due to divergences between results of its mutagenicity potential collected from different studies, more studies are needed. In this study, a cell population collected from rat livers were chosen for *in vivo* genotoxicity analysis because the importance of the liver in the metabolization of compounds. Analysis was performed using the micronuclei test using flow cytometry, allowing faster analysis, use of few materials and reduction in the number of animals, what is a subject much addressed currently in research. Irradiated rat diet did not show any genotoxic effect on liver

cell populations. The improvement of the techniques is important for the future of the research since the irradiation process is already consolidated.

2. Methods:

2.1 Chemicals

Normocaloric (about 3% of fat of total dry mass) rat industrial diet (Nuvilab[®]) was gamma-irradiated (DOSE, TAXA) using a ⁶⁰Co source (Gammacell 220) at room temperature. Type I Collagenase (CAS N.9001-12-1 Sigma Aldrich[®]) was solubilized (300 µg/mL) in Hank's Balanced Salt Solution (HBSS). Cyclophosphamide monohydrate (CAS N.6055-19-2 Sigma Aldrich[®]) and Methyl-Methane Sulphate (MMS, CAS N. 66-27-3 Sigma Aldrich[®]) were diluted in saline solution (NaCl 0,9%). Cell suspensions were properly incubated with SYTOX[®] Green (Molecular Probes, S7020) and ethidium monoazide bromide (EMA, Molecular Probes, E1374) to label nuclear and micronuclear DNA (SYTOX) and to discriminate nuclei from dead cells (EMA).

2.2 Animals

Groups of male Wistar rats were bred and maintained until the age of 8 months at IPEN Animal Facility under all principles of animal welfare (12/12 h day night cycles, room temperature: 22-23 °C, 44-65% relative atmospheric humidity, no more than three animals/cage), as specified by IPEN Ethical Animal Experimentation Committee (process number CEUA-IPEN N^o 148/14), including food and water *ad libitum* availability. Five animals were fed after weaning with normocaloric diet irradiated as described above, and three animals were fed with standard autoclaved diet. Positive controls for genotoxicity were represented by 2 animals injected intraperitoneally with cyclophosphamide (50 mg/kg) and other 2 injected same way with MMS (25 mg/kg) 24 hours prior the experiment. Negative controls were represented by 2 animals injected with 1 mL of vehicle control (NaCl 0,9%) (OECD).

2.3 Flow Cytometry

2.3.1. Hepatic cell isolation

Animals were euthanatized in a CO₂ chamber. Livers were exposed and fragments of 3 to 4 mm³ were dissociated passing through syringe needle in HBSS with collagenase (200 µg/mL). Tissue pieces were incubated at 37 °C for 1 hour, with vigorous shaking every 15 minutes. Suspensions were centrifuged (1500 rpm, 5 min, RT) and cell pellets were suspended in ammonium chloride (15.2 mM in water) to lyse erythrocytes and kept on ice for 5 minutes. Cells were centrifuged as described and suspended in ice-cold phosphate-buffered saline solution (PBS).

2.3.2. Flow cytometric analysis

Isolated liver cells from rats were plated (100 µL/well) in 96-well plates in quadruplicates. The used protocol for labelling nuclear/micronuclear DNA was described elsewhere (Bryce SM, 2007). Briefly, cells were incubated with EMA (5 µg/mL) and exposed to blue led light (30 W) in an ice bath to photoactivation of dye. Plates were centrifuged (1500 rpm, 15 min, RT) and cells were lysed with buffer containing SYTOX[®]-Green (0.4 µM) and RNase-A to avoid RNA labelling. After incubation, (1 h, 37 °C, dark) and pre-acquisition steps, cells were analyzed using a Accuri C6 Cytometer (BD Biosciences), through acquisition of fluorescence in FL1 (SYTOX[®]-Green) and FL3 (EMA) channels. Micronuclei frequencies from groups were compared by Kruskal-Wallis method.

3. Results:

Micronuclei were scored as shown in Fig 1. Examples of results were shown on Fig. 2. Results are shown in Fig 3.

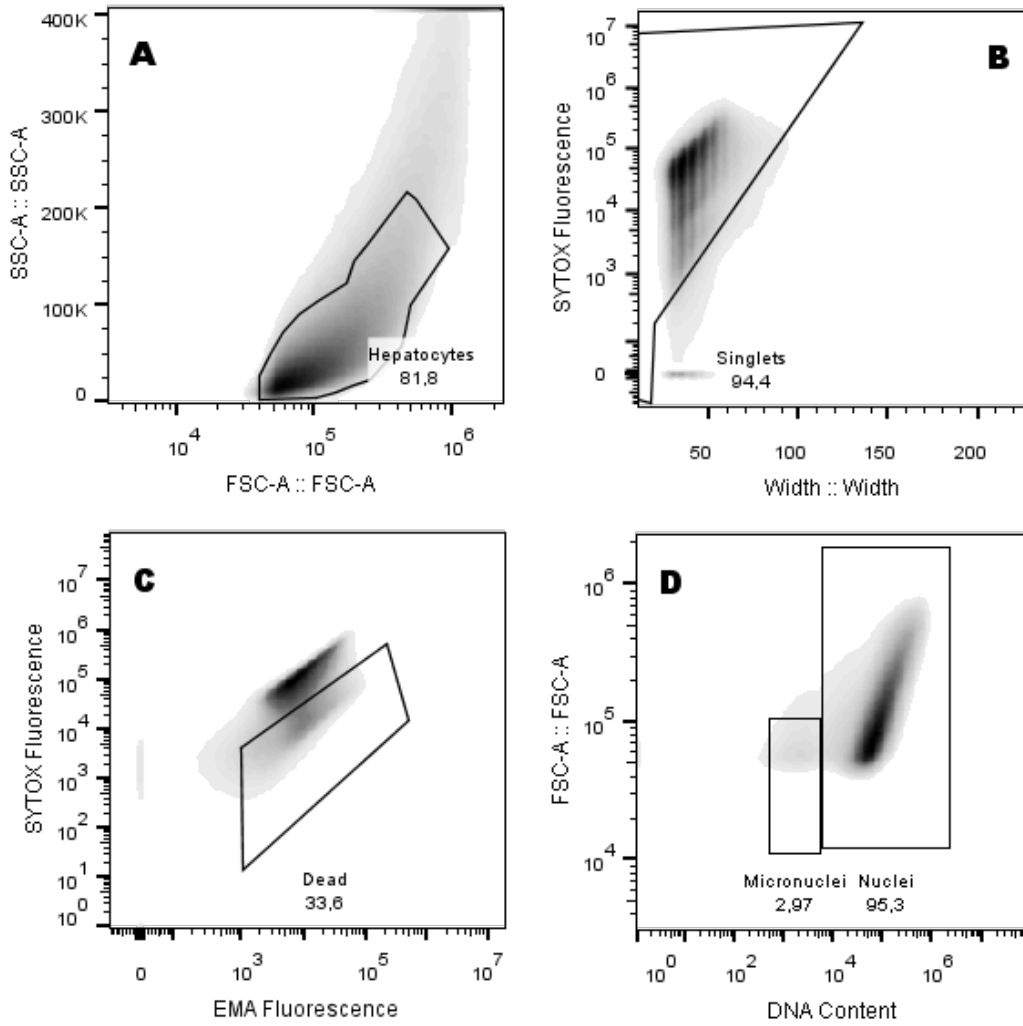


Figure 1: Gating strategy for analysis of micronucleus frequency from experiments. (A): Cell gating; (B): Doublet elimination/singlet characterization; (C) Dead cells exclusion from analysis; (D) Nuclei and MN regions delimited on plot. Numbers on plots refers to percentages of total events depicted on each plot.

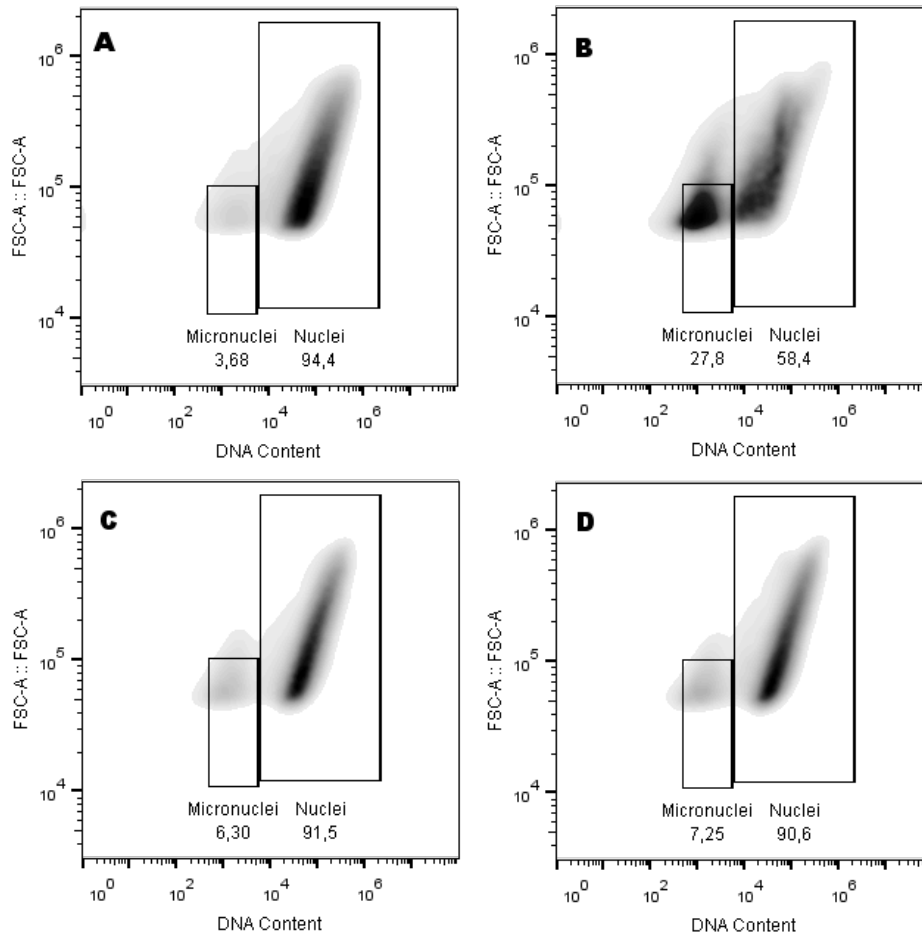


Figure 2: Examples of results from experimental groups. (A) NaCl 0,9%; (B) Ciclophosphamide, (C) MMS, (D) Irradiated diet

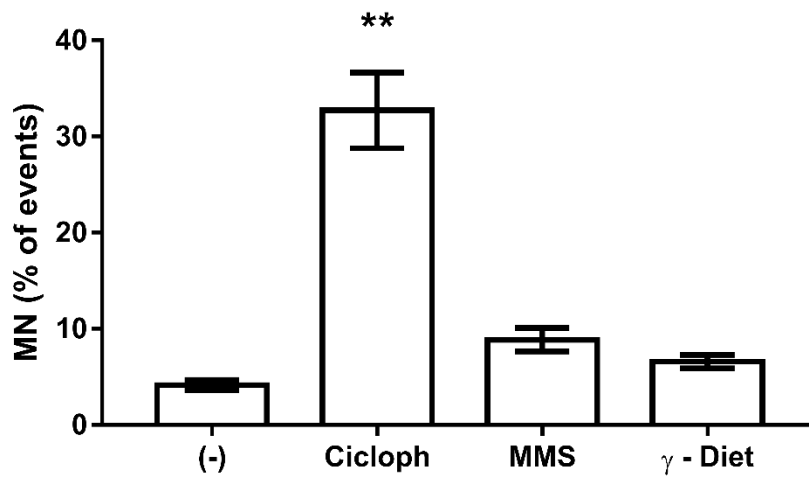


Figure 3: Percentage of MN (% of total events) of liver cells of rats treated with NaCl (-), Ciclophosphamide, MMS or irradiated diet (γ -diet). Bars: SEM. (**): $p < 0,01$ (difference from negative control)

4. Conclusions:

Although MMS did not induce micronuclei statistically different percentages from that found in the controls, cyclophosphamide induced damage, which leads to validation of the assay and to verify that there was no genotoxic damage in hepatic cells from animals fed for 8 months with irradiated diet, supposedly containing 2-ACBs. Further experiments (histopathology, visceral fat, hematology) will corroborate results.

References:

In vitro micronucleus assay scored by flow cytometry provides a comprehensive evaluation of cytogenetic damage and cytotoxicity Steven M. Bryce, Jeffrey C. Bemis, Svetlana L. Avlasevich, Stephen D. Dertinger Mutat Res. Author manuscript; available in PMC 2007 Aug 22. Published in final edited form as: Mutat Res. 2007 Jun 15; 630(1-2): 78–91. Published online 2007 Mar 19. doi: 10.1016/j.mrgentox.20

Towards the Detection of LET in the Modern Radiotherapy Clinic (Poster 11)

Humza Nusrat
Ryerson University, Toronto, ON, Canada

Purpose: Currently, treatment planning in radiation therapy is done by optimizing the amount of absorbed dose delivered to a certain region; the dose to the tumour is maximized while the dose to surrounding normal tissue is minimized. The use of absorbed dose alone as the metric of predicting biological response is fair in conventional high energy (> 1 MeV) photon and electron therapy; however, as the particle type is changed (e.g. protons, carbon-ions) or lower energies are used, the correlation between dose and relative biological effectiveness (RBE) begins to break down. In order to account for this, additional information is needed. The linear energy transfer (LET) is defined as the amount of energy absorbed per unit length along a charged particle's track, this quantity generally correlates well with RBE. The value of LET information in proton therapy treatment planning has been demonstrated [1], [2]. In this work, the need for LET information in increasingly popular photon treatments (e.g. intensity modulated radiation therapy (IMRT)) was evaluated and a novel LET detector design and measurement methodology was proposed.

Methods: Evaluating the need for LET information in photon therapy

In order to determine if the LET variation in modern photon therapy was significant, the LET spectra were scored inside and outside the treatment field of a simulated clinical radiation therapy beam. Using the Geant4.10.1 Monte Carlo software package, a phase space file representing a Varian Clinac 600C 6 MV photon beam was used to irradiate a 16 cm³ water tank (FIG. 1). The electron energy fluence was scored at various positions inside and outside the beam at two depths (1.5 cm and 5 cm); the NIST ESTAR database [3] was used to convert the energy fluence spectra to the unrestricted LET spectra.

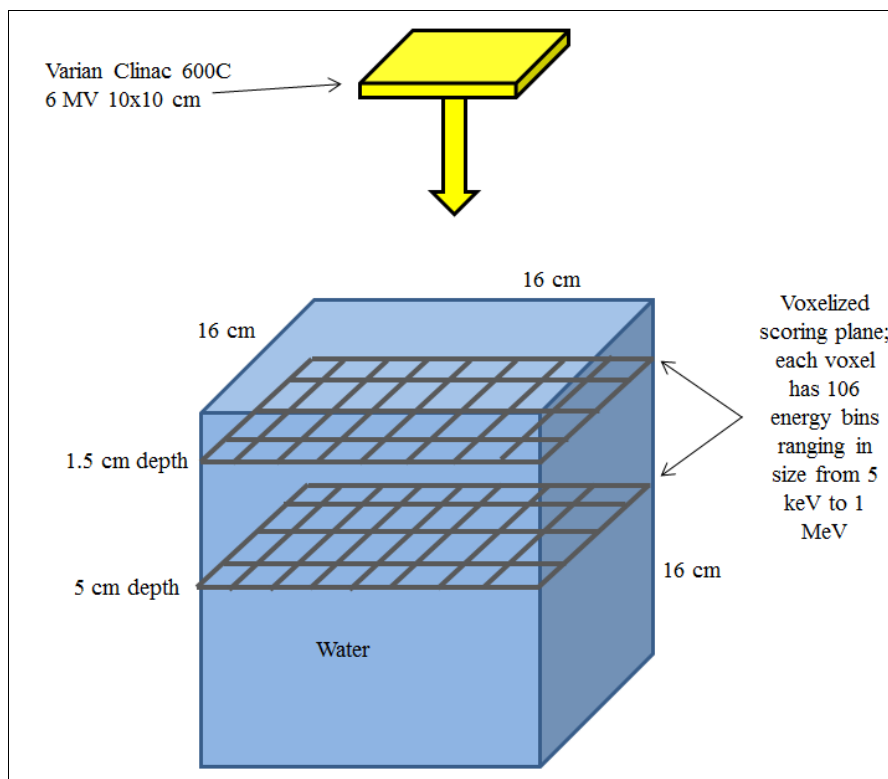


Figure 2: Geometry visualization of the Geant4.10.1 simulation carried out in order to examine the change in LET spectra at various positions in and outside the treatment field of a 6 MV clinical photon beam. Voxelized scoring planes were placed at depths of 1.5 cm and 5 cm; each two-dimensional voxel was 2 mm². The electron fluence going in both directions was determined and then sorted into energy bins ranging in size from 5 keV to 1 MeV.

LET measurement formalism

The signal (**S**) generated by a radiation sensitive detector to an incoming radiation spectrum is proportional to the response (**R**) to a certain energy multiplied by its fluence (Φ). In this case, the sensitive volume used is the plastic scintillator, the light output of which is intrinsically dependent on LET via Birks' Law. By measuring the light output of differently LET dependent plastic scintillator detectors, the LET fluence can be resolved through the relation $\mathbf{S}=\mathbf{R}\cdot\Phi$, given that **R** is invertible. **S** is signal measured using various plastic scintillators and a corresponding photodetector, and **R** is the Monte Carlo simulated ideal response matrix. The LET dependence of plastic scintillators can be tuned via doping with high-Z elements.

LET detector design

The current prototype of the LET measurement device contains a custom built scintillator housing (FIG. 2) which couples to a glass taper, leading to an optical fiber which transmits light signal outside the treatment room bunker to a photomultiplier tube. The scintillator housing is easily removable allowing the use of different scintillators when required. In this study, the effect of doping on scintillator response was examined using the undoped plastic scintillator as well as a 5% Pb-doped plastic scintillator. This was done by using the same measurement set-up for both scintillators and quantifying the light produced for different radiation types. The scintillator detector was irradiated using 9, 12, and 15 MeV electrons, as well as 100 kV and 250 kV x-rays.

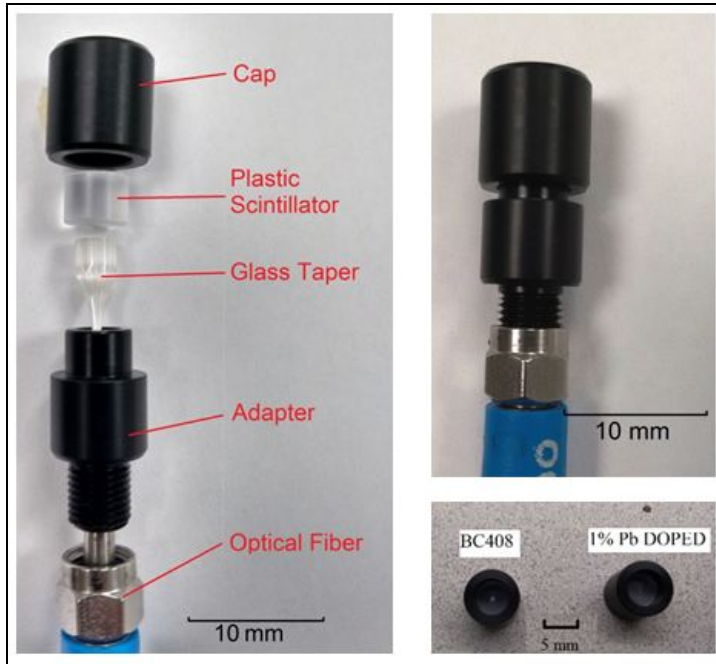


Figure 3: Detector setup shown in the open and closed configuration. The black acrylic opaque cap was used to prevent light from inside the treatment room from introducing noise to the measurement

Results:

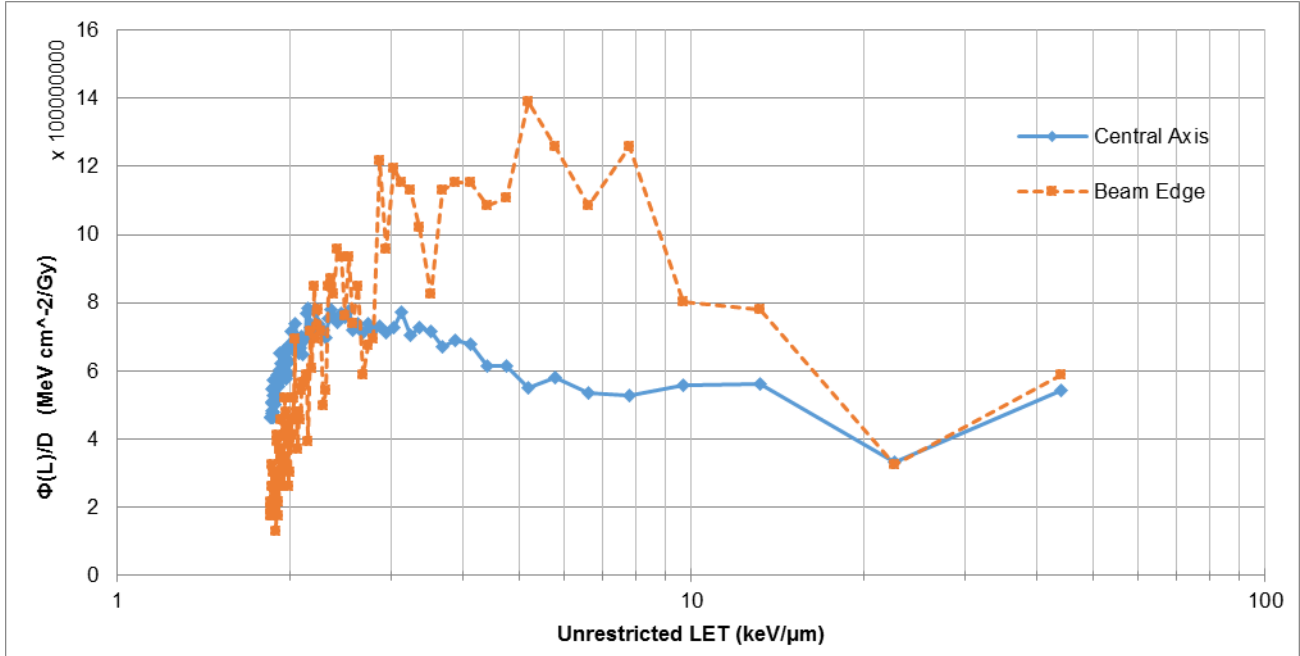


Figure 4: Significantly higher LET observed at the beam's edge relative to the central axis. Fluence was normalized to dose at each respective position

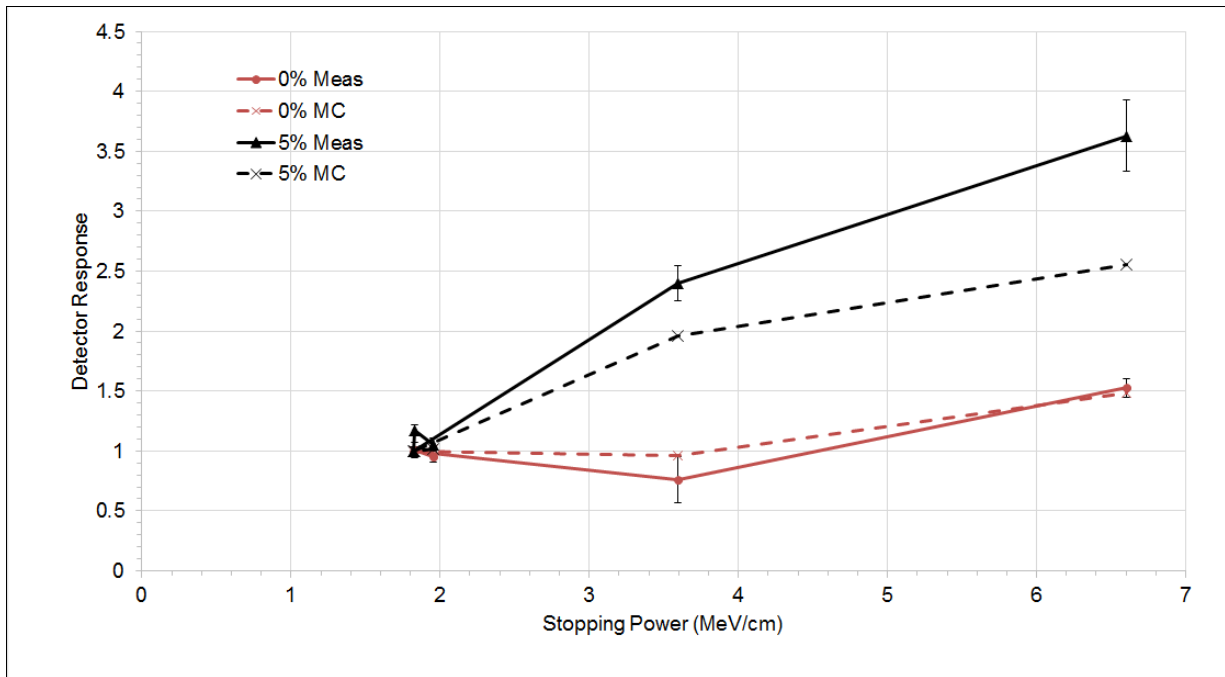


Figure 5: Preliminary measurements of undoped and 5%-Pb doped scintillator light emission demonstrate increased sensitivity as a result of metal doping to lower energy radiation

Conclusion

Preliminary results indicate that at the edge of the photon treatment beam, the LET for the same given dose is greater relative to the central axis due to the presence of increased low energy electrons and photons (due

to scattering). Initial scintillator doping measurements indicate that high-Z doping allows for increased sensitivity to lower energy radiation; the use of different dopants and concentrations in the future along with the formalism described above will lead to the measurement of LET in the clinic.

Works Cited:

- [1] C. Grassberger, A. Trofimov, A. Lomax and H. Paganetti, "Variations in linear energy transfer within clinical proton therapy fields and the potential for biological treatment planning," *Int J Radiat Oncol Biol Phys*, vol. 80, no. 5, pp. 1559-1566, 2011.
- [2] B. Jones, "Towards Achieving the Full Clinical Potential of Proton Therapy by Inclusion of LET and RBE Models," *Cancers*, vol. 7, no. 1, pp. 460-480, 2015.
- [3] M. J. Berger, J. S. Coursey, M. A. Zucker and J. Chang, "ESTAR, PSTAR, and ASTAR: Computer Programs for Calculating Stopping-Power and Range Tables for Electrons, Protons, and Helium Ions (version 1.2.3)," Gaithersburg, MD, 2005.

Relation to CIRMS mission and my Career Goals:

This work presents a novel measurement technique for ionizing radiation which can be potentially used not only in the clinical setting but in radiation protection and security as well. My career goals in the future involve becoming a clinical medical physicist and improving current treatment planning techniques to better predict biological response through the integration of new technologies.

Collaborators:

- Supervisor: Dr. Arman Sarfehnia
 - Medical Physicist, Odette Cancer Centre
 - Adjunct Professor, Ryerson University
- Collaborator: Dr. Geordi Pang
 - Senior Medical Physicist and Radiation Safety Officer, Odette Cancer Centre
 - Adjunct Professor, Ryerson University

Interplay Between MR Imaging and Radiotherapy: An Investigation of 3D Gel Dosimeters for Real-Time Quality Assurance (Poster 12)

Yvonne Roed^{1,2}, Hannah Lee², Mo Kadbi³, Lawrence Pinsky¹, Geoffrey Ibbott²

1 – Department of Physics, University of Houston, Houston, TX

2 – Department of Radiation Physics, UT MD Anderson Cancer Center, Houston, TX

3 – MR Therapy, Philips HealthTech, Cleveland, OH

Introduction: With the introduction of magnetic resonance-image guided radiotherapy (MR-IGRT) as an advanced treatment modality the need for new quality assurance (QA) standards for the machine and the treatment planning systems arises. These standards are currently developed to maintain the best possible patient care. The addition of a strong magnetic field presents new challenges for the physics of such treatment units and in the selection of QA devices. The installation of a non-clinical MR-Linac pilot system (Elekta AB, Stockholm, Sweden) that combines a 1.5T MR scanner with a 7MV linear accelerator (MR-Linac) at MD Anderson Cancer Center offers a new potential for gel dosimeters to be used for 3D dosimetry. The dosimeters don't have to be transported to a different device for read-out; they can be imaged and analyzed with the MR-component before, during, and after beam delivery. Furthermore, they can remain in the position of a patient, without needing to be moved and, therefore, simulate treatment.

Methods: Polymer-based gels were provided in cylindrical glass vials (5cm diameter, 4cm height) by MGS Research Inc. (Madison, CT). Iron-based Fricke-type gels were made in-house in 3% w/w gelatin, filled into cylindrical PET jars (8.5cm diameter, 6cm height) and stored at 4 °C for 24 hours prior to use. Two separate setups were used for this study. Polymer gels were irradiated at isocenter distance at 6 cm depth inside a full phantom. Half of the volume was positioned inside a 10x10cm² radiation field to capture

the penumbra region. A dose of 15Gy was delivered with the MR-Linac. Fricke gels were irradiated in air to a total dose of 30Gy in the center of the jar. Two 3x3 cm² fields were chosen to irradiate the gel to 10Gy with a gantry angle of 0° and 270°.

MR images were acquired in real-time with the MR-component of the MR-Linac for both setups using a balanced-Fast Field Echo (b-FFE) sequence. The sequence was started 30 seconds before irradiation and was stopped 30 seconds and 1 minute after irradiation for polymer gels and Fricke gels, respectively. Different imaging parameters were chosen for the two gel types depending on their radiation-induced chemical reaction. Polymer gels were imaged with repetition/echo times, TR/TE = 3.4/1.7ms and a temporal resolution of 277ms as the polymerization of monomers changes spin-spin relaxation rates. TR/TE = 4.4/2.2ms and a temporal resolution of 1800ms was selected for Fricke gels as spin-lattice relaxation rates change due to oxidation of ferrous ions.

Signal intensities (SI) inside and outside the radiation field were measured on all MR images. The difference in SI was calculated and normalized to the maximum value that was measured at the end of image acquisition. Time-lapse videos were prepared for both setups with a speed of 100 frames per second for polymer gels and 50 frames per second for Fricke gels.

Results: The resolution of the MR images was low and the images appeared coarse. The onset and the increase in polymerization of the polymer gels was visible in the contrast change on the MR images over the time of the irradiation. The irradiated region darkened gradually. The difference in SI between areas of the dosimeters inside and outside the radiation field was measured as early as the beam was turned on until 30 seconds after the beam was turned off. The SI difference increased monotonically during irradiation. A logarithmic increase was determined up to 97% of the maximum value at the completion of the exposure. The ongoing polymerization of the gel until 30 seconds after beam-off was indicated by the slow, continuous logarithmic increase in SI differences. This difference appeared to have reached a plateau at the end of image acquisition. The transition region from inside to outside the radiation field was clearly seen on line profiles drawn across this region.

The oxidation reaction from ferrous (Fe²⁺) to ferric (Fe³⁺) ions of the Fricke gels was visible on MR images due to the gradual brightening of the irradiated areas. This change in contrast became evident at beam initiation and increased for the duration of the beam delivery. The SI difference between regions of the dosimeters inside and outside the radiation field was determined from the start of the exposure until 1 minute after completion. The oxidation reaction continued after the exposure was completed, reaching a maximum at 1 minute following beam off. The SI difference increased linearly up to 32% of the maximum value with the gantry at 0° and 270°.

Time-lapse videos clearly visualized the chemical reactions that occurred when the gels were exposed to radiation.

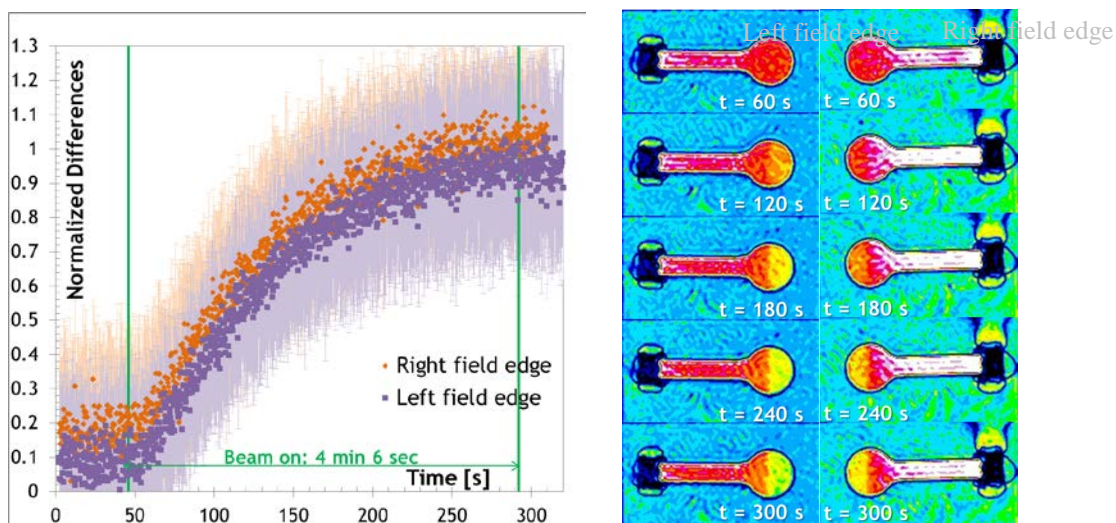


Figure 1: Difference in signal intensities for polymer gels measured for both field edges (left) and b-FFE color images generated every 60 seconds visualizing the radiation field edge (right).

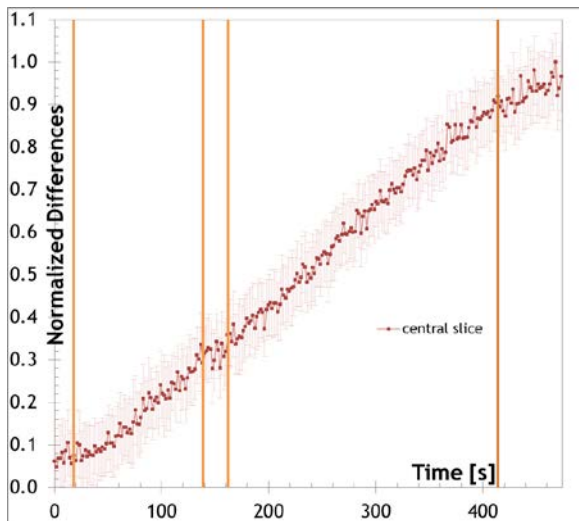


Figure 2: Difference in signal intensities for Fricke-type gels measured in the center of the dosimeter.

Conclusion: The appearance of a difference in SI at beam initiation showed that both gels reacted immediately to the delivered radiation. These results encourage further investigation and use of the gels for QA of MR-IGRT treatment units such as the MR-Linac, and especially for real-time QA. An optimization of the real-time imaging parameters is recommended to lower the noise of the MR images and obtain more qualitative and quantitative data.

Project relevance to CIRMS mission and to my career goals:

In the 2016 CIRMS Needs Report “3D dosimeters for Non-Standard External Beam Therapy Dosimetry” is described as an active measurement program description with medium priority. My graduate research on using a 3D radiosensitive gel to measure dose distributions from image-guided radiotherapy (IGRT) treatment units pertains directly to the needs for accurate treatment plan verification and high-precision dosimetry for which NIST does not yet provide standards. The rapid advancements of IGRT have led to the development of a combined MRI-linear accelerator system. Gels offer great potential as QA devices to measure 3D dose distributions from this novel, hybrid machine as they produce a signal that can be analyzed with MR. The results of my research will not only provide groundwork for the establishment of new QA standards for treatment plan verification but could even be expanded to include real-time verification as an alternative to conventional plan verification.

On the Impact Of The Scattering Angle For Direct Measurement Of The Energy Spectrum Of A Medical Linear Accelerator (Poster 13)

Sameer Taneja, Laura J. Bartol, Wesley S. Culberson, Larry A. DeWerd

University of Wisconsin, Medical Radiation Research Center

Objective: Dose calculation engines used in clinical radiation therapy treatment planning utilize the convolution-superposition algorithm to calculate dose to the patient accurately. The algorithm requires knowledge of a well-known energy spectrum, as previous work has shown significant differences in dose distributions resulting from minor changes in the energy spectrum (1-2). However, current methods for determining this energy spectrum rely on the use of a “self-tuning” approach, in which a starting spectrum determined through Monte Carlo methods is iteratively adjusted to match measured percent depth dose (PDD) curves (3-4). This method is indirect and is insensitive to small changes in the energy spectrum. At the same time, measurement of the energy spectrum is extremely challenging due to the high-energy, high-fluence nature of a linear accelerator photon beam. Indirect methods of spectrum measurement have been

completed, such as unfolding transmission measurements (5), decreasing mAs (6), and inserting a target material (7). All of these techniques have high uncertainties or are not applicable to a clinical beam. Previous work has shown that with the use of proper shielding and a Compton Scattering (CS) spectrometry geometry, the primary pulse height distribution (PHD) can be obtained above background, but high fluence rates caused pulse pileup (8). As a result, this work looks to use Monte Carlo N-Particle (MCNP) version 6 to investigate the effects of the CS angle on the expected PHD and fluence, both intended and unwanted.

Methods: A model of a Varian Clinac 21EX linear accelerator was experimentally benchmarked in MCNP6 using the methods outlined by Chibani et al. (9). The model was used to determine the photon energy distribution below the jaws of a (10x10) cm² field, which was subsequently used in all simulations. A custom built cylindrical shield and a reverse electrode high purity germanium (REGe) spectrometer were modeled in MCNP6 according to the manufacturer's schematics. The detector and shielding were placed at three CS angles including 35°, 44°, and 129° from a scattering rod placed at isocenter. An F8 detector pulse tally binned with an energy resolution of 0.512 keV (based on an energy calibration measurement) was performed in the active volume of the detector for each CS angle. In addition, unintended signal that could potentially convolute the measured signal was investigated, including CS scattered photons and wall scattered photons that penetrate the detector shield. In order to achieve reasonable statistics without having to use an impractical number of starting particles, multiple variance reduction techniques were implemented and optimized, including forced collisions, DXTRAN spheres, and weight windows (WWs).

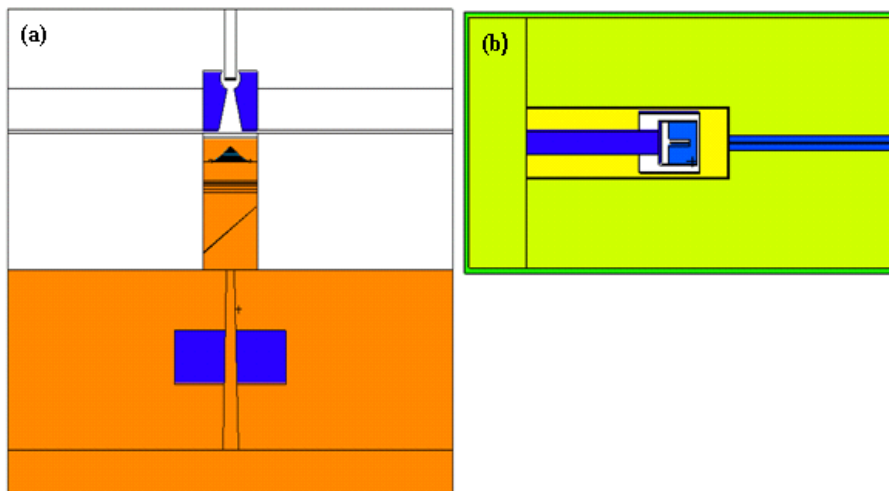


Fig. 1: A Visual Editor rendering of (a) an experimentally validated Varian Clinac 21EX linear accelerator and (b) a REGe detector and a custom built shield.

Results: Based on a calibration of 1 cGy/MU and a dose rate of 600 MU/minute, the Clinac 21EX linear accelerator model emits $5.1 \times 10^{16} \pm 0.5\%$ starting particles per minute (SP/min). Simulations show that as the CS angle increased from of 35° to 44° and 35° to 129°, the fluence entering the detector decreased by a factor of $11 \pm 3.4\%$ and $33 \pm 6.2\%$. Simulations show that increasing the CS angle from 35° to 120° decreased the maximum energy scattered toward the detector from 298 keV to 1.92 MeV, matching predicted values based on CS kinematics. The expected PHD at 35° shows a long tail and gradual falloff when compared with the PHD at 129°, which is evidenced by the relatively similar peak heights, located at 231 keV for 35° and 143 keV for 129° (Fig. 2). In addition, the contribution from CS-scattered photons and wall-scattered photons was on the order of 10^2 and 10^4 less than the intended signal, respectively.

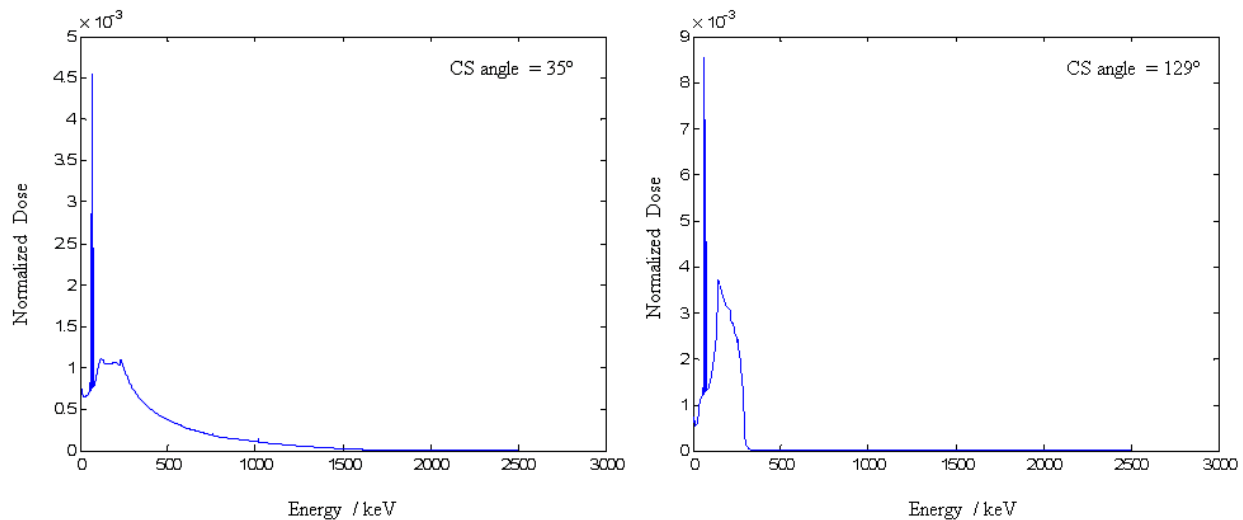


Fig. 2: Plots showing simulated pulse height distributions for CS angles of 35° and 129°.

Conclusion and Significance: Direct measurement of the energy spectrum of a medical linear accelerator has been extremely difficult due to pulse pileup. CS spectrometry has been applied in other high fluence, high energy environments in order to reduce detector pulse pileup. Previous work showed that when placing the detector out of the room and drilling through a concrete wall in this CS spectrometry setup, the decrease in the intended signal was too large and that the intended signal would not be decipherable above noise. Thus, this work investigated the effect of changing the CS angle on the expected PHD and count rate with the detector placed inside the vault. Simulations showed that as the angle increases, the fluence and the maximum energy of the expected PHD decreases. There is a tradeoff, however, with increased coherent scattering for high CS angles, and future work will investigate this effect. This work also shows expected PHD measurements using a well-characterized linear accelerator photon beam source and detector geometry. Future work will perform spectrum measurements in this CS spectrometry detector arrangement.

CIRMS 2017: This work fits the mold of the current conference theme of past, present, and future in its impacts of more accurately determining the energy spectrum of a clinical linear accelerator through a direct measuring technique. By characterizing the energy spectrum with a high degree of certainty, we can evaluate past and present spectrum determination techniques, investigate the impacts on patient calculations, and provide a baseline for comparison for future, more Monte-Carlo heavy treatment planning systems. Evaluating the optimal CS angle provides insight on the possibility of direct measurement.

- (1) P. M. Charland, I. J. Chetty, L. D. Paniak, B. P. Bednarz, and B. A. Fraass. Enhanced spectral discrimination through the exploitation of interface effects in photon dose data. *Med. Phys.*, 31:264–276, 2004.
- (2) B. L. Werner, I. J. Das, F. M. Khan, and A. S. Meigooni, “Dose perturbations at interfaces in photon beams,” *Med. Phys.* 14, 585–595 (1987).
- (3) R. Mohan, C. Chui, and L. Lidofsky. Energy and angular distributions for photons from medical linear accelerators. *Med. Phys.*, 12(5):592–597, 1985.
- (4) Das, I. J., Cheng, C.-W., Watts, R. J., Ahnesjö, A., Gibbons, J., Li, X. A., Lowenstein, J., Mitra, R. K., Simon, W. E. and Zhu, T. C. (2008), Accelerator beam data commissioning equipment and procedures: Report of the TG-106 of the Therapy Physics Committee of the AAPM. *Med. Phys.*, 35: 4186–4215.
- (5) E. S. M. Ali and D. W. O. Rogers. An improved physics-based approach for unfolding megavoltage bremsstrahlung spectra using transmission analysis. *Med. Phys.*, 39(3):1663–1675, 2012.
- (6) B. A. Faddegon. Pile-up corrections in pulsed-beam spectroscopy. *Nucl. Instrum. Methods Phys. Res. B*, 51(4):431–441, 1990.
- (7) N. K. Sherman, K. H. Lokan, R. M. Hutcheon, L. W. Funk, W. R. Brown, and P. Brown. Bremsstrahlung radiators and beam filters for 25 MeV cancer therapy. *Med. Phys.*, 1(4):185–192, 1974.
- (8) Laura Bartol. Spectroscopic characterization of high energy and high fluence rate photon beams. PhD thesis, University of Wisconsin-Madison, 2013.
- (9) O. Chibani, B. Mofteh, and C. M. Ma. On Monte Carlo modeling of megavoltage photon beams: a revisited study on the sensitivity of beam parameters. *Med Phys*, 38(1):188-201, 2011.

Measurement of Absorbed Dose to Water for a Low-Energy Miniature X-Ray Source with an Ionization Chamber (Poster 14)

Peter Watson

McGill University, Canada

Objective: In brachytherapy, miniature low-energy X-ray sources offer a number of advantages over traditional radioactive sources. These include their ease of portability, and reduced regulatory and shielding requirements. However, the dosimetry of these devices is challenging due to their steep dose gradients, soft X-ray spectra (< 100 keV) and influence of target spectral lines.

The objective of this work is to *evaluate and improve the dosimetry of miniature kilovoltage x-ray sources*. In particular, we have investigated the measurement of absorbed dose to water for the INTRABEAM System (Carl Zeiss, Germany), a 50 kVp X-ray source used in intraoperative radiotherapy. To evaluate the current dosimetry protocol recommended by the manufacturer, we have derived a formalism for calculating dose to water using an air-filled ionization chamber calibrated in terms of air-kerma. This formalism relies on a Monte Carlo (MC)-calculated conversion factor, C_Q , to go from a reference beam quality to the beam quality of interest. The effect of chamber geometry uncertainty and the effective point of measurement (POM) was also investigated.

Methods: Depth-dose rate measurements were performed with the INTRABEAM System using a dedicated water phantom offered by Zeiss. Ionization charge measurements were made using a soft X-ray PTW34013 parallel plate chamber, sealed in a waterproof holder. The absorbed dose rate to water was calculated from the measured charge by two methods: the absorbed dose formula recommended by Zeiss, and our own derived dose formalism.

The chamber conversion factor, C_Q , was calculated using the EGSnrc particle transport code. This calculation involved the use of a complete model of the PTW34013 ionization chamber (according to manufacturer specifications and dimension tolerances), the kV reference spectra used during chamber air-kerma calibration at PTB (Germany), and a previously validated model of the INTRABEAM source [1]. The dose to the chamber air cavity (D_{gas}) was simulated both in-air (with reference beam) and in-water (with INTRABEAM source). Dose to a small water voxel (D_w) was also calculated.

Results: The chamber conversion factor was found to depend heavily on the dimensions of the chamber air cavity (as shown in Figure 1). This difference was as large as 15% (@ 3 mm distance from source) between the thinnest and thickest cavity height within manufacturer tolerances. For the thinnest cavity investigated, there appears to be little to no depth dependence, while for the thickest cavity C_Q can vary by up to 10%. However, in all cases C_Q was larger than the value recommended by Zeiss.

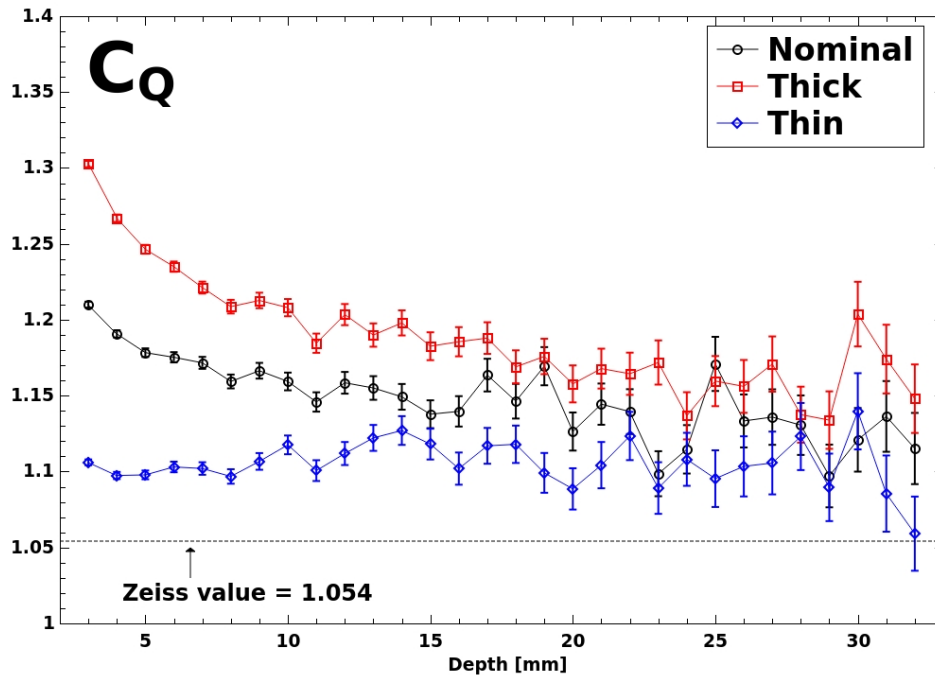


Figure 1: Ionization chamber conversion factor as a function of depth in water. POM was defined to be the inside of the entrance foil.

If the effective POM is shifted to the center of the chamber cavity (see Figure 2), the effect of dimension tolerance on C_Q is mitigated, with all three curves agreeing to within statistical uncertainty beyond 10 mm depth. Interestingly, beyond this depth C_Q is consistent with the recommended value of 1.054, despite the fact that Zeiss prescribes the chamber reference point as the entrance foil, not the cavity midpoint.

Due to steep dose gradients, source positioning was determined to be the dominant source of uncertainty (up to 7% at 3 mm depth for a 0.1 mm position uncertainty, see Figure 3). The dimensional tolerance uncertainty of the PTW34014 ionization chamber ranged from 5.6 to 1.8% (assuming a rectangular distribution), with the POM defined by the entrance foil. Our results suggest that this variance could be greatly reduced by setting the cavity midpoint as POM, however, the large dimension tolerance prevents an accurate determination of this midpoint. Unfortunately, the particular construction of the PTW34013 chamber prevents a mechanical or capacitive measurement of cavity size.

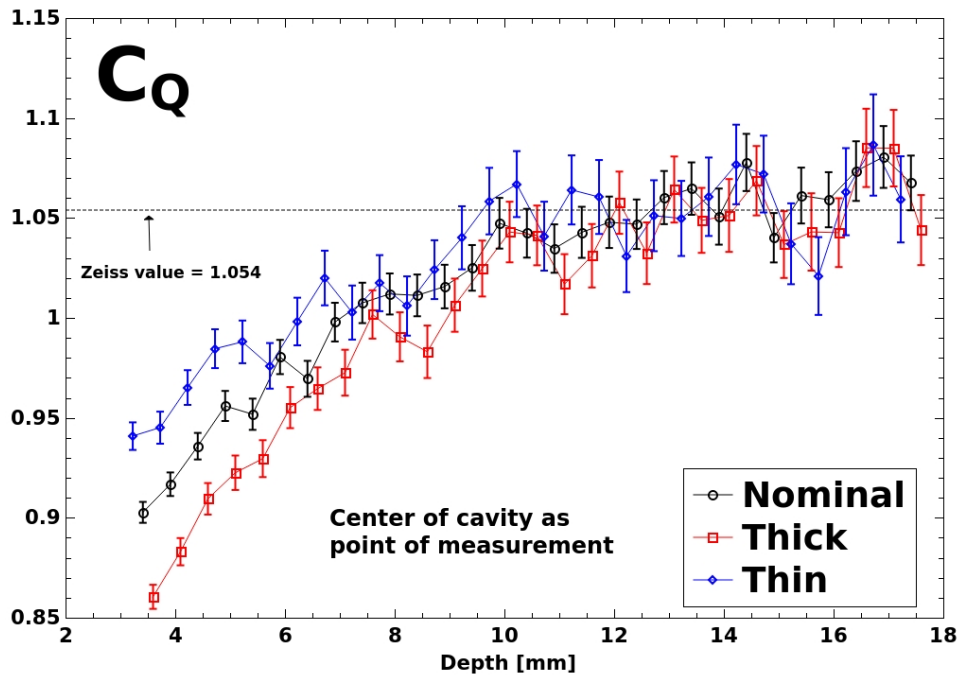


Figure 2: Ionization chamber conversion factor as a function of depth in water. POM was defined to be the midpoint of the cavity.

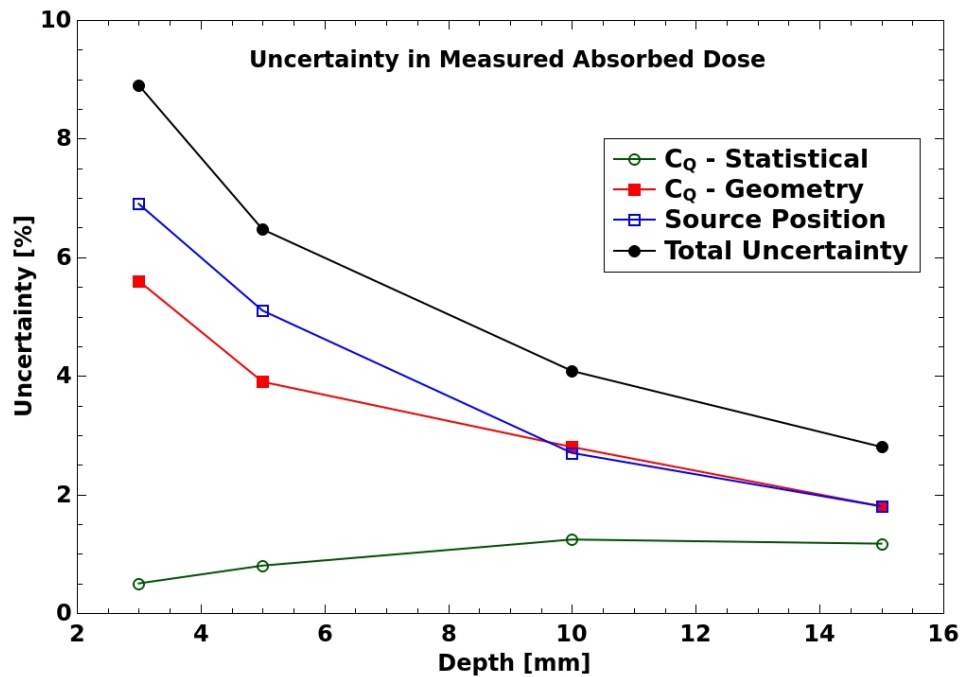


Figure 3: Uncertainty in dose measured with PTW34013 chamber following our derived dose formalism.

The total uncertainty in measured dose was found to range from 8.9% at 3 mm, to 2.8 % at 15 mm depth in water. While significant, this uncertainty does not account for the difference between absorbed doses calculated using the recommended formula and our method (up to 14.8% at 3 mm).

Conclusion: In this work, we have shown that the geometry uncertainty of the recommended ionization chamber (PTW34013) for absorbed dose to water measurements with the INTRABEAM System has a significant effect on the uncertainty of absorbed dose calculation. This geometry uncertainty also prevents the use of chamber cavity midpoint as POM, which has been shown to be more appropriate. It is

recommended that another soft X-ray ionization chamber with precise knowledge of cavity dimensions (ex. Exradin A20) be investigated for this purpose. Finally, the dose calculated with our formalism was found to be significantly larger than that of the manufacturer recommended formula, suggesting that dose to water could be underestimated by up to 23%.

[1] Watson, P., and J. Seuntjens. *Medical Physics* 41 8 (2014): 24-24.

Relation to CIRMS Mission:

This project addresses the pressing need for accurate and precise dosimetry of miniature X-ray, or “electronic brachytherapy”, sources. This aligns directly with the CIRMS mission of assessing the current needs of ionizing radiation measurements, specifically the goals of the subcommittee on absorbed dose standards for brachytherapy sources. Improving the knowledge of absorbed dose from these devices will allow for better confidence in dose delivery during treatment, ultimately improving the quality of treatment for patients. This is the reason I aspire to be a clinical medical physicist; to enhance the quality of care for patients.

Collaborators:

Marija Popovic^a and Jan Seuntjens^a

^aMedical Physics Unit, McGill University (Montreal, Canada)

Ionizing Radiation Effects on Reversibly Crosslinked Polymers (Poster 15)

Kejia Yang,¹ Roberto M. Uribe,² Walter Voit^{3*}

¹Department of Chemistry and Biochemistry, The University of Texas at Dallas, Richardson, TX.

²College of Applied Engineering, Sustainability and Technology, Kent State University, Kent, OH.

³Department of Materials Science and Engineering, The University of Texas at Dallas, Richardson, TX.

E-mail: walter.voit@utdallas.edu

Objectives: Dynamic covalent chemistry, specifically the Diels-Alder chemistry, has been used to prepare novel but difficult to achieve multifunctional smart polymer networks. The Diels–Alder reaction is a [4+2] cycloaddition between a dienophile and a diene. Some variants of the Diels-Alder reaction, such as furan–maleimide Diels–Alder (fmDA), are thermally reversible through a retro-Diels–Alder reaction, which can occur at elevated temperatures. Diels-Alder chemistries enable reversibly crosslinked materials, and have been applied to many types of smart materials, such as remendable materials,^{1–4} recyclable thermosets,^{5–7} thermoreversible dendrimers for drug delivery,⁸ stimuli-sensitive films,⁹ and others¹⁰. The fmDA chemistry is among the most commonly adopted ones for above applications due to the mild conditions under which its retro-Diels–Alder reaction occurs.¹⁰

The thermoreversibility of the aforementioned materials is crucial to enable their remendability, recyclability and other smart functions. While the higher percentage the fmDA linkages in the polymer network are, the more functionality the polymer has, higher amount of fmDA linkages could lead to unexpected secondary reactions and damage the thermoreversibility.^{11–13} Since the fmDA polymers usually require heating to go through retro-Diels–Alder reaction, studies have been carried out to investigate how a polymer’s thermoreversibility can be affected under heating conditions. However, as more and more smart materials have been used in medical device industry, it is worth to look into how ionizing radiation can affect the reversibility of fmDA linkages and further affect the materials’ bulk properties.

In this study, we will explore how the properties of reversible thermoset polymers, including their crosslinking density, glass transition temperatures, modulus, and toughness, are affected by e-beam radiation at various doses. We will also study how chemical structures of the polymers, including the fmDA adducts, can be changed during the e-beam radiation, that ultimately can affect the thermoreversibility of the materials.

Methods: *Polymer synthesis:* The model fmDA polymers were prepared by mixing the tris-furan monomer (ICN3F, shown in Figure 1) and bismaleimide (2M, shown in **Figure 1**) in stoichiometric ratio at 120 °C under constant stirring for 30 minutes before encased between two glass slides with two spacers of 1 mm thick. The resulting polymer was later cooled down slowly to room temperature overnight.

E-beam radiation: The polymer samples were irradiated with 3.8 MeV electrons with doses of 25 and 50 kGy at room temperature.

Characterization of polymers: The non-irradiated and irradiated samples were all characterized by dynamic mechanical analysis (DMA), differential Scanning Calorimetry (DSC), tensile test, and attenuated total reflectance Fourier transform infrared spectroscopy (ATR-FTIR).

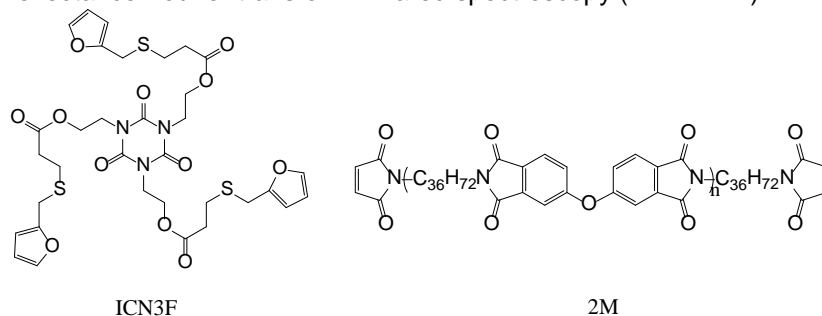


Figure 1. Monomers used for making model fmDA thermoset polymer

Results: DSC curves in **Figure 2a** show that the irradiated samples have higher glass transition temperatures (T_g) than the non-irradiated sample. All samples have endothermic transition with different onset temperatures—higher the dose of the radiation, higher the onset temperature the sample has.

DMA curves in **Figure 2b** confirm the increasing trend of T_g in irradiated samples. While irradiated samples both have higher rubbery modulus than the non-irradiated one, the sample irradiated at 50 kGy shows the highest storage modulus. All three samples show a storage modulus dramatic drop to below 0.1 MPa after entering the rubbery region, and their tan delta curves started to get noisy.

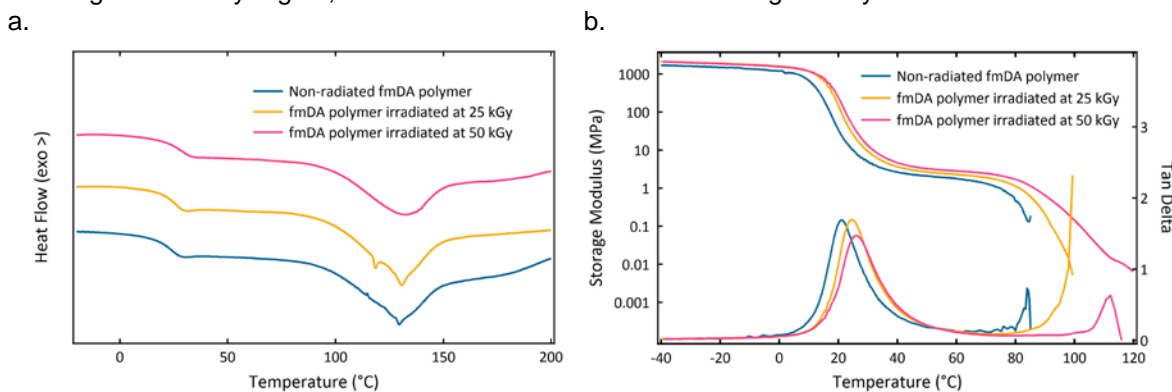


Figure 2. a. DSC curves and b. DMA curves of fmDA thermoset polymers with various doses of e-beam radiation

ATR-FTIR spectra of all three samples are shown in **Figure 3**. No obvious difference was observed among the three spectra.

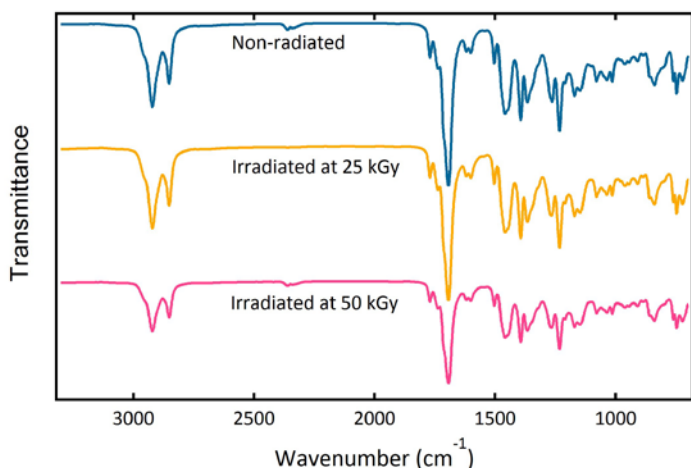


Figure 3. ATR-FTIR spectra of fmDA thermoset polymers with various doses of e-beam radiation. Stress–strain curves of non-radiated and irradiated fmDA thermoset polymers are shown in **Figure 4**. The Young’s modulus of the sample increases and the strain decreases as radiation dose increases, but the ultimate tensile stresses of the three samples are similar.

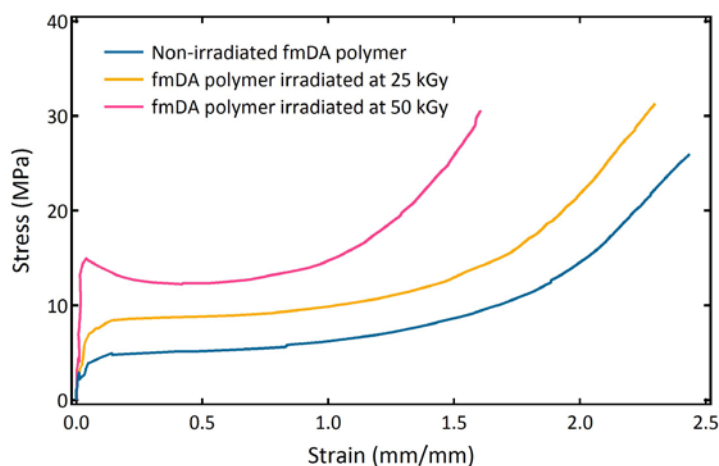


Figure 4. Stress–strain curves fmDA thermoset polymers with various doses of e-beam radiation

Discussion: The higher T_g 's and higher rubbery moduli of the irradiated samples from DMA and DSC, as well as the higher Young’s moduli of irradiated samples and less strains in the tensile tests verified that the e-beam radiation process on the model fmDA thermoset polymer at both 25 and 50 kGy resulted in higher crosslinking density in the networks.

Furthermore, ATR-FTIR did not show the fmDA adducts in the polymer networks have been changed by the radiation process. That indicates that the e-beam radiation at doses of 25 and 50 kGy did not damage the Diels–Alder adducts, i.e. the thermoreversibility of the fmDA adducts was not compromised and the polymer stayed remendable after e-beam radiation at doses of 25 and 50 kGy. The dramatic moduli drop and the noisy tan delta curves of all three samples in DMA also showed that all three samples entered the polymer flow region, indicating that all three samples, including the irradiated ones, were able to de-crosslink at higher temperatures, which was the feature of remendable polymers enabled by fmDA adducts.

Relevance to CIRMS mission:

The mission of CIRMS includes identification of research needs of radiation effects in industrial, medical and homeland security communities. As more and more smart materials have been developed and used for applications in industry, medical device, and homeland security, as well as the ionizing radiation process gets more involved in manufacturing, the studies focusing on radiation effects on those smart polymers become increasingly critical. Remendable polymers and composites are among the promising materials that could be a potential solution to the problems of repairing impact, delamination and cracking damage in engineering parts, medical device, aircraft and vehicles. We believe that our study on how the remendability

of the polymers can be affected by e-beam radiation will benefit the development of smart materials and their applications in aforementioned areas, and more importantly, to prevent the failure of the materials in critical applications.

Reference:

1. X. Chen, M. A. Dam, K. Ono, A. Mal, H. Shen, S. R. Nutt, K. Sheran, F. Wudl, *Science* **2002**, 295, 1698
2. X. Chen, F. Wudl, A. K. Mal, H. Shen, S. R. Nutt, *Macromolecules* **2003**, 36, 1802
3. P. Du, H. Jia, Q. Chen, Z. Zheng, X. Wang, D. Chen, *J. Appl. Polym. Sci.* **2016**, DOI: 10.1002/app.43971n/a
4. G. B. Lyon, A. Baranek, C. N. Bowman, *Adv. Funct. Mater.* **2016**.
5. L. M. Polgar, M. van Duin, A. A. Broekhuis, F. Picchioni, *Macromolecules* **2015**, 48, 7096
6. X. Zhang, Z.-C. Li, K.-B. Li, F.-S. Du, F.-M. Li, *J. Am. Chem. Soc.* **2004**, 126, 12200
7. Y.-L. Liu, C.-Y. Hsieh, Y.-W. Chen, *Polymer* **2006**, 47, 2581
8. F. Morgenroth, K. Müllen. *Tetrahedron* **1997**, 53, 15349
9. P.J. Costanzo, J.D. Demaree, F.L. Beyer. *Langmuir* **2006** 22, 10251
10. J. Lahann, *Click chemistry for biotechnology and materials science*, Wiley Online Library, **2009**.
11. F. Fringuelli, A. Taticchi, *The Diels-Alder reaction: selected practical methods*, John Wiley & Sons, **2002**
12. J. R. Jones, C. L. Liotta, D. M. Collard, D. A. Schiraldi, *Macromolecules* **1999**, 32, 5786
13. B. J. Adzima, H. A. Aguirre, C. J. Kloxin, T. F. Scott, C. N. Bowman, *Macromolecules* **2008**, 41, 9112

Other Submitted Abstracts

DoD Doctrine and Diagnostic Tools for Mass-Casualty Radiation and Nuclear Incidents (Poster 16)

David L. Bolduc and William F. Blakely

Scientific Research Department, Armed Forces Radiobiology Research Institute, Uniformed Services
University of the Health Sciences, Bethesda, MD USA

In the event of mass-casualty radiation or nuclear incidents, it will be imperative that triaging of victims is performed as accurately and quickly as possible in order to maximize first-responders' efficiency and scarce resources. This talk will discuss the Department of Defense doctrine pertaining to use of both radiation dose and Acute Radiation Syndrome (ARS) severity to assess radiation injury. Also presented, will be current diagnostic tools for assessing radiation dose and ARS risk, such as the Biodosimetry Assessment Tool (BAT), the First-responders' Radiological Assessment Triage (FRAT) tool, and the recent release of the Mobile FRAT tool for use on smart phones. The use of the MEDical TREatment ProtocOLs (METREPOL) radiation accident victims scoring sheet that has been incorporated into the AFRRRI Biodosimetry Worksheet, will also be reviewed. At AFRRRI METREPOL formed the basis for recently developed algorithms for assessing ARS risk that initially used animal radiation models. On-going activities include the planned integration of METREPOL's scoring system within the AFRRRI FRAT tool.

[The views expressed in this abstract are those of the authors and do not necessarily reflect the official policy or position of DoD, AFRRRI, USUHS, nor the U.S. Government. This research was supported under AFRRRI work units RBB43523.]

Effect of Low Dose Gamma Irradiation on Polymer Additives in Polyethylene Food Contact Materials (Poster 17)

Mary Dawn Celiz, Kim Morehouse, Lowri de Jager, Timothy Begley

Center for Food Safety and Applied Nutrition, U.S. Food and Drug Administration, 5001 Campus Drive,
College Park, Maryland 20740, USA

Food irradiation is used to eliminate or control the growth of spoilage organisms, pathogens and insects in food, and delay ripening and sprouting of fruits and vegetables; thereby, improving the safety of food and extending its shelf life. Certain food contact materials have been approved for use during the irradiation of prepackaged foods. As the need for convenience and food safety increases, irradiation of prepackaged foods may become prevalent. During irradiation, radiolysis products, from the polymer and polymer additives comprising the food contact material, may form. There is little information available on the effect of low dose irradiation on polymer additives. Hence, more data will be needed to assess the safety of food contact materials exposed to low doses of irradiation. This study is focused on determining the effect of gamma irradiation of less than 10 kGy on antioxidant polymer additives present in polyethylene resins. After irradiation, the antioxidants are extracted using accelerated solvent extraction, and the polymer extracts are analyzed using liquid chromatography with photodiode array (PDA) and a QTRAP[®] mass spectrometer (MS) as detectors. The MS is operated with atmospheric pressure chemical ionization as source in both positive and negative ionization modes. Data acquisition is performed in full scan MS and MS/MS modes. The amount of antioxidants extracted from the irradiated polymer resins are quantified using the MS/MS data. The formation of radiolysis products from the antioxidants are monitored using the PDA trace. The results demonstrate a decrease in the amount of the antioxidants present in the resins as the irradiation dose increases from 0 to 4 kGy. For Irganox 1076, a 39% decrease from 415 ppm is observed at 4 kGy. The major radiolysis product observed in the PDA trace has a 2 unit mass difference less than Irganox 1076. This indicates the loss of two hydrogens, which also corresponds to the fragments observed in the MS/MS spectrum. As the irradiation dose increases, the peak of this radiolysis product increases up to 60% relative to Irganox 1076 at 4 kGy, and then decreases to 6% at 20 kGy. Radiolysis products produced from polymer additives in food contact material during irradiation at low doses can potentially migrate to food. Determining

what these radiolysis products are and its amount will assist in the exposure based safety evaluation of food contact materials used with food irradiation at low doses.

An Electron/Photon Transport Bibliographic Database (Poster 18)

John C. Garth

Air Force Research Laboratory (retired)

This poster presents a bibliographic database containing over 5000 categorized references to articles on various areas of ionizing radiation physics. In 2005 the author gave a conference paper [1] that surveyed over 60 topics involving electron and photon transport in the energy range 10 eV - 30 MeV. Since that time, many references on these topics, including their abstracts, have been gathered and compiled into a comprehensive bibliographic database. For example, review and tutorial article references on nearly every topic are included. The author's intention is that this bibliographic "tool" can be regarded as a "textbook" that gives an integrated overview of many important radiation physics topics.

All references are categorized using 65 different topical headings. Topics include basic interactions of photons and electrons with matter, mathematical methods (e. g., Monte Carlo, the Boltzmann equation), popular computer codes, electron backscattering, transmission, energy and charge deposition, and various dosimetry topics. Medical physics areas include photon and electron beam therapy, brachytherapy, treatment planning, IMRT, medical imaging (including SPECT/CT and PET), nuclear medicine, radiation biology, and radiation protection. Other fields treated include radiation processing, radiation charging of insulators, physics of the earth's aurora, electron probe microanalysis, x-ray fluorescence analysis, x-ray photoelectron spectroscopy, microdosimetry, track structure, proton transport, ion beam transport, and electron energy loss spectroscopy.

References over the time period from 1940 to 2017 are contained in this database. It does not include many application-specific papers of particular interest only to specialists in a given area (e. g., medical physics, radiation processing). For example, most articles dealing with radiation therapy and imaging applications, as published in Medical Physics, would not be included. Yet the bibliography is still very comprehensive and large! The advantage of this database is that it should enable one to see how seemingly unrelated fields overlap and how they are connected through their common physics and mathematical transport models.

Most of the fields covered in this CIRMS meeting (medical physics, industrial applications, and radiation protection) are within the scope of this bibliography. At the poster session, this bibliographic database will be made available via electronic PC files to any conference participant. These files will include (1) a complete bibliographic Word file for all articles, (2) an Excel file database (excluding abstracts), and (3) an EndNote's library with abstracts for all references. We will also provide an executable file containing nearly all the data in the EndNote library, so that running EndNote need not be necessary. Finally, as a complement to this material, a summary "book" file will supply a brief introduction to each topical area contained in this database.

Reference:

1. J. C. Garth, "Electron/photon Transport and its Applications", Conference paper "The Monte Carlo Method: Versatility Unbounded in a Dynamic Computing World." Available on the web at: <http://cmpwg.ans.org/oct2007/Garth-Pub-Database/Garth%20MC2005.pdf>

Analysis of Fission Products Using Portable Gamma-ray Spectrometer Equipped with a Broad Energy Germanium Detector (BEGe) (Poster 19)

Joseph Hagan, Zhichao Lin, Stephanie Healey, Patrick Regan

Analytical Branch, Winchester Engineering and Analytical Center
Food and Drug Administration, 109 Holton Street, Winchester, MA 01890

Per the FDA food safety compliance and emergency response programs, 6 out of the 9 radionuclides that need to be monitored in the aftermath of a nuclear or radiological incident are fission products. Detection and quantification of gamma-emitting fission products in food with gamma spectrometry are complicated by a number of factors such as overlapping spectra, coincidence-summing effects, parent-progeny relationships, and variable sample self-attenuations. Many analysts practicing gamma-ray spectrometry have minimal experience in analyzing fresh fission products with commercial gamma spectrometry software owing to rare occurrence of nuclear reactor accidents and limited availability of applicable proficiency test materials. In order to address this laboratory competency concern, a proficiency test sample containing 13 fission product radionuclides was analyzed using a portable gamma-ray spectrometer equipped with electrically powered cryostat (Cryo-Pulse 5 Plus), ~40% broad energy germanium detector (BEGe), and Canberra Genie-2000/Apex-gamma spectroscopy software. A series of experiments were conducted to calibrate BEGe detector, optimize spectral processing parameters, correct coincidence summing effects, and define parent-progeny pairs that affect identification and quantification of the fission product radionuclides presented. The observations and results leading to the validation of detector calibrations and spectral analysis protocols are described. The performance characteristics of the method used for analyzing the fresh fission product radionuclides are also presented.

Status of Analysis of the Use of Co60 and Alternatives for Medical Device Sterilization (Poster 20)

Thomas K. Kroc

Fermilab

The Illinois Accelerator Research Center (IARC) at Fermilab has been asked by the National Nuclear Security Administration (NNSA) to conduct an analysis of the medical device validation process using radiation sterilization. The focus of this analysis is to understand the opportunities and challenges for replacing Co60 with electron beam or bremsstrahlung x-ray radiation. Fermilab is mid-way through its analysis having conducted an extensive review of the literature and regulations and has conducted a series of interviews with representatives of medical device manufacturers and processors.

The issue is very complex, ranging from intellectual property issues to multi-national regulation of medical devices. We will demonstrate this complexity with a few examples of successes and failures that have been attempted to date. We will offer some of our suggestions of actions that may improve the ability to accomplish this transition.

A System for the Measurement of Electron Stopping Powers (Poster 21)

Timothy Roy and Malcolm McEwen

Ionizing Radiation Standards, National Research Council Canada, Ottawa, ON

Introduction: Stopping powers are essential data in radiation dosimetry but there is little experimental data to confirm the calculated values provided in ICRU Report 37. A number of approaches to measure stopping powers have been investigated over the last two decades, with the best option being to use single-particle counting techniques similar to gamma spectroscopy.

Materials and Methods: The basis of the experiment is a large-volume HPGe detector with a thin entrance window. Monte Carlo simulations using EGSnrc were used to optimize the detector size, allowing the measurement of up to 35 MeV incident electrons with reasonable efficiency.

After initial commissioning with standard gamma sources, a test geometry was set up using a Y-90/Sr-90 source. The experimental setup is very simple to a 'classical' photon attenuation measurement, with a collimated source of ionizing radiation, an interaction medium, and a detector. By varying the amount of

scattering/absorbing material it is possible to obtain a parameter that is related to the electron stopping power. Measurements were made with two different materials – aluminum and copper – with a range of foil thicknesses for each. To obtain good statistics on the measured electron spectrum, long counting times were needed and measurements were repeated to ensure no variation with time (e.g., due to changes in the background spectrum). The full geometry was modelled in EGSnrc to obtain simulated spectra for comparison with the measurements.

Results and Discussions: In general, the agreement between measured and simulated spectra was very good. The biggest challenge for the simulation was validating the geometries of the source and detector. However, after a series of iterations, and by making small variations in the experimental geometry, a best estimate of the material thicknesses was achieved.

A high-order polynomial fitting routine was used to estimate the end-point energy for each absorber thickness. The end-point was very sensitive to the range of data used for the fit, which leads to an uncertainty in the stopping power parameter of around 5 %, too large to be useful. However, by applying the same fitting routine to both measured and simulated spectra, the uncertainty associated with the fitting routine is significantly reduced. Data for both materials yielded agreement between measurement and simulation at better than 2 %, which is very encouraging, given the challenges of using a continuous beta spectrum as the input to the measurement.

Conclusions: The HPGc detector has been successfully commissioned and tested in a manner relevant to its final application to stopping power measurements using a linear accelerator. The experimental geometry was successfully implemented in an EGSnrc simulation and a comparison between measured and calculated spectra gave very good agreement (around 2 % and within the combined uncertainties). This is a very good first step in the overall project and suggests that experimental stopping powers from linear accelerators can be measured with an uncertainty better than 0.5 %.

Identification of Irradiated Dietary Supplement Ingredients by Electron Paramagnetic Resonance Spectroscopy (Poster 22)

Kim M. Morehouse and Marc F. Desrosiers

Division of Analytical Chemistry, Center for Food Safety and Applied Nutrition, U.S. Food and Drug Administration, 5100 Paint Branch Parkway, College Park, MD 20740 Radiation Physics Division, National Institute of Standards and Technology, 100 Bureau Drive, Gaithersburg, MD 20899

Under current FDA regulations, dry or dehydrated aromatic vegetable substances may be treated with ionizing radiation for microbial disinfection if they are being used as ingredients in small amounts solely for flavoring or aroma. Radiation is not currently allowed if these plant-derived materials are used in non-trivial quantities in dietary substances. The Food Safety Modernization Act requires that food facilities conduct hazard assessments and if a hazard is reasonably likely to occur they must put in place preventive measures to control the hazard. Pathogens are reasonably likely to occur in some dry or dehydrated plant materials and manufacturers may choose to irradiate their products to control this hazard. The use of Electron Paramagnetic Resonance (EPR) to detect irradiated spices was demonstrated in the early 1990's for a limited number of spices. We have recently re-examined this technique to determine if EPR could be used to ensure products labeled as irradiated have indeed been irradiated, and those that are not authorized to be irradiated are not being treated. This paper presents data on the use of EPR for detecting irradiation in a variety of plant-derived materials used in the production of dietary supplements. We have investigated the resultant EPR spectra, including its stability with time. Most of the irradiated plant-derived products analyzed display an EPR spectrum that can be assigned to the cellulosic radical. Several products demonstrated a more complex radical spectrum which originates from other components found in the products. For most of the samples investigated, the EPR spectra of the irradiated products were markedly different from the non-irradiated product and this difference could be measured up to 90 days post irradiation treatment.

Application of the NRC Primary Standard Water Calorimeter to High-Energy Electron Beams (Poster 23)

Bryan Muir, Claudiu Cojocaru, Malcolm McEwen, Carl Ross

National Research Council Canada

Introduction: Water and graphite calorimeters, which directly measure absorbed dose from ionizing radiation via temperature increase, have been the primary standard for absorbed dose measurements in high-energy photon beams for more than two decades. However, the characteristics of electron beams (e.g, dose distribution) have limited, particularly, the application of water calorimetry to such beams. This study presents the results of electron beam water calorimetry measurements carried out at the National Research Council Canada (NRC), with specific focus on the photon-electron conversion factor, kecal in TG-51 (which is somewhat analogous to $k_{Qcross,Q0}$ in TRS-398) for several ion chamber types. There is substantial motivation to update kecal factors, a central parameter in reference dosimetry protocols that required assumptions and may therefore be in error.

Methods: An insulated enclosure with fine temperature control is used to maintain a constant temperature of the calorimeter phantom at 4 degrees Celsius to minimize effects from convection. Drifts in temperature are less than 0.1 mK/min. A parallel-plate glass vessel was specifically designed for measurements in high dose gradients in water irradiated by electron beams. This vessel houses two thermistor probes, traceable to the NRC primary standard of temperature, which measure the radiation induced temperature rise. The vessel is filled with high-purity water and saturated with N₂ gas to minimize the effect of radiochemical reactions on the measured temperature rise. Irradiations were performed with 18 MeV and 22 MeV beams from the NRC Elekta Precise linac. A set of secondary standard ion chambers were calibrated directly against the calorimeter. Finally, several other ion chambers (cylindrical and parallel-plate) were calibrated in the NRC cobalt-60 reference field and then cross-calibrated against the secondary standard chambers in electron beams to realize kecal factors.

Results: Measurements made in 22 MeV with two different vessel geometries are consistent within 0.2 % after correction for the vessel perturbation. Measurements of absorbed dose calibration coefficients for the same secondary standard chamber separated in time by 10 years are within 0.2 %. The reproducibility of the linac and transmission monitor chambers that would affect the transfer of the standard is typically at the 0.1 % level over the course of a day and less than 0.3 % over the course of 10 months, although these drifts are mitigated to the 0.1 % level by performing daily ion chamber normalization measurements. Calibration coefficients for secondary standard ion chambers can be achieved with uncertainty less than 0.4 % ($k=1$) in high-energy electron beams. The additional uncertainty in deriving calibration coefficients for well-behaved chambers indirectly against the secondary standard reference chambers is not significant. These kecal factors differ by up to 2.1 % from those in TG-51, a potentially significant change for reference dosimetry measurements.

Conclusions: The measurements made here of kecal factors for eight plane-parallel and six cylindrical ion chambers will impact future updates of reference dosimetry protocols by providing some of the highest quality measurements of this crucial dosimetric parameter.

Analysis of ⁸⁹Sr in Food by Cerenkov Liquid Scintillation Counting (Poster 24)

Jingjing Pan, Kathryn Emanuele, Eileen Maher, Zhichao Lin, Stephanie Healey, Patrick Regan

Winchester Engineering and Analytical Center
Food and Drug Administration
109 Holton Street, Winchester, MA 01890

Among the radionuclides of greatest concern for food safety, radioactive strontium, i.e., ⁸⁹Sr ($T_{1/2} = 50.5$ days and $E_{max} = 1.5$ MeV) and ⁹⁰Sr ($T_{1/2} = 28.9$ years and $E_{max} = 0.55$ MeV), are mostly monitored in protecting public health given their high bioavailability, skeletal accumulation, and known carcinogenicity. Both ⁸⁹Sr and

^{90}Sr can be released from nuclear detonation, nuclear power plant accident, or malevolent radiological attack. Because ^{89}Sr decays $>10^4$ times faster than ^{90}Sr , ^{89}Sr contributes a significant short-term radiation dose in the early stage of nuclear emergencies and needs to be quantified to enable inclusive radiation risk assessment along with ^{90}Sr . The radioanalytical procedure for differential quantification of ^{89}Sr and ^{90}Sr is complicated by their identical chemical properties and overlapping beta spectra. This presentation describes a liquid scintillation method that applies $\text{Ca}_3(\text{PO}_4)_2$ coprecipitation for matrix removal, Sr resin for elimination of radiometric interferences, enriched stable isotope for determination of Sr yield, and Cerenkov counting for quantification of ^{89}Sr radioactivity in a variety of foods. A preliminary study demonstrated that the method is capable of detecting and quantifying ^{89}Sr in a 100 g food sample at $\sim 1/10$ and $\sim 1/5$ of regulatory limit, respectively. Other method performance characteristics including robustness, accuracy, precision, and uncertainty are also evaluated based on various experimental results. The method provides an essential radioanalytical capability needed by FDA in responding to a nuclear or radiological event that involves radioactive ^{89}Sr .

Characterization of a Commercial Optically Stimulated Luminescence Dosimetry System (Poster 25)

Bryan Remley
Georgetown University and NIST

There is a need to better understand the risks of low level radiation dose. This includes radiation doses delivered by medical diagnostic procedures. In this respect it is important that radiation doses measured in clinics by medical and health physicists are accurate and traceable to national standards. Users of instruments typically calibrate their dosimeters in one type of radiation beam with a specific photon energy spectrum (referred to as beam quality) and then may use these dosimeters to measure radiation in other types of radiation beam qualities over a different range of photon energies. This may not represent much of a problem, if the dosimeter response is relatively constant for a broad range of photon energies. However, the optically stimulated luminescent (OSL) dosimeters studied in this work have demonstrated a relatively strong energy dependence in low photons with energy less than 100 keV. This means that close attention shall be paid to how the system is calibrated, and when used to measure a radiation dose from low energy photons. For the OSL dosimetry system studied in this work, the vendor provides pre-exposed OSLs to calibrate the OSL reader for dose measurements in a ^{137}Cs gamma-ray beam and in a beam of x-rays with a tube voltage of 80kVp. This calibration is adequate if the OSLs will be used to measure doses in such radiation fields or beam qualities. However, if the OSLs are to be used in radiation fields with different energy spectrum (or beam quality) the dose measurement will need to be corrected to account for differences in the photon energy spectrum. In this work an OSL dosimetry system was characterized to measure doses in radiation fields for which the OSL system was calibrated from the vendor provided OSLs (80 kVp x-rays). But in addition, the OSL dosimetry system was characterized to measure doses in other x-ray beams that have energy spectra similar to those found in x-ray diagnostic units. A comparison of the doses measured by the OSL dosimetry system using the vendor's calibration was made with an independent calibration presented in this work. As a result of this comparison, a set of beam quality correction factors were developed to correct the dose values measured by the vendor's unit taking into account for the difference in beam quality. The OSL dosimetry system calibrations performed in this work were made using multiple calibration sets of OSLs. These calibrations sets were irradiated in the National Institute of Standards and Technology (NIST) reference x-ray beams. Because of this, the conversion factors developed as a result of this work, when applied to dose measurements made with the vendor's OSL dosimetry system, will result in a dose measurement that are traceable to the national standard for air kerma for the beam qualities studied here.

The Use of Systems Engineering Methods and Human Factors Analysis to Identify and Mitigate Safety Issues in Cranial Stereotactic Radiation Surgery (CSRS) (Poster 26)

Jimmy Stringer
University of Cincinnati

Purpose: Technology utilized in radiation oncology is robust, continues to grow at a rapid pace, and is clinically mature. However, safe guards have lagged behind the rate of advancement. These technological advancements have led to a culture of hypo-fractionation, where higher doses are now being delivered in shorter periods of time. While this is more convenient for the patient and is more radio biologically advantageous, hypo-fractionation presents a higher risk of patient injury as compared to conventionally fractionated treatments. A safety systems engineering approach towards clinical processes could ensure that dose delivery in these high stakes treatments are safely executed. This research utilized Failure Mode and Effect Analysis (FMEA) to evaluate hypo-fractionated cranial stereotactic radiation surgery(CSRS) processes from prescription to the final fraction. The goal of this project was to complete an overall hazard assessment of the CSRS process and ultimately cultivate ways to eliminate or reduce the risk in these high stakes treatments.

Method: A FMEA was performed for CSRS at Tri Health Medical Center.

- 1) Created a mapping of each of the processes associated with CSRS.
- 2) Failure modes were identified and placed in a risk assessment matrix to determine the level of risk and hazard.
- 3) A risk probability number was assigned to each failure mode based on tabulated scores on a scale of 1 to 10.
- 4) We identify and presented recommended improvements to the Medical Director and Chief Physicist.

Results: We identified 25 processes associated with CSRS. We identified 20 possible failure modes. 5 of the top-ranked failure modes were considered for process redevelopment. Redevelopment suggestions were presented to the Medical Director and Chief Physicist for possible clinical implementation.

The Development of Hard X-ray Detectors Calibration Facility (Poster 27)

Jinjie Wu¹, Jia Wang¹, Xufang Li², Xu Zhou², Congzhan Liu², Chenze Li¹, Haoran Liu¹, Juncheng Liang¹,
Zhi Chang², XinQiao Li²

¹ National Institute of Metrology, Beijing, China

² Institute of High Energy Physics, Beijing, China

The Hard X-ray Modulation Telescope (HXMT) is the high energy astrophysics mission in China. The High Energy X-ray Telescope (HE) is a core payload of HXMT. It has a cylindrical structure, consisting of 18 NaI (TI)/CsI (Na) phoswich modules. To ensure the reliability of the space observational results, the detectors need to be well calibrated on the ground, by measuring the response of the detectors to incident X-ray photons. Its ground calibration mainly includes measurements of the energy linearity, the energy resolution and the detection efficiency.

A hard X-ray calibration facility (HXCF) is established for the calibration which mainly includes an X-ray tube (the high voltage range is 10-225 kV), a double crystal monochromator used for getting a fixed beam direction, and two collimators with lead shield.

The HXCF covers 15 to 170 keV energy band and has a high fraction of monochromatic X-ray and good monochromaticity. The spot size is measured by CCD detector and GEM detector. The absolute fluence of the monochromatic X-ray is obtained by low energy germanium (LEGe) detector which is calibrated by Monte Carlo simulation and experiment with radionuclides. The results of Monte Carlo simulations and experimental calibration with radionuclides show good agreement between each other with the largest relative discrepancy of -1.8%. The relative expanded uncertainty of fluence arrive 3.8% (k=2) in the range of 15 to 170 keV monoenergetic x-ray.

The energy linearity, the energy resolution and the detection efficiency of 18 NaI (TI)/CsI (Na) phoswich modules has been calibrated by HXC

PAST PRESIDENTS OF CIRMS

1993 - Marshall R. Cleland, IBA Industrial, Inc.	1994 - Peter Almond, Univ. of Louisville
1995 - R. Thomas Bell, U.S. Dept. of Energy	1996 - Anthony J. Berejka, Ionicorp
1997 - Larry A. DeWerd, Univ. of Wisconsin	1998 - Robert M. Loesch, U.S. Dept. of Energy
1999 - Thomas W. Slowey, K&S Associates	2000 - X. George Xu, RPI
2001 - Joseph C. McDonald, PNNL	2002 - Arthur H. Heiss, Bruker BioSpin Corp.
2003 - Geoffrey S. Ibbott, UT M.D. Anderson	2004 - James A. Deye, Nat'l Cancer Institute
2005 - R. Craig Yoder, Landauer, Inc.	2006 - Mohamad Al-Sheikhly, Univ. of MD
2007 - Shawna Eisele, Los Alamos Nat'l Lab.	2008 - Manny Subramanian, Best Medical
2009 - Nolan Hertel, GA Tech	2010 - Kim Morehouse, US FDA
2011 - Chip Starns, ScanTech	2012 - Roberto Uribe, Kent State University
2013 - Robert Rushton, Hopewell Designs Inc.	2014 - Kim M. Morehouse, US FDA
2015 - Walter E. Voit, UT Dallas	2016 - present: Mark S. Driscoll, SUNY - ESF

CIRMS Award for Distinguished Achievement in the Field of Ionizing Radiation Measurements and Standards

2000 **Randall S. Caswell**, National Institute of Standards and Technology (retired)

Randall S. Caswell Award for Distinguished Achievement in the Field of Ionizing Radiation Measurements and Standards:

2002 **H. Thompson Heaton, II**: Center for Devices and Radiological Health, US FDA (retired)
2004 **Anthony J. Berejka**, Ionicorp +
2006 **Kenneth L. Swinth**, Swinth Associates
2007 **Bert M. Coursey**, National Institute of Standards and Technology, U.S. DHS (retired)
2008 **Larry A. DeWerd**, University of Wisconsin
2009 **Marshall R. Cleland**, IBA Industrial, Incorporated
2010 **Geoffrey S. Ibbott**, UT MD Anderson Cancer Center
2011 **Kenneth G.W. Inn**, National Institute of Standards and Technology (retired)
2012 **Joseph C. McDonald**, Pacific Northwest National Laboratory (retired)
2014 **Stephen M. Seltzer**, National Institute of Standards and Technology (retired)
2015 **X. George Xu**, Rensselaer Polytechnic Institute
2016 **James A. Deye**, National Cancer Institute, RRP
2017 **Peter R. Almond**, UT MD Anderson Cancer Center (retired)

Student Travel Grant Recipients

2017	Alexandra Bourgouin James Renaud Susannah Hickling Manik Aima	Carleton University, Canada McGill University, Canada McGill University, Canada University of Wisconsin - Madison
2016	Manik Aima Khalid Gameil Yvonne Roed Blake Smith Kejia Yang	University of Wisconsin - Madison National Research Council of Canada UT MD Anderson Cancer Center University of Wisconsin - Madison University of Texas at Dallas
2015	Mitchell Carroll Travis Dietz Jon Hansen Sameer Taneja	UT MD Anderson Cancer Center University of Maryland - College Park University of Wisconsin - Madison University of Wisconsin - Madison
2013/2014	Mitchell Carroll Kuan-Chih Huang Cameron Maher Dwayne Riley S��verine Rossomme Steven Shaffer Anjali Srivastava Samantha Steele Angela Weier Bennett Williams Yana Zlateva	MD Anderson Cancer Center Rensselaer Polytechnic Institute Texas A&M University University of Wisconsin Universit�� Catholique de Louvain University of Texas at Dallas Missouri University of Science and Technology SUNY ESF University of Wisconsin – Madison University of Illinois McGill University
2012	Kevin Casey Olivia Huang Fahima Islam Lisa Meyers Joshua Reed James Renaud Dwayne Riley Vaibhav Sinha John Michael Briceno	MD Anderson Cancer Center MD Anderson Cancer Center Missouri U. of Sci. & Technology University of Cincinnati University of Wisconsin McGill University University of Wisconsin Missouri U. of Sci. and Technology UTexas Health Science Center San Antonio
2011	Austin Faught Adam Paxton Gina Paek	University of Texas University of Wisconsin Chapman University
2010	Keith Hearon	Texas A&M University

	Steven Horne Regina Kennedy Charlotte Rambo	LLNL Nuclear Forensics Internship Program University of Wisconsin Texas A&M University
2009	Marina K. Chumakov Ryan Grant Jessica R. Snow Walter Voit	University of Maryland University of Texas M.D. Anderson Cancer Center University of Wisconsin Georgia Institute of Technology
2008	Regina M. Kennedy Matthew Mille	University of Wisconsin Rensselaer Polytechnic Institute
2007	Jianwei Gu Arman Sarfehnia Sarah Scarboro Zachary Whetstone	Rensselaer Polytechnic Institute McGill University Georgia Institute of Technology University of Michigan
2006	Kimberly Burns Maisha Murry Karl Benjamin Richter Reed Selwyn	Georgia Institute of Technology University of Cincinnati University of Minnesota University of Wisconsin
2005	Eric Burgett Mark Furler Andrew Jensen	Georgia Institute of Technology Rensselaer Polytechnic Institute University of Wisconsin
2004	Jennifer R. Clark Stephen D. Davis Carlos Roldan	University of Kentucky University of Wisconsin University of Massachusetts – Lowell
2003	Sheridan L. Griffin Malcolm P. Heard Shannon Miller-Helfinstine Baodong Wang	University of Wisconsin University of Texas M.D. Anderson Cancer Center Kent State University Rensselaer Polytechnic Institute
2002	Wes Culberson Ramazan Kizil Dickerson Moreno Michael Shannon	University of Wisconsin Penn State University University of Missouri Georgia Institute of Technology
2001	Matt Buchholz Michael Czayka Bridgette Reniers Kurt Stump	Oregon State University Kent State University Universite' Catholique de Louvain University of Wisconsin
2000	Lesley Buckley Peter Caracappa Scott Larsen	University of Wisconsin Rensselaer Polytechnic Institute State University of New York
1999	Ahmet Bozkurt Ariel Drogin Kurt Marlow Oleg Povetko Jennifer Smilowitz	Rensselaer Polytechnic Institute University of Kentucky Idaho State University Oregon State University University of Wisconsin

CIRMS Meetings and Workshops

April 2016	Annual Meeting Focus: "A Matter of Scale: Measurement Standards from the Nano to the Giga" Working groups: Industrial Applications and Materials Effects Medical Applications Radiation Protection / Homeland Security
April 2015	Annual Meeting Focus: "Fundamentals of Ionizing Radiation" Working groups: Industrial Applications and Materials Effects Medical Applications Radiation Protection / Homeland Security
March 2014	Annual Meeting Focus: "Advanced Manufacturing and Technology" Working groups: Industrial Applications and Materials Effects Medical Applications Radiation Protection / Homeland Security
October 2012	Annual Meeting Focus: "Confidence through Measurement Traceability" Working groups: Industrial Applications and Materials Effects Medical Applications Radiation Protection / Homeland Security
October 2011	Annual Meeting Focus: "Public Perception of Radiation" Working groups: Industrial Applications and Materials Effects Medical Applications Radiation Protection / Homeland Security
October 2010	Annual Meeting Focus: "Ionizing Radiation Sources: Users, Availability, and Options" Working groups: Industrial Applications and Materials Effects Medical Applications Radiation Protection / Homeland Security
October 2009	Annual Meeting Focus: "Radiation Measurements and Standards for Incident Response" Working groups: Industrial Applications and Materials Effects Medical Applications Radiation Protection / Homeland Security
October 2008	Annual Meeting Focus: "Radiation Measurements and Standards at the Molecular Level" Panel Discussion: Radiation Source Use and Replacement Break-out session workshops: Industrial Applications and Materials Effects Medical Applications Radiation Protection / Homeland Security

October 2007 Annual Meeting Focus: "Measurements and Standards for Radiation Based Imaging"
Break-out session workshops:
Industrial Applications and Materials Effects
Medical Applications: "Imaging for Radiation Therapy Planning and Delivery"
Radiation Protection / Homeland Security

October 2006 Annual Meeting Focus: "Implications of Uncertainty in Radiation Measurements and Applications"
Break-out session workshops:
Industrial Applications and Materials Effects
Medical Applications: "Imaging for Radiation Therapy Planning and Delivery"
Radiation Protection / Homeland Security

October 2005 Annual Meeting Focus: "The Impact of New Technologies on Radiation Measurements and Standards"
Break-out session workshops:
Industrial Applications and Materials Effects
Radiation Protection
Medical Applications: "Unconventional Measurements and Standards"

October 2004 Annual Meeting Focus: "Biological Dosimetry Measurements and Standards"
Break-out session workshops:
Medical Applications
Homeland Security
Industrial Applications and Materials Effects
Radiation Protection
Department of Homeland Security and CIRMS workshop on the Development of REALnet - Radiological Emergency Analytical Laboratory Network

October 2003 Annual Meeting Focus: "Radiation/Radioactivity Measurements and Standards in Industry"
Break-out session workshops:
Medical Applications
Homeland Security
Industrial Applications and Materials Effects
Radiation Protection

April 2003 Advances in High Dose Dosimetry

October 2002 Annual Meeting Focus: "Traceability for Radiation Measurements and Standards"
Break-out session workshops:
Traceability and Standards in High-Dose Applications
Traceability and Standards for Homeland Security
Traceability and Standards in the Medical Physics Community

September 2002 Electron Beam Treatment of Biohazards

February 2002 Ultra-Sensitive Uranium Isotopic Composition Intercomparison Planning Meeting

October 2001 Annual Meeting Focus: "Radiation Standards for Health and Safety"
Break-out session workshops:
Specifications for Standard *In-Vivo* Radiobioassay Phantoms

Food Irradiation Technology Advancements and Perspectives
Measurements and Standards for Intravascular Brachytherapy Sources

October 2000	Annual Meeting Focus: "Advanced Radiation Measurements for the 21st Century" Break-out session workshops: Dosimetry for Radiation Hardness Testing: Sources, Detectors, and Computational Methods Measurements and Standards Infrastructure for Brachytherapy Sources Laboratory Accreditation Program for Personnel Dosimetry: Review of the Status of Implementation of New Standards Drum Assay Intercomparison Program
May 2000	Estimating Uncertainties for Radiochemical Analyses
April 2000	Computational Radiation Dosimetry: New Applications and Needs for Standards and Data Radiation Measurements in Support of Nuclear Material and International Security
May 1999	R-level Measurements and Standards for Public and Environmental Radiation Protection
April 1999	Measurements and Standards for Prostate Therapy Seeds Standards, Intercomparisons and Performance Evaluations for Low-level and Environmental Radionuclide Mass Spectrometry and Atom Counting
September 1998	Radiation Dosimetry Protection
April 1998	Measurements and Standard for Intravascular Brachytherapy
March 1998	NIST Radiochemistry Intercomparison Program
October 1997	High Dose E-Beams Electronic Personnel Dosimetry
March 1997	Iodine -125 Brachytherapy
February 1997	NIST Radiochemistry Intercomparison Program
September 1996	Standards and Measurements for Therapeutic Radionuclides for Use in Bone Palliation
July 1996	Mid-year workshops Mutual Accreditations
June 1996	Radiation Sterilization Medical Devices
April 1996	Mutual Accreditations Absolute Dose
September 1995	MQA Gamma Processing
March 1995	New NVLAP Criteria Radionuclide Speciation
June 1994	Ocean Studies SRM

Please save the date:

26th Annual Meeting CIRMS 2018

April 16-18*, 2018

* Exact dates still to be confirmed

Visit www.cirms.org for

- ▶ more information about CIRMS
- ▶ presentations from the previous Annual Meetings
- ▶ CIRMS Report on Needs in Ionizing Radiation Measurement and Standards
- ▶ membership application
- ▶ and more...

Contact us at: CIRMS@CIRMS.org



Council on Ionizing Radiation Measurements and Standards

P.O. Box 262333, Plano, TX 75026 • 301-591-8776 • email: cirms@cirms.org • www.cirms.org

CIRMS 2017 Corporate Sponsorship

Benefits to all corporation members/sponsors:

- Company branding through Sponsors List on CIRMS website and on all announcements and mailings
- Editorial position on the CIRMS "Needs Report" Panel
- Can be elected to the Executive Committee
- Up to six 2017 individual employee memberships to CIRMS
- Free tabletop display and/or poster space at CIRMS 2017 Annual Meeting (March 27-29, 2017)

Corporate Sponsor (\$1000 per year)

- Company branding through Sponsors List
- Editorial position on the CIRMS "Needs Report" Panel
- Can be elected to the Executive Committee
- One free registration to CIRMS 2017
- Two free 2017 individual employee memberships to CIRMS

Bronze Sponsor (\$2000 per year)

- Benefits of Corporate Sponsorship
- Extra support and branding through one of the following:
 - Named Sponsorship of Student Travel Grant
 - Names and Logos on CIRMS 2017 Bags
 - Names and Logos on CIRMS 2017 Portfolio
 - Names and Logos on CIRMS 2017 Flash Drives
 - Names and Logos on CIRMS 2017 Lanyards

Silver Sponsor (\$3000 per year)

- Benefits of Bronze Sponsorship
- Named Sponsorship of Coffee Break or second Bronze perk
- One additional free registration to CIRMS 2017 (total: 3)
- Two additional free individual employee memberships (total: 4)

Gold Sponsor (\$5000 per year)

- Benefits of Silver Sponsorship
- Named Sponsorship of Smokey Glen Farm BBQ Happy Hour or Dessert
- One additional free registration to CIRMS 2017 (total: 3)
- Two additional free individual employee memberships (total: 6)

Platinum Sponsor (>\$10,000 per year)

- Benefits of Gold Sponsorship
- Sponsor for Smokey Glen Farm BBQ Dinner
- Free CIRMS 2017 conference registrations for up to 10 people from your organization
- Free individual employee memberships for up to 20 people from your organization



CIRMS Membership Application

Instructions

Complete this form and print it. Fax to 872-883-7202 or mail the completed form and send your payment to: CIRMS, P.O. Box 262333, Plano, TX 76026.

Membership Class

Select which membership class:

- Corporate Sponsor \$1,000.00
- Corporate Sponsor Bronze \$2,000.00
- Corporate Sponsor Silver \$3,000.00
- Corporate Sponsor Gold \$5,000.00
- Corporate Sponsor Platinum \$10,000.00
- Government / Non-Profit Organization Sponsors \$250.00
- Individual Member \$50.00
- Student Member \$25.00

Member Information

Name and Address of Applicant. Corporate and Organizational Sponsors may name up to six

Representative Name: _____
Organization: _____
Address: _____
City: _____
State: _____
Zip- Code: _____
Phone: _____
Fax: _____
Email: _____

Representative 2 Name: _____
Phone: _____
Email: _____

Representative 3 Name: _____
Phone: _____
Email: _____

Representative 4 Name: _____
Phone: _____
Email: _____

Representative 5 Name: _____
Phone: _____
Email: _____

Representative 6 Name: _____
Phone: _____
Email: _____



Council on Ionizing Radiation Measurements and Standards
P.O. Box 262333 Plano, TX 750026 Phone: 301-591-8776 Fax: 972-883-7202
www.cirms.org

Area Of Interest

	Rep 1	Rep 2	Rep 3	Rep 4	Rep 5	Rep 6
Homeland Security	<input type="checkbox"/>					
Industrial Applications & Materials Effects (IAME)	<input type="checkbox"/>					
Medical Applications (MED)	<input type="checkbox"/>					
Radiation Protection (RP)	<input type="checkbox"/>					

Payment Options

Check # _____

Please make Check payable to CIRMS and mail or fax information to the address above.

Credit Card Type:

Visa

Master Card

American Express

Name On Card:

Expire Date:

Card Number:

Signature: